Carbon cycling across ecosystem succession in a north temperate forest: controls and management implications

Lucas Nave[1], Christopher M. Gough[2], Cameron Clay[3], Fernanda Santos[4], Jeff W. Atkins[5], Sonja Benjamins-Carey[3], Gil Bohrer[6], Buck Castillo[3], Robert T. Fahey[7], Brady Hardiman[8], Kathryn Hofmeister[9], Valeriy Y. Ivanov[10], Jennifer Kalejs[3], Ashley M. Matheny[11], Angela Menna[2], Knute J. Nadelhoffer[3], Brooke Propson[12], Adam Schubel[3], Jason Tallant[3]

[1]Michigan Technological University, College of Forest Resources and Environmental Science

[2]Virginia Commonwealth University, Department of Biology

[3]University of Michigan Biological Station

[4]Oak Ridge National Laboratory

[5]USDA Forest Service, Southern Research Station

[6]Ohio State University, Department of Civil, Environmental and Geodetic Engineering

[7]University of Connecticut, Department of Natural Resources and the Environment

[8]Purdue University, Department of Forestry and Natural Resources

[9]University of Wisconsin- Oshkosh, Environmental Studies Program

[10]University of Michigan, Department of Civil and Environmental Engineering

[11]University of Texas at Austin, Department of Earth and Planetary Sciences

[12]University of Wisconsin- Madison, Department of Soil Science

For Review Only

Open Research: Datasets used in this research are as follows: canopy attributes (Atkins 2022; doi.org/10.5281/zenodo.6452902), chronosequence C stock, flux, and soils (Nave et al. 2024;

doi.org/10.6073/pasta/b47e7e6f05d6fcd7136c1e28f23e5217), and flux tower data (Gough et al. 2023a; 2023b; doi.org/10.17190/AMF/2204882; doi.org/10.17190/AMF/1881597). Additional datasets will be published in an EDI repository upon manuscript acceptance.

This manuscript has been authored by UT-Battelle, LLC, under contract DE-AC05-00OR22725 with the US Department of Energy (DOE). The US government retains and the publisher, by accepting the article for publication, acknowledges that the US government retains a nonexclusive, paid-up, irrevocable, worldwide license to publish or reproduce the published form of this manuscript, or allow others to do so, for US government purposes. DOE will provide public access to these results of federally sponsored research in accordance with the DOE Public Access Plan (https://www.energy.gov/doe-public-access-plan).

For Review Only

Abstract

Despite decades of progress, much remains unknown about successional trajectories of carbon (C) cycling in north temperate forests. Drivers and mechanisms of these changes, including the role of different types of disturbances, are particularly elusive. To address this gap, we synthesized decades of data from experimental chronosequences and long-term monitoring at a well-studied, regionally representative field site in northern Michigan, USA. Our study provides a comprehensive assessment of changes in above- and belowground ecosystem components over two centuries of succession, links temporal trends in major C pools and fluxes with underlying drivers, and offers several conceptual insights to the field of forest ecology. The first of these concepts is that temporal dynamics in several ecosystem components are consistent across severe disturbances that reset succession and partial disturbances that slightly modify it. Namely, both types of disturbance increase soil N availability, alter fungal community composition, and affect aboveground growth and interspecific competition as short-lived pioneer trees succeed to longer-

lived taxa. These changes in turn affect soil C stocks, respiratory emissions, and other belowground processes. In contrast, other ecosystem components have inconsistent effects on C cycling over succession. For example, canopy structure does not influence C uptake early in succession, but becomes important as stands develop, with the importance of individual structural properties changing over the course of two centuries of stand development. In recent decades, we find that climate change is masking or overriding effects of community compositional change on C uptake; respiratory emissions appear sensitive to both climatic and successional compositional change. In synthesis, we emphasize that time is not a driver of C cycling, it is a dimension within which ecosystem drivers such as canopy structure, tree and microbial community composition change. Changes in those drivers, not in forest age, are what control forest C trajectories, and those changes can happen quickly or slowly, through natural processes or deliberate intervention. Stemming from this view and a whole-ecosystem perspective on forest succession, we offer management applications from this work and assess its broader relevance to understanding long-term change in other north temperate forest ecosystems.

For Review Only

Key words: forest disturbance, ecosystem development, biogeochemistry, community composition, climate change

1. Introduction

The general trajectories of carbon (C) stocks and sequestration rates over the course of secondary succession in north temperate forests are well known. Rapid sequestration during the initial decades after disturbance begins to decline later in the first century of stand development, while standing C stocks continue to increase, potentially for centuries (Pan et al. 2011; Pregitzer and Euskirchen 2004). However, there is considerable variation in these trends, evidenced by large amounts of variance in age-C relationships within individual sites, sites that show the same general patterns over very different timescales, and sites that depart from general trends altogether (Birdsey et al. 2023; Bradford and Kastendick 2011; Keeton et al. 2011; Thom and Keeton 2019). This variation indicates that our understanding of the factors controlling forest C trajectories has room to grow; it also highlights the fact that forest age is far from the only thing that influences C cycling over decade to century timescales.

Because all approaches to studying ecosystem succession struggle with its long timescales, sites that combine multiple complementary approaches can make powerful contributions to our understanding of the topic. Chronosequences have limitations, but as yet they are the only way to empirically quantify C pools and fluxes over centuries (Wardle et al. 2012; Yanai et al. 2003). The other empirical approach—long-term monitoring—allows for longitudinal observation and evaluation of trends inferred through chronosequences, but even the longest-running of such studies cannot capture the centuries-long process of ecosystem succession (Eisen and Barker Plotkin 2015; Fahey et al. 2005; Hoover et al. 2011; Novick et al. 2018). In combination, these two complementary approaches can identify patterns and mechanisms of successional change, but even still it can be challenging to place results in the context of north temperate forests more

For Review Only

broadly. Such context, however, is necessary to produce transferable insights based on mechanistic understanding.

Long-term studies indicate several factors likely to control C stocks and sequestration rates over successional timescales in north temperate forests. The importance of forest structure—particularly canopy structure—to C cycling has often been demonstrated, though typically not through a successional lens (Gough et al. 2019; Ishii et al 2004; Reich 2012). Where it has been investigated as an ecosystem property that develops over the course of succession, increasing canopy structural complexity has been shown to increase forest C uptake by increasing resource use efficiency (Gough et al. 2022; Hardiman et al. 2013; Pan et al. 2013; Scheuermann et al. 2018). However, canopy structural complexity is to some extent linked to another important driver of forest C: forest community composition (Pedro et al. 2017). Trees are the most readily observed aspect of the forest community, and their compositional change over time is used almost synonymously with succession (although succession is a whole-ecosystem process). As a driver, the composition of the tree community determines canopy functional traits that influence many ecosystem processes, including C cycling (Fahey et al. 2019). Tree community composition also affects forest C in other ways, including interspecific variation in hydraulic strategies, wood density, aboveground vs. belowground C allocation, and interactions with the composition of other organismal communities, such as soil microbial communities (Abramoff and Finzi 2016; Davidson et al. 2002; Prescott and Grayston 2013, Woodcock and Shier 2002).

Soil microbial communities in turn connect to a third major driver of forest C pools and fluxes: soil biogeochemistry. Soil biogeochemistry in this sense encompasses successional changes in soil properties such as pH (Compton et al. 1998; Flinn and Marks 2007), as well as microbial communities and the C- and nutrient-transforming processes that they mediate (Goodale and

For Review Only

Aber 2001; Knelman et al. 2017; Lewis et al. 2014; Lovett et al. 2018). Nitrogen (N) is particularly important among nutrients because it limits primary production, and the forms of it that are available for plant and microbial uptake change over the course of succession (Leduc and Rothstein 2010; Nave et al. 2009). Moreover, different microbial taxa play different roles in mineralizing organic matter and releasing soil N (Phillips et al. 2013). In acidic northern forest soils, ectomycorrhizal (EcM) fungi are major players in N cycling, and EcM taxa that explore larger volumes of soil or produce organic matter depolymerizing enzymes play more prominent roles as succession advances and a larger share of soil N pool is held in less accessible organic forms (Chen et al. 2019; Hobbie et al. 2013; Leduc et al. 2013). Successional interactions between soil N availability, photobiont C supply, and mycobiont enzyme production and N foraging are as yet better characterized in boreal forest soils, but are relevant to the N economy and C balance of temperate forest soils as well (Baldrian et al. 2023; Fosmark et al. 2024; Hay et al. 2015; Jorgensen et al. 2022). Research that places these biogeochemical processes in the context of aboveground ecosystem dynamics (e.g., forest composition, canopy structure) is particularly needed to better understand succession as a whole-ecosystem process.

In working towards the goal of transferable, predictive science, enumerating the factors that influence forest C over succession is arguably less important than describing how these factors operate holistically in ecosystems. Inspired by recent multi-decadal C cycling assessments from intensively studied north temperate forests (Desai et al. 2022; Finzi et al 2020; Hollinger et al. 2021), we synthesize new data and past results from long-term monitoring and chronosequence experiments at a well-studied site, the University of Michigan Biological Station (UMBS), in northern Lower Michigan. Our analysis is intended to extend this body of work by investigating longer-term successional changes spanning decades to centuries, by: (1) identifying trends and

For Review Only

drivers of major C pools and fluxes; (2) describing mechanisms by which they operate; (3) assessing relevance to the ecology and management of north temperate forests. The first two of these objectives are facilitated by offering several predictions that inform the C pools, fluxes, and drivers we have elected to focus on here. First, we predict that successional development of forest structure regulates vegetation growth and overall ecosystem C accumulation. Second, we predict that changes in aboveground (tree) and belowground (microbial) community composition are coupled through successional time, with corresponding influences on biogeochemical functioning. Third, we predict that concurrent changes in composition and environmental drivers have influenced trends in ecosystem C uptake and loss over recent decades.

2. Methods

2.1 Study site- UMBS (45.56^{o}, -84.72 ^{o}) is in northern Lower Michigan, in the southeastern 1/3 of the 261,000 km^2 Laurentian Mixed Forest Province of the USDA Forest Service ecosystem classification framework (Cleland et al. 1997; McNab et al. 2007). The province has a humid continental climate with cold winters and warm summers; at UMBS, mean annual temperature (MAT; 6.9^{o}) and mean annual precipitation (MAP; 893 mm, including 284 cm snowfall; 1991-2020 for all parameters) fosters mixtures of warmer-temperate (*e.g.,* oak, maple) and cold-tolerant boreal (*e.g.,* spruce, fir, birch) forest types. Land use and disturbance history is broadly consistent throughout the province, where millennia of Native American ecosystem management activities were displaced by clearcutting and uncontrolled wildfires beginning with Euro-American colonization in the late 1800s and extending into the early 1900s (Lorimer 2001; Rhemtulla et al. 2009; Whitney 1987). Modern forest management began around the middle of the 20th century, and is more extensive than intensive: early-successional deciduous and mixed forests are clearcut and regrown over 40-80 year rotations, longer-lived deciduous cover types

For Review Only

156 experience selection harvests at 10-20 year intervals, and upland conifers (mostly pines) are
157 managed with periodic thinning and regeneration harvests at 60-100 years of age (Bates et al.
158 1993; Gahagan et al. 2015; Gerlach et al. 2002; Palik et al. 2003; Stone 2002).

159 A detailed description of the landscape setting and experimental design of UMBS (Nave et al.
160 2017a) is summarized here. The regional Silurian and Devonian sedimentary bedrock lays buried
161 beneath 100-200 m of glacial and lacustrine sediments deposited during the late Pleistocene. The
162 highest elevations on the landscape are moraines of poorly-sorted till deposited directly by the
163 continental ice mass; these are exceeded in area by lower-lying outwash plains, which were
164 deposited by meltwater flowing away from ice margins. These landforms were modified during
165 regional glacial re-advances 12,600 -10,500 years before present, and, at the lowest elevations,
166 by lacustrine processes 4,300 - 3,000 years before present (Schaetzl et al. 2002; Nave et al.
167 2017b). Soils formed in till are mostly coarse-loamy Lamellic and Alfic Haplorthods (USDA
168 Subgroups), outwash soils are predominantly sandy Entic Haplorthods, and soils in the lowest
169 positions are predominantly Endoaquods, Endoaquents, and Haplosaprists (USDA Great Groups)
170 formed in lake-modified outwash sediments and Holocene organic deposits.

171 Current vegetation at UMBS is the local result of the land use history that occurred across the
172 wider ecological province. Namely, clearcutting and wildfires between 1870-1923 replaced pre-
173 exploitation forests of long-lived species including red pine (*Pinus resinosa*), white pine (*P.*
174 *strobus*), eastern hemlock (*Tsuga canadensis*), sugar maple (*Acer saccharum*), American beech
175 (*Fagus grandifolia*), and red oak (*Quercus rubra*) with mixed deciduous-conifer forests
176 dominated by early-successional taxa such as bigtooth aspen (*Populus grandidentata*) and paper
177 birch (*Betula papyrifera*) in xeric to mesic settings, and trembling aspen (*P. tremuloides)* and
178 balsam fir (*Abies balsamea*) in mesic to hydric settings. Most UMBS forestland is dominated by

For Review Only

early-successional taxa, which have been increasingly replaced by longer-lived species in the last 20-30 years, due to lack of disturbances or management (Gough et al. 2010). Isolated portions of UMBS property were cut partially, or not at all, or were burned before cutting could occur and therefore serve as older reference forests, with composition and structure that might be more extensive today if not for the widespread disturbances of a century ago. Upland forests at UMBS are broadly representative of the wider Laurentian Mixed Forest Province in terms of their composition, growth rates, and disturbance history (Gough et al. 2007; Nave et al. 2017a).

2.2 Experimental design- This study is based upon data collected through 2020 from several long-term experimental designs at UMBS (Fig. 1), with unique aspects detailed below.

2.2.1. Chronosequences and old reference forests- Two experimental chronosequences, differing in the type of stand-replacing disturbance, allow for the observation of stands ranging in age from 22 – 109 years. All chronosequence stands are on sandy outwash plains and have similar soil properties. Individual chronosequence stands were established either by clearcut + residue burning (known as the Burn Plots; Scheiner and Teeri 1981), or by a clearcut not followed by an intentional residue fire. Given that nearly all of the UMBS landscape (and the region) experienced clearcutting and fire ~100 years ago, the two chronosequences therefore differ in whether they have experienced one stand-replacing cut-and-burn disturbance (hereafter 1x cut+burn) or two stand-replacing cut-and-burn disturbances (2x cut+burn). In 2020, stand ages in the 1x cut+burn chronosequence were 33, 48, 68, and 109 years old (reflecting clearcutting in 1987, 1972, 1952, and 1911, respectively); 2x cut+burn stands were 22, 40, 66, 72, and 84 years old (clearcut + residue burning in 1998, 1980, 1954, 1948, and 1936, respectively).

The experimental chronosequences are complemented by observations of older reference stands, some of which have been monitored since the 1940s (Fig. 1). The oldest of the three reference

For Review Only

stands reported here, Indian Point, is a hemlock-northern hardwoods forest with a long history of Native American management (Albert and Minc 1987); it is uneven-aged, but in the area that has been intensively monitored, dominant trees date to *ca.* 1830 (i.e., stand age = 190 years). The two other old reference stands are pine-dominated, with canopy dominants dating to 1885 – 1890 (stand age = 130 years). One of these stands was partially cut and lightly burned; the best available records (and site evidence) suggest the other was initiated after a stand-replacing fire. Due to their unique disturbance histories and differences in soils, landforms, and topoclimate, none of the three reference stands is an ideal representation of conditions that would be expected on the paired chronosequences after additional decades of development (Nave et al. 2019).

In both the experimental chronosequences and the old reference stands, individual stands range from just over 1 ha to more than 10 ha in size; in each stand, most data collection occurs within 3 plots, each 0.1 ha in size (except for 2 plots, 0.07 and 0.14 ha, in the 22-year-old "Burn Plot"). Throughout the remainder of this paper, we use the term "stand" to describe an area of forest of a known common age, composition, and disturbance, from one to several hectares in size. We distinguish stands from plots, which are sampling units of logistical convenience, but note that in many stands, individual plots were arrayed to sample across measurable or visually apparent spatial variation in ecosystem structure, disturbance severity, or to minimize edge effects. The sole exception to the "stand" vs. "plot" terminology is the Burn Plots, which by this definition consist of stands differing in ages, but whose name we reference (with capitalization) owing to their immediate recognition for generations of UMBS researchers.

2.2.2 Flux towers- The other experimental design that we draw upon for this analysis consists of paired reference and treatment flux towers known in the AmeriFlux Network as the US-UMB (reference) and US-UMd (disturbed) core sites (Fig. 1). The reference tower has a ~100 ha

For Review Only

footprint and is supported by ground-based monitoring of ecosystem properties, C pools and fluxes across an array of 81 permanent plots since 1997. The treatment tower, erected in 2006, has a ~30 ha footprint where all of the aging, early-successional trees (aspen and birch) were stem girdled in 2008 to accelerate an incipient successional transition to longer-lived taxa- a process that has continued to unfold in the reference footprint since that time. The treatment footprint holds 22 permanent sampling plots. In each footprint, a single 1.1 ha plot surrounds the flux tower, and the remainder of the plots (0.08 ha each) are located at 100 m intervals along transects that radiate away from the tower. Within the scientific literature, comparisons of ecosystem processes and C cycling between the reference and treatment footprints have occasionally been reported as results of the Forest Accelerated Succession ExperimenT (FASET; Nave et al. 2011). In this paper, we refer to the reference vs. treatment towers explicitly when differentiating between slower natural background succession vs. experimentally accelerated succession, or to FASET (as a paired design) when drawing inferences from the two footprints collectively. Like the paired chronosequences, the footprints of both flux towers are located principally on sandy, high-level outwash plains.

2.3 Data collection methods- This paper synthesizes existing and presents previously unpublished data collected over the last 40 years on the experimental designs described in section 2.2. The following subsections provide overview descriptions; details are provided in references cited here and in Appendix S1.

2.3.1 Ecosystem C stocks- Inventories supporting the estimation of aboveground live tree, standing dead tree, and coarse down woody debris C stocks are typically completed at 5-year intervals in the experimental designs reported in this paper. At each census, permanent plots are inventoried for all trees ≥1.37 m in height, which are identified to species and measured for

For Review Only

diameter at breast height. Aboveground biomass C stocks are calculated from these inventory data using a combination of site-specific and generalized allometric equations (Nave et al. 2017a) and appropriate plot area expansion factors. For presentation and discussion, live trees are grouped into short-lived deciduous (aspen, paper birch), long-lived deciduous (all other deciduous taxa), and long-lived coniferous functional groups (all coniferous species found in these plots are long-lived). Coarse down woody debris (DWD) is censused for dimensions, density, and species on 3 subplots per 0.1 ha permanent plot, and scaled up using expansion factors (Clay et al. 2022). Soil, coarse and fine root C stocks were inventoried in 2014 to a depth of 1 m, as described in Nave et al. (2019). All data are publicly available (Nave et al. 2024).

2.3.2 Canopy structure- In this paper we report canopy structural parameters collected using ground-based portable canopy LiDAR in the individual plots located in each chronosequence and old reference forest stand. These parameters were collected along two perpendicular transects (40 m each) in each plot (Fahey et al. 2019; Scheuermann et al. 2018). From the raw LiDAR returns, we used the *forestr* package to compute three canopy structural parameters for analysis, including leaf area index (LAI), mean maximum canopy height, and canopy rugosity (Hardiman et al. 2013; Atkins et al. 2018). These canopy structural data have been previously published (Atkins 2002; Fahey et al. 2019; Scheuermann et al. 2018), but not used to address the specific questions of the present synthesis.

2.3.3 Biometric C flux measurements- This paper reports four major C fluxes derived from plot-based biometric measurements: wood net primary production (NPP_w), soil respiration (Rs), fine root production, and leaf litterfall. Wood NPP was calculated for all experimental chronosequence and old reference forest stands as the change in woody biomass C between 2019 and 2014 census intervals, divided by the 5-year remeasurement interval. Soil respiration

For Review Only

measurements were made on *in situ* collars across a range of dates and soil temperatures each year in the experimental chronosequence and old reference forest stands from 2014-2021, and from 1998-2020 and 2008-2017 in the UMB and UMd tower footprints, respectively. Detailed description of data collection and scaling to stand-level means is available in Clay et al. (2022) and Appendix S1. Fine root production, measured in chronosequence and old reference stands during the 2016-2019 growing seasons, is also described in Clay et al. (2022). Briefly, we used plastic mesh cores packed with freshly sieved, root-free native soil in each stand to quantify growing season root production (5-6 month) each year, averaged across all years within each stand. Soil respiration and fine root production data are publicly available (Nave et al. 2024).

Leaf litterfall fluxes reported in this paper come from a temporally consistent subset of the 0.08 ha permanent plots in the reference (n=12, 1997-2019) and treatment (n=14, 2006-2019) flux tower footprints. In each plot, the contents of individual traps (n=3) were aggregated into plot-level total leaf litterfall, which was sorted by species and component, and used to calculate annual means according to Gough et al. (2008).

2.3.4 Tower-based CO_2 and water vapor fluxes- In this paper, we report annual values of gross ecosystem C uptake (as gross primary production; GPP), gross ecosystem C emission (as ecosystem respiration; R_{eco}), and net ecosystem C uptake (as net ecosystem exchange; NEE) from publicly available AmeriFlux data for the US-UMB (2000-2020) and US-UMd (2008-2020) towers using the AmeriFlux-FLUXNET processed version of the data (Gough et al 2023a; 2023b). Annual values have been screened, gap-filled, and computed from the raw flux data collected on the two towers according to FLUXNET methods described in Pastorello et al. (2020). We also present growing season, midday (1100 – 1400 local time) ecosystem water use

For Review Only

efficiency (WUE) for reference (2001-2020) and treatment (2007-2020) towers (calculated from the same AmeriFlux-FLUXNET data sources), computed only for non-gap-filled periods.

2.3.5 Soil C dynamics- We examine changes in soil C using two distinct datasets and approaches to address two distinct questions. First, to assess soil C trajectories over a century of stand development, we compiled data from five known sampling campaigns on the Burn Plots. Across these campaigns, only O horizons were sampled consistently. Assuming differences in individual judgment and specific sampling techniques, we used unweighted effect-size meta-analysis to quantify the magnitude and temporal patterns of O horizon C stocks following cut+burn disturbance. Statistical methods follow Nave et al. (2021). Second, to assess how soil C stocks have changed in recent decades, we report results from a longitudinal re-sampling of an unmanipulated reference area adjacent to the Burn Plots. This area of 1911-origin (clearcut + unintentional residue fire) forestland was sampled in 1980, and again in 2009, providing an opportunity to compare mineral soil C stocks by genetic horizon over a 29-year period, independent of any disturbances other than the original region-wide cut+burn disturbance.

2.3.6 Soil biogeochemistry and microbial communities- In this paper, we report results from a systematic 2015 biogeochemical and microbial characterization of Burn Plots topsoils (A horizons). These samples allowed for comparison of fungal communities, extracellular enzyme activity, root biomass, microbial biomass C, soil N availability, soil C and N concentrations, pH, and soil moisture across the 5 experimental stands comprising the 2x cut+burn Burn Plots (data published in Nave et al. 2024). All preparation and most analysis steps were completed in the UMBS Analytical Laboratory, with sequencing at the Microbial Systems Molecular Biology Laboratory at the University of Michigan. Detailed methods are provided in Appendix S1. To inform fungal N cycling aspects of these measurements, we collected fungal sporocarps in 2022

For Review Only

316 from paired plots (n=6 plots) in the reference and treatment flux tower footprints that received
317 ^{15}N tracer additions in 2010 (Nave et al. 2013). We analyzed these fungal samples by isotope
318 ratio mass spectrometry in the UMBS Analytical Laboratory in order to assess long-term N
319 foraging of several ectomycorrhizal (EcM) fungal taxa, using ^{15}N-enrichment as an indicator.

320 *2.3.7 Climatology and atmospheric deposition*- Daily climatology and weekly atmospheric
321 deposition have been monitored since the late 1970s on the main campus of UMBS on the south
322 shore of 1,700 ha Douglas Lake (Fig. 1). We present MAT as the average of daily maximum and
323 minimum values and MAP as the sum of daily water-equivalent values (UMBS 2024). For
324 atmospheric deposition, we present annual total inorganic N deposition values, as obtained from
325 the National Atmospheric Deposition Program, of which UMBS is site MI09.

326 *2.4 Data analysis*- This paper is intended to provide a holistic view of interactions between
327 ecosystem components over time, and how they influence C cycling. This required synthesizing
328 and analyzing many different types of data according to a range of appropriate approaches and
329 techniques. Analytical details are provided here, in Appendix S1, and in figure captions. The
330 following narrative enumerates the specific statistical tests used to address each topic of interest;
331 parenthetical references to figures are provided to aid in connecting these statistical tests to the
332 results we present and the inferences we draw from them. To test for differences in total
333 ecosystem C stocks (and in individual pools) over succession (Fig. 2a), we treated each plot in
334 each chronosequence and old reference stand as an experimental unit, binned plots into 40-year
335 age classes, and used one-way ANOVAs with Fisher's Least Significant Difference post-hoc
336 tests to identify significant differences between age classes. Changes in composition over the
337 same 40-year age classes (Fig. 2b) are expressed as the proportion of aboveground live tree
338 biomass in each of three functional groups (short-lived deciduous, long-lived deciduous, long-

For Review Only

lived coniferous); these data are presented for visualization but are not analyzed statistically. To test relationships between canopy structure and C uptake over succession (Fig. 3), we treated each plot in each chronosequence and old reference stand as an experimental unit, selected NPP_w as the response variable, and used multiple linear regression to determine the predictive capacity (as partial r^2) of leaf area index (LAI), maximum canopy height, and rugosity. We conducted separate regressions for young (22-48 years; n=11), middle-aged (66-84 years; n=6), and old (>100 years; n=12) stands. We standardized the values for the three structural parameters by subtracting their means and dividing by their standard deviations. To examine successional trajectories of canopy production in taxonomic detail in recent decades (Fig. 4), we treated individual plots in the reference and treatment tower footprints as experimental units, selected leaf litterfall mass as the response variable, and used year as the predictor variable in simple linear regressions to predict temporal trajectories in leaf production (total across all species), and for individual species (red oak), genera (red +sugar maples), and functional groups (early-successional species, i.e., aspen and birch). To test for successional trends in soil respiration (Fig. 5), we treated each chronosequence and old reference stand as an experimental unit, and used simple linear regression to test for temporal trends (i.e., as a function of stand age) in Rs fluxes and proportions. We ran separate regressions for annual vs. growing-season only trends, for each of the following fluxes and proportions: 1) total soil respiration [Rst], 2) autotrophic soil respiration [Rsa], 3) heterotrophic soil respiration [Rsh], and 4) heterotrophic proportion [Rsh/Rst]. To examine relationships between stand age, fine root production, and soil respiration (Fig. 6), we conducted two regressions: first, stand age vs. mean growing season fine root production (averaged to the stand level across all available years of ingrowth core incubation); second, mean growing season fine root production vs. annual total soil respiration. To examine

For Review Only

long-term successional patterns in O horizon C stocks on the Burn Plots (section 3.2 narrative), we used unweighted effect size meta-analysis to test (1) for a significant effect of past disturbance on C stocks using categorical meta-analysis and (2) whether O horizon C stock changes vary significantly with time since disturbance using continuous meta-analysis. To test for long-term changes in soil properties across the Burn Plots (Fig. 7a), we treated individual stands as experimental units, selected A horizon pH, %C, and microbial biomass C as response variables, and used stand age as the predictor variable in simple linear regressions. To test for relationships between soil properties and biogeochemical function (Figs. 7b, c), we treated individual Burn Plot stands as experimental units, selected α-glucosidase activity rate as the response variable, and regressed it against pH and %C as predictor variables (respectively) using simple linear regressions. To test for changes in fungal community composition over succession on the Burn Plots (Fig. 8), we treated individual soil samples from each stand as experimental units. In QIIME, we (1) identified fungal families driving community dissimilarity across stands using ANCOM, (2) visualized fungal communities with a PCoA biplot, and (3) tested for statistical significance of community dissimilarity along a Bray-Curtis dissimilarity matrix. To identify soil properties driving community dissimilarity (Fig. 9), we again selected individual Burn Plots soil samples as experimental units and used a (1) dbRDA biplot to visualize dissimilarity in soil properties across stand ages, and (2) forward stepwise regression, including α-glucosidase activity, microbial biomass C and N, soil NH_4-N availability, soil C and N concentrations, pH, and water content as predictor variables, to identify statistically significant predictors of variation in community dissimilarity. To test for significant differences in competition for N among different EcM fungal families (Fig. 10), we treated individual plots in the reference and treatment tower footprints as experimental units, selected the ^{15}N value of bulk

For Review Only

fungal sporocarps from each family as the response variable, and used family as the predictor variable in a one-way ANOVA. To test for significant changes in mineral C stocks in recent decades (Fig. 11), we treated individual soil profiles as experimental units, selected total C stock as the response variable, and used a two-way ANOVA to test for significant effects of horizon (A, E, B), sampling year (1980, 2009), and their interaction on C stocks. To test for significant temporal trends in GPP, R_{eco}, NEE, and WUE (Figs. 12a-c), we used multiple linear regressions. For each response variable, we ran a multiple regression model with year (continuous) and treatment (dummy variable, coded relative to the reference footprint) to test for significant temporal trajectories and significant differences between footprints. Flux timeseries were 2000-2020 for the reference tower and 2008-2020 for the treatment tower. We used a paired t-test to determine whether mean cumulative growing season soil respiration efflux differed in reference vs. treatment tower footprints over the long-term timeseries. To test for significant temporal changes in MAT and MAP (Figs. 12d, 12e) we ran simple linear regressions with year as the predictor, for a 1980-2020 climatology period. To test for significant changes in atmospheric N deposition, we used piecewise regression to examine break-point timing and slope for annual total inorganic N deposition values from the UMBS NADP station, 1980-2020.

In the case of all tests, we used data transformations as necessary to mitigate non-normality or unequal variances, and set $P<0.05$ as the threshold for accepting test results as statistically significant. In a limited number of cases and in the context of results significant at $P<0.05$, we discuss several results with $P>0.05$ but $P<.0.10$ as marginal trends. We completed t-tests, ANOVAs, and regressions in SigmaPlot 14.0 (SYSTAT Software, San Jose, CA US). We used MetaWin 3.0 (Rosenberg 2022) to analyze Burn Plots soil C data. Data processing and analyses of fungal community composition were completed in R and QIIME.

For Review Only

3. Results

3.1 Ecosystem C stocks and aboveground dynamics over succession- Total ecosystem C stocks in UMBS upland forests increase over 200 years of succession ($P<0.001$), largely due to increases in aboveground biomass ($P<0.001$), which exceed soil as the largest C pool by ~50 years of stand development (Fig. 2a). Smaller C pools also show significant temporal dynamics, including larger standing dead tree C stocks in the 40-80 and 80-120 year age classes ($P<0.001$), larger O+A horizon C stocks in 120-160 and >160 year old stands, and larger DWD ($P<0.001$) and smaller fine root ($P=0.05$) C stocks in >160 year old stands (Appendix S1). As this successional increase in total ecosystem C unfolds, forest composition changes, with short-lived pioneer species giving way to longer-lived deciduous or coniferous taxa (Figure 2b).

Rates of biomass increase (as NPP_w) also vary over succession, with the aspects of canopy structure influencing NPP_w shifting over time (Fig. 3). Early in succession (plots in stands that are 22-48 years old), NPP_w varies nearly four-fold between plots, but this variation is unrelated to structural parameters (multiple regression $P>0.05$). In middle-aged stands (66-84 years old) NPP_w is less variable among plots, and is significantly related (multiple regression $P=0.03$) to canopy height (partial $r^2=0.72$), leaf area index (partial $r^2=0.21$), and, to a lesser extent, canopy rugosity (partial $r^2=0.04$). Old stands (>100 years old) possess the widest between-plot variance in NPP_w, which is significantly related (multiple regression $P=0.02$) to leaf area index ($r^2=0.60$), and to a lesser extent canopy height and rugosity (both partial $r^2<0.05$).

Leaf litterfall data from the flux tower footprints detail the changes in forest composition that occur as pioneer species give way to longer-lived taxa at the close of the first century of succession. In the reference tower footprint where background natural succession is ongoing, a 23-year decline in leaf production by early-successional aspen and birch (Fig. 4A; regression

For Review Only

P<0.001) has been offset by a significant increase by red oak (Fig. 4B; P<0.001), maintaining whole-canopy leaf production at the same level (Fig. 4A; regression P>0.05). Leaf production by maple (primarily *A. rubrum,* secondarily *A. saccharum*) has remained unchanged over this interval (Fig. 4B; regression P>0.05). The 14-year litterfall record for the treatment tower footprint reveals a pattern of compositional change that is functionally similar, but greater in rate and magnitude. There, where the mortality of early-successional taxa was accelerated by stem girdling (Fig. 4A), leaf production by oak and maple both increased significantly (Fig. 4C; P<0.001), albeit threefold more rapidly for oak, based on slope coefficients for the two taxa. Indeed, oak transitioned from being subdominant to maple during the first 5 years of litterfall collections in the treatment footprint, to consistently being the canopy dominant over more recent years.

3.2 Belowground C, soil biogeochemistry, and microbial dynamics over succession- Soil respiration is the largest loss term in the UMBS C budget, and is dominated by emissions during the growing season (Fig. 5). On an annual basis, total soil respiration (Rst) does not vary with successional stage (P=0.29), but marginal decreases in autotrophic (Rsa; P=0.07) and increases in heterotrophic (Rsh; P=0.06) components lead to an overall increase in the proportion of total emissions that are heterotrophic (Figs. 5a, 5b). During the growing season, successional trends in soil respiration are more evident, with Rst (P=0.04) and Rsa (P=0.03) declining with stand age, and Rsh/Rst increasing with stand age (Figs. 5c, 5d). Growing season fine root production, which is unrelated to stand age (Fig. 6a, P=0.22), is in fact a stronger predictor of Rst than stand age itself (Fig. 6b; P<0.01).

Soils data from the Burn Plots chronosequence reveal changes in soil C, biogeochemical, and microbial properties over the course of succession. Categorical meta-analysis of the 5 known

For Review Only

sampling campaigns shows that O horizon C stocks were diminished by the clearcut+burn that established these stands (-29%, bootstrapped confidence interval -14% to -42%), with no temporal trend to imply recovery over the duration of the chronosequence (meta-regression, P=0.74). In contrast to O horizons, topsoils appear to be recovering as stands develop over the course of the chronosequence. Successional trends (Fig. 7a) include increased soil %C (P=0.03) and microbial biomass C (P<0.01), and decreased pH (P=0.03). These trends in turn have biogeochemical consequences, with higher %C and lower pH being linked to higher rates of cellulose-degrading enzyme activity (α-glucosidase; Figs. 7b, 7c; P=0.03).

Across the Burn Plots, successional changes in soil pH, %C, microbial biomass, and α-glucosidase activity are accompanied by significant changes in fungal community composition (Fig. 8; P=0.025). During the initial decades after disturbance, taxa in the EcM Amanitaceae and mixed saprotrophic/EcM Clavariaceae dominate. Stand development progresses through stages dominated by EcM taxa in the Tricholomataceae and Russulaceae, and by a century of succession, the fungal community is dominated by EcM taxa in the Cortinariaceae (Fig. 8; see Appendix S1 for specific taxa). This long-term fungal community shift has been accompanied by the topsoil property changes in Fig. 7, as well as increased moisture and root biomass, and a successional decline in soil NH_4-N availability (Fig. 9; P<0.05). Of all these soil properties, pH, moisture, α-glucosidase activity, root biomass, and NH_4-N availability are most strongly related to shifts in the fungal community over the course of succession on the Burn Plots (Fig. 9).

Patterns from the Burn Plots are informed by two results from other experimental designs that address fungal N cycling and soil C stocks. First, fungal sporocarp analyses from the decadal ^{15}N tracer experiment in the ~110 year old forests of the flux tower footprints reveal that of the four most frequently observed EcM families, sporocarps of taxa in the Cortinariaceae have

For Review Only

477 significantly higher ^{15}N enrichment (Fig. 10; P=0.01). Second, multidecadal soil monitoring in
478 the 1911-origin reference stand adjacent to the Burn Plots demonstrates significant declines in A
479 and E horizon C stocks in the last 30 years in this ~110 year old reference stand (Fig. 11).

480 *3.3 Ecosystem C fluxes and climate forcings*- Two decades of flux tower observations reveal
481 significant changes in whole-ecosystem C fluxes and their environmental drivers (Fig. 12).
482 Ecosystem C uptake (GPP, negative=uptake) has become significantly more negative with time,
483 with no difference in the rate of change between reference and experimentally accelerated
484 succession footprints (Fig. 12a, lower portion). Concurrently, R_{eco} has increased significantly in
485 the reference footprint, but not in the treatment footprint (Fig. 12a, upper portion). In both
486 footprints, WUE has increased concurrently with GPP, with no difference in the rate of increase
487 between footprints (Fig. 12b). In terms of net C balance, NEE has become more negative with
488 time in both footprints, but this increase in net C uptake has been significantly weaker in the
489 background natural succession footprint due to the long-term increase in R_{eco} (Fig. 12c). Over the
490 common period of record, cumulative mean growing season Rst has been significantly larger in
491 the reference footprint than the treatment footprint (P<0.001, Appendix S1).

492 Changes in C and water fluxes observed in the past 15-20 years have been accompanied by
493 ongoing changes in climate and atmospheric deposition over the past 40 years. From 1980 to
494 2020, UMBS became significantly warmer (Fig. 12d) and wetter (Fig. 12e), with increases of
495 +0.25º MAT and +5.0 cm MAP per decade. Over the same period, wet inorganic N deposition
496 declined significantly (-25%; Fig. 12f), primarily since the year 2000.

497 **4. Discussion**

498 *4.1 Synthesis of ecosystem changes over succession*

For Review Only

Our synthesis illustration (Fig. 13) integrates this multitude of ecosystem components, their changes and interactions over the range of timescales and experimental designs at UMBS. This illustration is a simplified representation of results reported above, which are parenthetically referenced in the text below and complemented with UMBS-relevant citations.

Following stand-replacing disturbance on the sandy outwash plains of UMBS, aboveground biomass accumulation is initially rapid and unrelated to canopy structural development (Figs. 2a, 3b, 13a). As stands approach mid-succession, vertical canopy development drives the accumulation of aboveground biomass, which soon exceeds soil as the largest ecosystem C pool (Figs. 2a, 3b). Increases in aboveground biomass C continue later into succession, where between-stand variation in leaf area explains rates of continued increase (Figs. 2a, 3b, 13c).

Stand-replacing disturbance diminishes O horizon C stocks (section 3.2, meta-analysis) for 100 years, but soil C and related soil physicochemical, biogeochemical, and microbial properties begin to recover during the first century of succession. Recovery encompasses increases in A horizon moisture, exchangeable acidity, root and microbial biomass, and Bs horizon pedogenic iron concentrations, and decreases in A horizon pH, base cations, cation exchange capacity, and soil N availability (Figs. 7a, 9, 13a; Nave et al. 2019; White et al. 2004). These soil property changes have functional consequences including increased rates of α-glucosidase activity and a successional increase in the heterotrophic fraction of soil respiration (Figs. 7b, 7c, 5a, 5c, 13a), and are accompanied by long-term shifts in fungal and tree community composition (Figs. 13a, 13b). Over this 100-year timescale, communities shift from being dominated by short-lived aspen and birch with mixed saprotrophic/enzymatically weak EcM fungal communities, to increased representation of longer-lived deciduous trees and fungal communities dominated by EcM taxa in the Cortinariaceae, with known organic matter decomposition abilities (Figs. 2b, 8,

For Review Only

13a, 13b; Bödeker et al. 2014; Kyaschenko et al. 2017). As these compositional shifts unfold over decades, the heterotrophic fraction of total soil respiration increases (Figs. 5a, 5c). After a century of succession, combined O + A horizon C stocks recover from stand-replacing disturbance (Fig. 13c).

By 100 years of succession after stand-replacing disturbance, aspen and birch have begun to die out, at rates that naturally vary according to soil and landform properties, and in the case of the experimental girdling disturbance, have been deliberately accelerated (Figs. 2b, 4a, 13b; Nave et al. 2014). Similar to the Burn Plots but over a shorter timescale, accelerated aspen-birch mortality in the treatment flux tower footprint causes a temporary increase in soil N and an accompanying excursion in fungal community composition, with increased saprotrophic and decreased EcM taxa (Fig. 13b; Castillo et al. 2018; Nave et al. 2011a; 2013; 2014). As aspens die, oak outcompetes maple for canopy gaps and N, especially in the treatment tower footprint, with its EcM associates in the Cortinariaceae proving highly competitive for N (Figs. 4a, 4b, 10, 13ab; Nave et al. 2013). In reference forests where gradual background mortality of aspen and birch is ongoing (i.e., the reference flux tower footprint and the 1911-origin reference stand adjacent to the Burn Plots), soil and total ecosystem respiration increase as surface soil C stocks decline, resulting in a weaker overall C sink than in the experimentally accelerated succession footprint (Figs. 11, 12a top, 13b). In both footprints, GPP and WUE exhibit ongoing increases with mean annual temperature and precipitation (Figs. 12a bottom, 12b, 12d, 12e).

Predictions of C cycling and its drivers through the end of a second century of succession are hindered by the prospects of continued climate change and the unique conditions on which the three old reference forests in our experimental design are found (Fig. 13c). While some of the more robust chronosequence trends may hold into the future, such as long-term aboveground

For Review Only

biomass increases, (Fig. 2a), others are less clear. For example, differences in LAI and NPP_w between the ~130 year old pine-dominated stands on outwash and the ~190 year old hemlock-hardwoods on moraine may be successional trends, or results of unique landform and soil properties (Fig. 13c, Albert and Minc 1987; Nave et al. 2017; 2019; Scheuermann et al. 2018).

4.2 Detailed discussion of ecosystem components

4.2.1 Aboveground wood production and canopy structure- Our finding that the canopy metrics that drive aboveground growth change over the course of succession (Fig. 2) addresses the first of the predictions enumerated at the close of the Introduction. In young stands, canopy structural complexity does increase with age, but it is not the driving force for aboveground growth. Instead, the severity of the stand-establishing disturbance may be a more important determinant of between-stand variation in NPP_w (Scheuermann at al. 2018). Canopy structural control of NPP_w becomes stronger in middle aged stands, evidenced by low residual variance in the structure – NPP_w relationship, and suggests that the rate at which a deeper canopy develops fundamentally constrains NPP_w during this period of rapid vertical growth, possibly involving a tradeoff between vertical growth and lateral crown expansion (i.e., increased LAI). Beyond a century of development, variation in LAI explains the majority of the variance in NPP_w. This may indicate that as rates of overstory tree vertical growth begin to slow with succession, canopy stratification (including the developing understory) becomes more important to whole-canopy photosynthetic C fixation (Murphy et al. 2023).

4.2.2 Soil C – microbial interactions over succession- Soil C stocks and microbial communities were profoundly altered by region-wide stand-replacing disturbances a century ago, but have begun to recover during the century of succession that has unfolded since. The meta-analytic reduction in O horizon C stocks that we report (-29%, section 3.2) falls in the range of losses

For Review Only

reported in meta-analyses of harvest and fire for temperate forest soils generally (Nave et al. 2010; 2011b), but is larger than typical in the Lake States (Nave et al. 2021). This may reflect a compound effect of the second (experimental) cut-and-burn disturbance applied to create each Burn Plot (i.e., chronosequence stand) throughout the 20th century, which is in addition to the landscape-wide cutting and fires that occurred in the latter 19th through early 20th centuries (Gough et al. 2007). In contrast to persistently diminished O horizons, A horizons across the Burn Plots appear to be recovering, with %C, microbial biomass C, and pH showing significant relationships with stand age (Fig. 7a). These results independently confirm a previously reported decrease in topsoil pH across the Burn Plots (Nave et al. 2019), and add mechanistic insight by revealing that as topsoils begin their post-disturbance recovery of acidity and organic matter, the microbial community and its enzymatic functions (Fig. 7b, 7c) follow suit.

4.2.3 Coupled tree-fungal compositional-functional changes- Our synthesis of results from the Burn Plots and FASET reveals that stand-replacing and partial disturbances induce microbial and N cycling responses that are similar in pattern, but different in timescale and magnitude. On the Burn Plots, clearcutting + fire causes soil N availability and nitrophilic fungi (EcM and saprotrophs) to increase abruptly, then decline over 100 years as N-foraging EcM decomposers in the Cortinariaceae rise in dominance (Figs. 8, 9; Birkebak et al. 2013; Bödeker et al. 2014; Chen et al. 2019; Kyaschenko et al. 2017; Nave et al. 2019; White et al. 2004). Similarly, in FASET, the pulse of aspen and birch mortality in the treatment footprint led to a 2-4 year increase in soil N availability relative to the reference footprint, accompanied by a decline in EcM and an increase in saprotrophic fungi (Castillo et al. 2018; Nave et al. 2011a; 2013; 2014). Since that time, EcM fungi and their N uptake have recovered, with taxa in the Cortinariaceae outcompeting taxa in the Amanitaceae, Boletaceae, and Russulaceae for the ecosystem ^{15}N tracer

For Review Only

591 that was applied during the disturbance period (Fig. 10). Based on their strong decomposing
592 enzyme production, the shift in the fungal community towards the Cortinariaceae would seem to
593 favor increased rates of soil C mineralization and CO_2 emission.

594 Successional changes in microbial communities and their functions go hand-in-hand with
595 changes in tree community composition and functioning, addressing our second prediction
596 (coupled aboveground-belowground compositional-functional linkages). Increases in the
597 enzymatically proficient Cortinariaceae may mean that these EcM taxa are increasing the ability
598 of longer-lived hosts (primarily red oak) to access less available forms of soil N (Jorgensen et al.
599 2022; Leduc et al. 2013; Lindahl et al. 2021). Indeed, red oak has outcompeted red maple for soil
600 N during the successional transition out of aspen-birch dominance (Nave et al. 2013), has higher
601 foliar N concentrations (Nave et al. 2009), rates of stomatal conductance, photosynthesis, and
602 sap flux (Gough et al. 2021; Matheny et al. 2017). These acquisitive vs. conservative traits may
603 underpin the multi-decadal trends in canopy production by the two species. Over this period, oak
604 has had the clear competitive advantage (Fig. 4), especially in the treatment footprint, where
605 water and N availability were elevated for 2-4 years following experimentally accelerated aspen
606 mortality (He et al. 2014; Nave et al. 2014). Compared to the aspen they are replacing, however,
607 oak and maple both have lower rates of photosynthesis and stomatal conductance, and lower
608 foliar N concentrations (Gough et al. 2021; Nave et al. 2009). Thus, this successional transition
609 to longer-lived species may have longer-term consequences for functions such as water use, C
610 uptake and respiratory emissions at the ecosystem scale.

611 *4.2.4 Ecosystem C fluxes, net balance, and environmental drivers*- Over the course of succession,
612 compositional change from aspen to longer-lived tree taxa with lower photosynthetic rates would
613 seem to favor reduced whole-canopy GPP. Decades of monitoring in the flux tower footprints

For Review Only

614 shows that the opposite has occurred (Fig. 12). This addresses our third prediction and implies
615 that external forcings, such as warming and wetting, are overriding compositional influences on
616 successional trajectories of C cycling, at least on the uptake side. On the emissions side, the
617 picture is more complex. Respiratory emissions should be decreasing with succession in the
618 tower footprints, because the longer-lived taxa replacing aspen and birch have higher C use
619 efficiency (less C respired per unit C fixed; Gough et al. 2021), and the chronosequences suggest
620 long-term declines in Rst and Rsa with age (Fig. 5). Counter to that prediction, R_{eco} has remained
621 stable in the treatment footprint where composition has changed rapidly over the last decade, and
622 increased in the reference footprint. Some portion of this increase in R_{eco} in the reference
623 footprint has been due to increased Rst emissions, which have been larger than in the treatment
624 footprint in the last 1-2 decades (section 3.3. and Appendix S1). These elevated respiratory
625 losses are consistent with surface soil C stock declines observed over recent decades in the 110
626 year old Burn Plot reference stand, which is in all regards similar to the UMB reference footprint
627 (Fig. 11). Collectively, these patterns imply an overarching, climate-driven increase in
628 respiratory emissions, which is being canceled out in the treatment footprint by rapid
629 successional change to tree taxa with lower specific respiration rates.

630 Though it is unclear whether climate or composition has the stronger influence on its constituent
631 fluxes, the increasing C sink strength (NEE) over time in both footprints indicates that GPP has
632 increased more rapidly than R_{eco} (Fig. 12). This strengthening C sink over the past 1-2 decades of
633 succession has been concurrent with increased WUE in both footprints, due in part to the
634 replacement of aspen and birch with oak and maple, which have higher WUE (Matheny et al.
635 2014). However, similar trends in NEE and WUE are occurring in other humid north temperate
636 forests where compositional change is less likely to be a substantial mechanism, implying a role

For Review Only

637 for broader environmental drivers such as warming, wetting, CO_2 fertilization, and N
638 oligotrophication (Finzi et al. 2020; Groffman et al. 2018; Hollinger et al. 2021; Keenan et al.
639 2013). The key takeaway from this trend is thus much the same as for respiratory emissions:
640 there is evidence for a broader climatic influence on ecosystem C balance and water use, and an
641 influence of successional change in composition. Unfortunately, our experimental design cannot
642 be parse these factors as independent drivers.

643 One factor that may be influencing respiratory emissions at UMBS is non-native earthworms.
644 Most of the earthworm taxa present at UMBS in recent decades have been present since the
645 early- to mid-1900s, but changes in their spatial distribution and community composition have
646 occurred (Crumsey et al. 2014). One of the more notable changes has been the expansion of
647 *Lumbricus terrestris*, which directly consumes and vertically redistributes larger quantities of
648 surface leaf litter than other taxa (Crumsey et al. 2015). On balance, *L. terrestris* and other taxa,
649 including those that consume and redistribute mineral soil organic matter, have a small negative
650 effect on soil C UMBS (Crumsey et al. 2013). This implies that declining soil C stocks and
651 increasing soil and ecosystem respiration is due, in some part, to the activity of these organisms.
652 Overall, earthworm spatial distribution and community structural will likely continue to change
653 over time at UMBS, in a patch dynamic influenced by factors such as road proximity, soil
654 texture, and tree community composition (Crumsey et al. 2014). As these changes unfold,
655 earthworm dietary preferences may interact with forest successional dynamics to affect C cycling
656 outcomes, as maple leaf litter is much preferred, and more quickly consumed, than oak litter
657 (Crumsey et al. 2013).

658 *4.3 Context and broader relevance to north temperate forest ecosystems and their management-*
659 Our study is both representative and unique within the context of its region, in ways that help to

For Review Only

understand its relevance to C cycling in other north temperate forests. In its composition, UMBS is broadly representative, as the aspen-birch cover type is the most extensive at the site and across the broader Laurentian Mixed Forest Province (Nave et al. 2017a; Ruefenacht et al. 2008). In its age, UMBS is unique, as aspen-birch forests tend to be younger because their persistence depends on large-scale disturbance or management that has not occurred at UMBS (Carson et al. 2023; Friedman and Reich 2005). In terms of broader relevance, many of the general patterns that we report here are similar to other empirical studies across the U.S. Lake States, Northeast, and adjacent Canada. These include a strengthening C sink in a maturing forest over recent decades (Finzi et al. 2020; Hollinger et al. 2021), successional increases in ecosystem C stocks that are driven by aboveground biomass (Alban and Perala 1992; Keeton et al. 2011), and long-term recovery of soil properties following disturbance (Poirier et al. 2016; Roy et al. 2021). However, for every one of these general patterns across the region, there are studies that show divergent or more nuanced trends (Arain et al. 2022; Desai et al. 2023; Gao et al. 2018; Prest et al. 2014; Wang et al. 2014). This highlights that even if some successional trends are predictable (e.g., increases in total ecosystem C) and some drivers are known (e.g., leaf area, soil texture), site specifics (e.g., disturbance history, management prescriptions) can still be equally or more important (Ford and Keeton 2017; Hoover 2011; Kern et al. 2021; Latty et al. 2004).

In the north temperate forest literature, the lack of any one consistent successional C trajectory or set of drivers reflects diversity in forest ecosystems, including in the ways that they have been managed or otherwise altered by people. Accepting this diversity and the uncertainty that it introduces into future forest functioning is part of forest management. Of particular note in this context are the many factors we show other than stand age that influence C cycling, and the possibility that these factors can serve as explicit targets for manipulation when C is a

For Review Only

management objective. Managing forests means much more than managing their age, e.g., by clearcutting to restart, or allowing to "mature" by leaving them untouched. Directly and indirectly, managing forests means manipulating structure (above and belowground), composition (plants and microbes), and relationships between ecosystem components, including their functional and biogeochemical outcomes. Taking this ecological view of forest management, and setting aside the notion that forest age is a driver itself, we offer several management applications relevant to north temperate forests.

The most timely management application of our results emerges from the decadal trends in C uptake and emissions in the two flux tower footprints. In the treatment footprint, the intentional killing of over one-third of the live trees has had a paradoxical effect: an increase in C sequestration. There, altering forest composition redistributed resources (access to light, soil N) from resource-demanding to resource-efficient taxa. This action decreased canopy structural complexity—a driver usually positively associated with C sequestration (Gough et al. 2021; Hardiman et al. 2011; Thom and Keeton 2020)—and nonetheless increased C sequestration, implying a greater role for N than light limitation of C uptake. In contrast, in the reference footprint, natural succession towards an older and more structurally complex condition has been accompanied by a weaker increase in C sink strength, due to a concurrent increase in respiratory losses. Collectively, this difference between footprints implies that partial harvests to manipulate composition may be a way to simultaneously increase within-forest C sequestration, while removing C that would otherwise be respired and instead storing it in harvested wood products (Gahagan et al. 2015; Powers et al. 2011). Our results suggest such treatments will be most effective where there is a wide difference in resource efficiency between the dominant trees that are removed, and the codominant or suppressed trees that are released, with greater trait diversity

For Review Only

706 in released species facilitating climate adaptation and C mitigation (Clark and D'Amato 2021;
707 Thom et al. 2021; Wiechmann et al. 2022).

708 Our findings provide a belowground view on the typically aboveground-focused work of
709 managing forests. We show that predictable tree community composition changes over
710 succession are linked to concurrent changes in soil properties and microbial communities.
711 Whether severe and stand-replacing or partial and patchy, disturbances that kill trees accelerate
712 the N cycle and shift the fungal community from low-N EcM fungi that are strong decomposers,
713 to more nitrophilic EcM and saprotrophic fungi. These shifts can be subtle and short-lived, as in
714 the experimental girdling that accelerated succession in FASET, or more persistent, as in the
715 clearcut harvest + fire of the Burn Plots, where fundamental soil properties are still changing
716 many decades later. In both cases, aboveground dynamics (tree growth, community composition)
717 have successional implications for belowground processes, including root production, soil CO_2
718 emissions, and long-term soil C stock changes.

719 The final management consideration of our synthesis emerges from its landscape context. At
720 4,000 ha, UMBS is large enough to host multiple experimental designs on the same kind of
721 "site"—sandy outwash plains—yet also large enough that its landscape holds other ecosystem
722 types where findings from these study sites do not apply. Thus across UMBS and other humid
723 temperate glaciated landscapes with mosaics of mixed hardwood-conifer forests, our results will
724 be most relevant on drier landforms and soils with lower nutrient availability. On more
725 productive landforms and soils, successional patterns and C cycle trajectories may be different,
726 or similar but for different underlying reasons. Drawing management applications from this and
727 other long-term studies will therefore be most effective when disturbances and succession are
728 seen as whole-ecosystem processes, with bottom-up and belowground factors given equal weight

For Review Only

to the plant communities that usually capture the most attention (Barnes et al. 1982). Vegetation treatments to achieve C cycle objectives can then be optimized to the kinds of ecosystems where they are most likely to be effective. For example, our results imply that partial harvests to release codominant or overtopped oak can increase ecosystem C sequestration, but that this outcome is most likely on drought-prone, low-nutrient soils where its water- and N-acquisitive traits make it best suited to capitalizing on release from competition. On more mesic, productive soils, treatments to release maple and capitalize on its high levels of water and C use efficiency may be more effective at increasing C sequestration. Still other management strategies, approaches, and tactics may be needed to balance C with other objectives in other settings. In this way, moving beyond stand-level thinking to landscape management mosaics can diversify the composition, structure, connectivity, climate adaptation capacity, and C management strategies of larger forested areas (Ontl et al. 2020; Thom and Keeton 2020). Ultimately, as climate, disturbance regimes, and species distributions continue to change, management must be conducted in this larger context in order to maintain forest functions- and in some areas, forests at all.

4.4 Key unknowns- Our work struggles with several limitations, and also highlights several areas in need of future research. Its most significant limitation emerges from its greatest strength, in the sense that so many experimental designs and datasets can be brought to bear on so many aspects of the ecosystem at a single site. While this allows for a holistic view of C cycling and its drivers, the lack of consistency in individual studies precludes an elegant, balanced synthetic analysis. The resulting narrative synthesis is as complex as the ecosystem itself, and in simplifying this complexity for clearer communication, we have minimized attention to potential issues such as stand-level variation in disturbance histories and the disconnect between inferences from a 20-year flux record vs. a 200-year chronosequence. The spatial and temporal

For Review Only

752 distribution of past clearcutting and fire at UMBS is more nuanced than we communicate here,
753 and in focusing on what is consistent across disturbance types, we overlook the potential that
754 localized past events may be influencing the results we report (Cooper 1981; D'Amato et al.
755 2017; Farmer 1958; Kilburn 1957). Similarly, we emphasize consistencies, rather than
756 differences between the decadal patterns of succession in the flux tower footprints and the
757 centuries-long continuum of chronosequence and old reference stands. Notably, our NEP
758 estimates over these longer timescales indicate that only one of these stands is definitively a C
759 sink (Clay et al. 2022), a result which is at odds with tower-based observations showing a
760 consistent C sink over time.

761 One of the key unknowns in this study is the degree to which several unaddressed belowground
762 processes and C fluxes vary over successional time. In this work, we are limited to relatively
763 coarse metrics of belowground C cycling, such as soil respiration and fine root production. More
764 detailed investigations of processes such as root exudation, fungal hyphal production, and
765 bacterially-mediated C and nutrient transformations would result in more mechanistic inferences
766 into microbial and biogeochemical drivers of belowground C cycling over succession. This is
767 particularly true for N cycling processes, given the likelihood that this site's strong N limitation
768 will only increase with CO_2 fertilization and N oligotrophication (Groffman et al. 2018).

769 Another key unknown in our study is the broader spatial (and longer-term temporal) relevance of
770 our results pertaining to the ecophysiology and growth trajectories of red oak. The similarity of
771 oak's increase at UMBS and the long-term Harvard Forest AmeriFlux site (Finzi et al. 2020),
772 concurrent with the increasing C sink strength at both sites, implies a potential connection
773 between composition and C cycling functions, not to mention a bright future for oak. In contrast,
774 a recent synthesis of oaks in the context of climate change indicates more complex, and likely

For Review Only

775 negative prospects for the genus. Namely, the same acquisitive traits that have facilitated oak's
776 competitive rise at these humid sites predispose them to decline as warming continues and vapor
777 pressure deficit increases (Novick et al. 2022). Here, there are clear management implications for
778 how drought, pests and pathogens, and C cycling interact in oak forests throughout the East. As
779 climate change and other pressures continue to increase, management interventions such as
780 thinning and prescribed fire may be necessary to support oak persistence, while accepting novel
781 structures, reduced densities, and increased mortality as inevitable (Clark et al. 2022, Isaacson et
782 al. 2023; Refsland et al. 2020). As conditions continue to change, further research will be needed
783 to examine the ecological mechanisms by which management affects composition and C cycling,
784 across a range of structures and successional stages, in oak and other forest types.

785 **Acknowledgements**

786 This work is based on the effort of over 100 researchers who have conducted studies at UMBS
787 over many decades, and to acknowledge each individual is impossible. Individuals who have
788 made especially important contributions to the work presented here include Peter Curtis, John
789 Den Uyl, Renee Kinney, Jim Le Moine, Bob Vande Kopple, Nick Van Dyke, Renee Veresh, and
790 Chris Vogel. Two anonymous referees provided attentive reviews and feedback that improved
791 the manuscript substantially after its initial submission. This work is supported by the National
792 Science Foundation (Award No. DEB-2245670), and funding for the UMBS AmeriFlux core site
793 is provided by the U.S. Department of Energy's Office of Science. Contributions to this work
794 from F.S. were supported in part by the Laboratory Directed Research and Development
795 Program of Oak Ridge National Laboratory, managed by UT-Battelle, LLC, for the U. S.
796 Department of Energy (Project Number 11176).

797

For Review Only

References

Abramoff, R. Z., and A. C. Finzi. 2016. Seasonality and partitioning of root allocation to rhizosphere soils in a midlatitude forest. Ecosphere **7**.

Alban, D. H., and D. A. Perala. 1992. CARBON STORAGE IN LAKE STATES ASPEN ECOSYSTEMS. Canadian Journal of Forest Research-Revue Canadienne De Recherche Forestiere 22:1107-1110.

Albert, D.A., and L. D. Minc. 1987. The natural ecology and cultural history of the Colonial Point red oak stands. University of Michigan Biological Station, Technical Report, 80pp.

Arain, M. A., B. Xu, J. J. Brodeur, M. Khomik, M. Peichl, E. Beamesderfer, N. Restrepo-Couple, and R. Thorne. 2022. Heat and drought impact on carbon exchange in an age-sequence of temperate pine forests. Ecological Processes 11.

Atkins, J. 2022. Initial release of the pcl data package including canopy structural data for 3,118 individual portable canopy lidar transects from 25 sites across North America. doi.org/10.5281/zenodo.6452902.

Atkins, J., G. Bohrer, R. Fahey, B. Hardiman, C. Gough, T. Morin, A. Stovall, N. Zimmerman, and C. Black. 2018. forestr: Ecosystem and Canopy Structural Complexity. Metrics from LiDAR. R package version 1.1. doi.org/10.5281/zenodo.6452902.

Baldrian, P., R. López-Mondéjar, and P. Kohout. 2023. Forest microbiome and global change. Nature Reviews Microbiology 21:487-501.

Barnes B.V., K.S. Pregitzer, T.A. Spies, and V.A. Spooner. 1982. Ecological Forest Site Classification. Journal of Forestry 493-498.

Bates, P. C., C. R. Blinn, and A. A. Alm. 1993. Harvesting impacts on quaking aspen regeneration in northern Minnesota. Canadian Journal of Forest Research-Revue

For Review Only

Canadienne De Recherche Forestiere **23**:2403-2412.

Birdsey, R. A., D. A. DellaSala, W. S. Walker, S. R. Gorelik, G. Rose, and C. E. Ramirez. 2023. Assessing carbon stocks and accumulation potential of mature forests and larger trees in US federal lands. Frontiers in Forests and Global Change **5**.

Birkebak, J. M., J. R. Mayor, K. M. Ryberg, and P. B. Matheny. 2013. A systematic, morphological and ecological overview of the Clavariaceae (Agaricales). Mycologia **105**:896-911.

Bödeker, I. T. M., K. E. Clemmensen, W. de Boer, F. Martin, Å. Olson, and B. D. Lindahl. 2014. Ectomycorrhizal *Cortinarius* species participate in enzymatic oxidation of humus in northern forest ecosystems. New Phytologist **203**:245-256.

Bradford, J. B., and D. N. Kastendick. 2010. Age-related patterns of forest complexity and carbon storage in pine and aspen-birch ecosystems of northern Minnesota, USA. Canadian Journal of Forest Research **40**:401-409.

Castillo, B. T., L. E. Nave, J. M. Le Moine, T. Y. James, and K. J. Nadelhoffer. 2018. Impacts of experimentally accelerated forest succession on belowground plant and fungal communities. Soil Biology & Biochemistry **125**:44-53.

Chen, J., J. Heikkinen, E. A. Hobbie, K. T. Rinne-Garmston, R. Penttilä, and R. Mäkipää. 2019. Strategies of carbon and nitrogen acquisition by saprotrophic and ectomycorrhizal fungi in Finnish boreal *Picea abies*-dominated forests. Fungal Biology **123**:456-464.

Clark, K. L., C. Aoki, M. Ayres, J. Kabrick, and M. R. Gallagher. 2022. Insect infestations and the persistence and functioning of oak-pine mixedwood forests in the mid-Atlantic region, USA. Plos One 17.

Clark, P. W., and A. W. D'Amato. 2021. Long-term development of transition hardwood and<i>

For Review Only

Pinus strobus- Quercus mixedwood forests with implications for future adaptation and mitigation potential. Forest Ecology and Management 501.

Clay, C., L. Nave, K. Nadelhoffer, C. Vogel, B. Propson, J. Den Uyl, L. J. Hickey, A. Barry, and C. M. Gough. 2022. Fire after clear-cut harvesting minimally affects the recovery of ecosystem carbon pools and fluxes in a Great Lakes forest. Forest Ecology and Management **519**.

Cleland, D.T., P.E. Avers, W.H. McNab, M.E. Jensen, R.G. Bailey, T. King, and W.E. Russell. 1997. National hierarchical framework of ecological units. In: Boyce, M.S., and A. Haney (eds.). Ecosystem management: Applications for sustainable forest and wildlife resources. Yale University Press, New Haven, CT, pp. 181-200.

Compton, J. E., R. D. Boone, G. Motzkin, and D. R. Foster. 1998. Soil carbon and nitrogen in a pine-oak sand plain in central Massachusetts: Role of vegetation and land-use history. Oecologia **116**:536-542.

Cooper, A. W. 1981. Aboveground biomass accumulation and net primary production during the first 70 years of succession in *Populus grandidentata* stands on poor sites in northern Lower Michigan. In: West, D. C., Shugart, H. H., and D. B. Botkin (eds.). Forest succession: concepts and application. Springer-Verlag, New York, pp. 339-360.

Crumsey, J. M., Y. Capowiez, M. Goodsitt, S. Larson, J. Le Moine, J. Bird, G. Kling, and K. J. Nadelhoffer. 2015. Exotic earthworm community composition interacts with soil texture to affect redistribution and retention of litter-derived C and N in northern temperate forest soils. Biogeochemistry **126**:379-395.

Crumsey, J. M., J. Le Moine, Y. Capowiez, M. Goodsitt, S. Larson, G. Kling, and K. J. Nadelhoffer. 2013. Community-specific impacts of exotic earthworm invasions on soil

For Review Only

carbon dynamics in a sandy temperate forest. Ecology **94**:2827-2837.

Crumsey J. M., J. Le Moine, C. S. Vogel, and K.J. Nadelhoffer. 2014. Historical patterns of exotic earthworm distributions inform contemporary associations with soil physical and chemical factors across a northern temperate forest. Soil Biology and Biochemistry **68**:503-514.

D'Amato, A. W., D. A. Orwig, D. R. Foster, A. B. Plotkin, P. K. Schoonmaker, and M. R. Wagner. 2017. Long-term structural and biomass dynamics of virgin Tsuga-canadensis-Pinus strobus forests after hurricane disturbance. Ecology 98:721-733.

Davidson, E. A., K. Savage, P. Bolstad, D. A. Clark, P. S. Curtis, D. S. Ellsworth, P. J. Hanson, B. E. Law, Y. Luo, K. S. Pregitzer, J. C. Randolph, and D. Zak. 2002. Belowground carbon allocation in forests estimated from litterfall and IRGA-based soil respiration measurements. Agricultural and Forest Meteorology **113**:39-51.

Desai, A. R., B. A. Murphy, S. Wiesner, J. Thom, B. J. Butterworth, N. Koupaei-Abyazani, A. Muttaqin, S. Paleri, A. Talib, J. Turner, J. Mineau, A. Merrelli, P. Stoy, and K. Davis. 2022. Drivers of Decadal Carbon Fluxes Across Temperate Ecosystems. Journal of Geophysical Research-Biogeosciences **127**.

Eisen, K., and A. B. Plotkin. 2015. Forty years of forest measurements support steadily increasing aboveground biomass in a maturing, Quercus-dominant northeastern forest. Journal of the Torrey Botanical Society **142**:97-112.

Fahey, R. T., J. W. Atkins, C. M. Gough, B. S. Hardiman, L. E. Nave, J. M. Tallant, K. J. Nadehoffer, C. Vogel, C. M. Scheuermann, E. Stuart-Haentjens, L. T. Haber, A. T. Fotis, R. Ricarts, and P. S. Curtis. 2019. Defining a spectrum of integrative trait-based vegetation canopy structural types. Ecology Letters **22**:2049-2059.

For Review Only

Fahey, T. J., T. G. Siccama, C. T. Driscoll, G. E. Likens, J. Campbell, C. E. Johnson, J. J. Battles, J. D. Aber, J. J. Cole, M. C. Fisk, P. M. Groffman, S. P. Hamburg, R. T. Holmes, P. A. Schwarz, and R. D. Yanai. 2005. The biogeochemistry of carbon at Hubbard Brook. Biogeochemistry **75**:109-176.

Farmer, R. E. 1958. Some effects of prescribed burning following clear-cutting in poor site aspen. School of Forestry, University of Michigan, Ann Arbor. M.S. Thesis, 53pp.

Finzi, A. C., M. A. Giasson, A. A. B. Plotkin, J. D. Aber, E. R. Boose, E. A. Davidson, M. C. Dietze, A. M. Ellison, S. D. Frey, E. Goldman, T. F. Keenan, J. M. Melillo, J. W. Munger, K. J. Nadelhoffer, S. V. Ollinger, D. A. Orwig, N. Pederson, A. D. Richardson, K. Savage, J. W. Tang, J. R. Thompson, C. A. Williams, S. C. Wofsy, Z. X. Zhou, and D. R. Foster. 2020. Carbon budget of the Harvard Forest Long-Term Ecological Research site: pattern, process, and response to global change. Ecological Monographs **90**.

Flinn, K. M., and P. L. Marks. 2007. Agricultural legacies in forest environments: Tree communities, soil properties, and light availability. Ecological Applications **17**:452-463.

Ford, S. E., and W. S. Keeton. 2017. Enhanced carbon storage through management for old-growth characteristics in northern hardwood-conifer forests. Ecosphere 8:20.

Forsmark, B., T. Bizjak, A. Nordin, N. P. Rosenstock, H. Wallander, and M. J. Gundale. 2024. Shifts in microbial community composition and metabolism correspond with rapid soil carbon accumulation in response to 20 years of simulated nitrogen deposition. Science of the Total Environment 918.

Gahagan, A., C. P. Giardina, J. S. King, D. Binkley, K. S. Pregitzer, and A. J. Burton. 2015. Carbon fluxes, storage and harvest removals through 60 years of stand development in red pine plantations and mixed hardwood stands in Northern Michigan, USA. Forest

For Review Only

913 Ecology and Management **337**:88-97.
914 Gao, B. L., A. R. Taylor, E. B. Searle, P. Kumar, Z. L. Ma, A. M. Hume, and H. Y. H. Chen.
915 2018. Carbon Storage Declines in Old Boreal Forests Irrespective of Succession
916 Pathway. Ecosystems 21:1168-1182.
917 Gerlach, J. P., D. W. Gilmore, K. J. Puettman, and J. C. Zasada. 2002. Mixed-species forest
918 ecosystems in the Great Lakes region: a bibliography.*in* F. S. U.S. Department of
919 Agriculture, editor. Minnesota Agricultural Experiment Station, St. Paul, MN USA.
920 Goodale, C. L., and J. D. Aber. 2001. The long-term effects of land-use history on nitrogen
921 cycling in northern hardwood forests. Ecological Applications **11**:253-267.
922 Gough, C. M., J. W. Atkins, R. T. Fahey, P. S. Curtis, G. Bohrer, B. S. Hardiman, L. J. Hickey,
923 L. E. Nave, K. M. Niedermaier, C. Clay, J. M. Tallant, and B. Bond-Lamberty. 2022.
924 Disturbance has variable effects on the structural complexity of a temperate forest
925 landscape. Ecological Indicators **140**.
926 Gough, C. M., J. W. Atkins, R. T. Fahey, and B. S. Hardiman. 2019. High rates of primary
927 production in structurally complex forests. Ecology **100**.
928 Gough, C. M., G. Bohrer, and P.S. Curtis. 2023a. AmeriFlux FLUXNET-1F US-UMB Univ. of
929 Mich. Biological Station, Ver. 3-5, AmeriFlux AMP, (Dataset).
930 https://doi.org/10.17190/AMF/2204882
931 Gough, C. M., G. Bohrer, and P.S. Curtis. 2023b. AmeriFlux FLUXNET-1F US-UMd UMBS
932 Disturbance, Ver. 3-5, AmeriFlux AMP, (Dataset).
933 https://doi.org/10.17190/AMF/1881597
934 Gough, C. M., G. Bohrer, B. S. Hardiman, L. E. Nave, C. S. Vogel, J. W. Atkins, B. Bond-
935 Lamberty, R. T. Fahey, A. T. Fotis, M. S. Grigri, L. T. Haber, Y. Ju, C. L. Kleinke, K. C.

For Review Only

Mathes, K. J. Nadelhoffer, E. Stuart-Haëntjens, and P. S. Curtis. 2021. Disturbance-accelerated succession increases the production of a temperate forest. Ecological Applications **31**.

Gough, C. M., C. S. Vogel, B. Hardiman, and P. S. Curtis. 2010. Wood net primary production resilience in an unmanaged forest transitioning from early to middle succession. Forest Ecology and Management **260**:36-41.

Gough, C. M., C. S. Vogel, K. H. Harrold, K. George, and P. S. Curtis. 2007. The legacy of harvest and fire on ecosystem carbon storage in a north temperate forest. Global Change Biology **13**:1935-1949.

Gough, C. M., C. S. Vogel, H. P. Schmid, H. B. Su, and P. S. Curtis. 2008. Multi-year convergence of biometric and meteorological estimates of forest carbon storage. Agricultural and Forest Meteorology **148**:158-170.

Groffman, P. M., C. T. Driscoll, J. Duran, J. L. Campbell, L. M. Christenson, T. J. Fahey, M. C. Fisk, C. Fuss, G. E. Likens, G. Lovett, L. Rustad, and P. H. Templer. 2018. Nitrogen oligotrophication in northern hardwood forests. Biogeochemistry **141**:523-539.

Hardiman, B. S., G. Bohrer, C. M. Gough, C. S. Vogel, and P. S. Curtis. 2011. The role of canopy structural complexity in wood net primary production of a maturing northern deciduous forest. Ecology **92**:1818-1827.

Hardiman, B. S., C. M. Gough, A. Halperin, K. L. Hofmeister, L. E. Nave, G. Bohrer, and P. S. Curtis. 2013. Maintaining high rates of carbon storage in old forests: A mechanism linking canopy structure to forest function. Forest Ecology and Management **298**:111-119.

Hay, T. N., L. A. Phillips, B. A. Nicholson, and M. D. Jones. 2015. Ectomycorrhizal community

For Review Only

structure and function in interior spruce forests of British Columbia under long term fertilization. Forest Ecology and Management 350:87-95.

He, L., V. Y. Ivanov, G. Bohrer, K.D. Maurer, C. S. Vogel, and M. Moghaddam. 2014. Effects of fine-scale soil moisture and canopy heterogeneity on energy and water fluxes in a northern temperate mixed forest. Agricultural and Forest Meteorology **184**: 243-256.

Hobbie, E. A., A. P. Ouimette, E. A. G. Schuur, D. Kierstead, J. M. Trappe, K. Bendiksen, and E. Ohenoja. 2013. Radiocarbon evidence for the mining of organic nitrogen from soil by mycorrhizal fungi. Biogeochemistry 114:381-389.

Hollinger, D. Y., E. A. Davidson, S. Fraver, H. Hughes, J. T. Lee, A. D. Richardson, K. Savage, D. Sihi, and A. Teets. 2021. Multi-Decadal Carbon Cycle Measurements Indicate Resistance to External Drivers of Change at the Howland Forest AmeriFlux Site. Journal of Geophysical Research-Biogeosciences **126**.

Hoover, C. M. 2011. Assessing Seven Decades of Carbon Accumulation in Two US Northern Hardwood Forests. Forests **2**:730-740.

Isaacson, B. N., Y. Yang, M. C. Anderson, K. L. Clark, and J. C. Grabosky. 2023. The effects of forest composition and management on evapotranspiration in the New Jersey Pinelands. Agricultural and Forest Meteorology 339.

Ishii, H. T., S. Tanabe, and T. Hiura. 2004. Exploring the relationships among canopy structure, stand productivity, and biodiversity of temperature forest ecosystems. Forest Science **50**:342-355.

Jörgensen, K., G. Granath, J. Strengbom, and B. D. Lindahl. 2022. Links between boreal forest management, soil fungal communities and below-ground carbon sequestration. Functional Ecology **36**:392-405.

For Review Only

Keenan, T. F., D. Y. Hollinger, G. Bohrer, D. Dragoni, J. W. Munger, H. P. Schmid, and A. D. Richardson. 2013. Increase in forest water-use efficiency as atmospheric carbon dioxide concentrations rise. Nature **499**:324-+.

Keeton, W. S., A. A. Whitman, G. C. McGee, and C. L. Goodale. 2011. Late-Successional Biomass Development in Northern Hardwood-Conifer Forests of the Northeastern United States. Forest Science **57**:489-505.

Kern, C. C., L. S. Kenefic, C. Kuehne, A. R. Weiskittel, S. J. Kaschmitter, A. W. D'Amato, D. C. Dey, J. M. Kabrick, B. J. Palik, and T. M. Schuler. 2021. Relative influence of stand and site factors on aboveground live-tree carbon sequestration and mortality in managed and unmanaged forests. Forest Ecology and Management 493:12.

Kilburn, P. D. 1957. Historical development and structure of the aspen, jack pine, and oak vegetation type on sandy soils in northern Lower Michigan. School of Forestry, University of Michigan, Ann Arbor. Dissertation, 267pp.

Knelman, J. E., E. B. Graham, S. Ferrenberg, A. Lecoeuvre, A. Labrado, J. L. Darcy, D. R. Nemergut, and S. K. Schmidt. 2017. Rapid Shifts in Soil Nutrients and Decomposition Enzyme Activity in Early Succession Following Forest Fire. Forests **8**.

Kyaschenko, J., K. E. Clemmensen, A. Hagenbo, E. Karltun, and B. D. Lindahl. 2017. Shift in fungal communities and associated enzyme activities along an age gradient of managed *Pinus sylvestris* stands. Isme Journal **11**:863-874.

Latty, E. F., C. D. Canham, and P. L. Marks. 2004. The effects of land-use history on soil properties and nutrient dynamics in northern hardwood forests of the Adirondack Mountains. Ecosystems 7:193-207.

Leduc, S. D., E. A. Lilleskov, T. R. Horton, and D. E. Rothstein. 2013. Ectomycorrhizal fungal

For Review Only

succession coincides with shifts in organic nitrogen availability and canopy closure in post-wildfire jack pine forests. Oecologia **172**:257-269.

Leduc, S. D., and D. E. Rothstein. 2010. Plant-available organic and mineral nitrogen shift in dominance with forest stand age. Ecology **91**:708-720.

Lewis, D. B., M. J. Castellano, and J. P. Kaye. 2014. Forest succession, soil carbon accumulation, and rapid nitrogen storage in poorly remineralized soil organic matter. Ecology **95**:2687-2693.

Lindahl, B. D., J. Kyaschenko, K. Varenius, K. E. Clemmensen, A. Dahlberg, E. Karltun, and J. Stendahl. 2021. A group of ectomycorrhizal fungi restricts organic matter accumulation in boreal forest. Ecology Letters **24**:1341-1351.

Lorimer, C. G. 2001. Historical and ecological roles of disturbance in eastern North American forests: 9,000 years of change. Wildlife Society Bulletin **29**:425-439.

Lovett, G. M., C. L. Goodale, S. V. Ollinger, C. B. Fuss, A. P. Ouimette, and G. E. Likens. 2018. Nutrient retention during ecosystem succession: a revised conceptual model. Frontiers in Ecology and the Environment **16**:532-538.

Matheny, A. M., G. Bohrer, C. S. Vogel, T. H. Morin, L. L. He, R. P. D. Frasson, G. Mirfenderesgi, K. V. R. Schäfer, C. M. Gough, V. Y. Ivanov, and P. S. Curtis. 2014. Species-specific transpiration responses to intermediate disturbance in a northern hardwood forest. Journal of Geophysical Research-Biogeosciences **119**:2292-2311.

Matheny, A. M., R. P. Fiorella, G. Bohrer, C. J. Poulsen, T. H. Morin, A. Wunderlich, C. S. Vogel, and P. S. Curtis. 2017. Contrasting strategies of hydraulic control in two codominant temperate tree species. Ecohydrology **10**.

McNab, W.H., D.T. Cleland, J.A. Freeouf, J.E. Keys, G.J. Nowacki, and C.A. Carpenter. 2007.

For Review Only

Description of Ecological Subregions: Sections of the Conterminous United States. USDA Forest Service, Washington, D.C. 80pp.

Murphy, B. A., J. A. May, B. J. Butterworth, C. G. Andresen, and A. R. Desai. 2022. Unraveling Forest Complexity: Resource Use Efficiency, Disturbance, and the Structure-Function Relationship. Journal of Geophysical Research-Biogeosciences 127.

Nave, L. E., K. DeLyser, G. M. Domke, M. K. Janowiak, T. A. Ontl, E. Sprague, B. F. Walters, and C. W. Swanston. 2021. Land use and management effects on soil carbon in US Lake States, with emphasis on forestry, fire, and reforestation. Ecological Applications **31**.

Nave, L. E., P. E. Drevnick, K. A. Heckman, K. L. Hofmeister, T. J. Veverica, and C. W. Swanston. 2017b. Soil hydrology, physical and chemical properties and the distribution of carbon and mercury in a postglacial lake-plain wetland. Geoderma **305**:40-52.

Nave, L. E., C. M. Gough, K. D. Maurer, G. Bohrer, B. S. Hardiman, J. Le Moine, A. B. Munoz, K. J. Nadelhoffer, J. P. Sparks, B. D. Strahm, C. S. Vogel, and P. S. Curtis. 2011a. Disturbance and the resilience of coupled carbon and nitrogen cycling in a north temperate forest. Journal of Geophysical Research-Biogeosciences **116**.

Nave L., C. Gough, and K. Nadelhoffer. 2024. Forest tree, woody debris, root ingrowth, soil respiration and characterization data from long-term research plots for LTREB at the University of Michigan Biological Station. Version 9. Environmental Data Initiative. https://doi.org/10.6073/pasta/b47e7e6f05d6fcd7136c1e28f23e5217 Link last verified 15 February 2024.

Nave, L. E., C. M. Gough, C. H. Perry, K. L. Hofmeister, J. M. Le Moine, G. M. Domke, C. W. Swanston, and K. J. Nadelhoffer. 2017a. Physiographic factors underlie rates of biomass production during succession in Great Lakes forest landscapes. Forest Ecology and

For Review Only

Management **397**:157-173.

Nave, L. E., J. M. Le Moine, C. M. Gough, and K. J. Nadelhoffer. 2019. Multidecadal trajectories of soil chemistry and nutrient availability following cutting vs. burning disturbances in Upper Great Lakes forests. Canadian Journal of Forest Research **49**:731-742.

Nave, L. E., K. J. Nadelhoffer, J. M. Le Moine, L. T. A. van Diepen, J. K. Cooch, and N. J. Van Dyke. 2013. Nitrogen Uptake by Trees and Mycorrhizal Fungi in a Successional Northern Temperate Forest: Insights from Multiple Isotopic Methods. Ecosystems **16**:590-603.

Nave, L. E., J. P. Sparks, J. Le Moine, B. S. Hardiman, K. J. Nadelhoffer, J. M. Tallant, C. S. Vogel, B. D. Strahm, and P. S. Curtis. 2014. Changes in soil nitrogen cycling in a northern temperate forest ecosystem during succession. Biogeochemistry **121**:471-488.

Nave, L. E., E. D. Vance, C. W. Swanston, and P. S. Curtis. 2010. Harvest impacts on soil carbon storage in temperate forests. Forest Ecology and Management **259**:857-866.

Nave, L. E., E. D. Vance, C. W. Swanston, and P. S. Curtis. 2011b. Fire effects on temperate forest soil C and N storage. Ecological Applications **21**:1189-1201.

Nave, L. E., C. S. Vogel, C. M. Gough, and P. S. Curtis. 2009. Contribution of atmospheric nitrogen deposition to net primary productivity in a northern hardwood forest. Canadian Journal of Forest Research **39**:1108-1118.

Novick, K. A., J. A. Biederman, A. R. Desai, M. E. Litvak, D. J. P. Moore, R. L. Scott, and M. S. Torn. 2018. The AmeriFlux network: A coalition of the willing. Agricultural and Forest Meteorology **249**:444-456.

Novick, K., I. Jo, L. D'Orangeville, M. Benson, T. F. Au, M. Barnes, S. Denham, S. L. Fei, K.

For Review Only

Heilman, T. Hwang, T. Keyser, J. Maxwell, C. Miniat, J. McLachlan, N. Pederson, L. X. Wang, J. D. Wood, and R. P. Phillips. 2022. The Drought Response of Eastern US Oaks in the Context of Their Declining Abundance. Bioscience 72:333-346.

Ontl, T. A., M. K. Janowiak, C. W. Swanston, J. Daley, S. Handler, M. Cornett, S. Hagenbuch, C. Handrick, L. McCarthy, and N. Patch. 2020. Forest Management for Carbon Sequestration and Climate Adaptation. Journal of Forestry **118**:86-101.

Palik, B., K. Cease, L. Egeland, and C. Blinn. 2003. Aspen regeneration in riparian management zones in northern Minnesota: Effects of residual overstory and harvest method. Northern Journal of Applied Forestry **20**:79-84.

Pan, Y., J. M. Chen, R. Birdsey, K. McCullough, L. He, and F. Deng. 2011. Age structure and disturbance legacy of North American forests. Biogeosciences **8**:715-732.

Pan, Y. D., R. A. Birdsey, O. L. Phillips, and R. B. Jackson. 2013. The Structure, Distribution, and Biomass of the World's Forests. Pages 593-+ *in* D. J. Futuyma, editor. Annual Review of Ecology, Evolution, and Systematics, Vol 44.

Pastorello, G., C. Trotta, E. Canfora, H. S. Chu, D. Christianson, Y. W. Cheah, C. Poindexter, J. Q. Chen, A. Elbashandy, M. Humphrey, P. Isaac, D. Polidori, A. Ribeca, C. van Ingen, L. M. Zhang, B. Amiro, C. Ammann, M. A. Arain, J. Ardö, T. Arkebauer, S. K. Arndt, N. Arriga, M. Aubinet, M. Aurela, D. Baldocchi,, et al.. 2020. The FLUXNET2015 dataset and the ONEFlux processing pipeline for eddy covariance data. Scientific Data **7**.

Pedro, M. S., W. Rammer, and R. Seidl. 2017. Disentangling the effects of compositional and structural diversity on forest productivity. Journal of Vegetation Science **28**:649-658.

Phillips, R. P., E. Brzostek, and M. G. Midgley. 2013. The mycorrhizal-associated nutrient economy: a new framework for predicting carbon-nutrient couplings in temperate forests.

For Review Only

New Phytologist 199:41-51.

Poirier, V., M. R. Coyea, D. A. Angers, and A. D. Munson. 2016. Silvicultural treatments and subsequent vegetation impact long-term mineral soil biogeochemistry in mixedwood plantations. Forest Ecology and Management 368:140-150.

Powers, M., R. Kolka, B. Palik, R. McDonald, and M. Jurgensen. 2011. Long-term management impacts on carbon storage in Lake States forests. Forest Ecology and Management 262:424-431.

Pregitzer, K. S., and E. S. Euskirchen. 2004. Carbon cycling and storage in world forests: biome patterns related to forest age. Global Change Biology **10**:2052-2077.

Prescott, C. E., and S. J. Grayston. 2013. Tree species influence on microbial communities in litter and soil: Current knowledge and research needs. Forest Ecology and Management **309**:19-27.

Prest, D., L. Kellman, and M. B. Lavigne. 2014. Mineral soil carbon and nitrogen still low three decades following clearcut harvesting in a typical Acadian Forest stand. Geoderma 214:62-69.

Refsland, T., B. Knapp, K. Stephan, and J. Fraterrigo. 2020. Sixty-five years of fire manipulation reveals climate and fire interact to determine growth rates of Quercus spp. Ecosphere 11.

Reich, P. B. 2012. Key canopy traits drive forest productivity. Proceedings of the Royal Society B-Biological Sciences **279**:2128-2134.

Rhemtulla, J. M., D. J. Mladenoff, and M. K. Clayton. 2009. Legacies of historical land use on regional forest composition and structure in Wisconsin, USA (mid-1800s-1930s-2000s). Ecological Applications **19**:1061-1078.

For Review Only

Rosenberg, M. S. 2022 MetaWin v 3.0.8. https://www.metawinsoft.com

Roy, M. E., Y. Surget-Groba, S. Delagrange, and D. Rivest. 2021. Legacies of forest harvesting on soil properties along a chronosequence in a hardwood temperate forest. Forest Ecology and Management 496:10.

Ruefenacht, B., M. V. Finco, M. D. Nelson, R. Czaplewski, E. H. Helmer, J. A. Blackard, G. R. Holden, A. J. Lister, D. Salajanu, D. Weyermann, and K. Winterberger. 2008. Conterminous US and Alaska Forest Type Mapping Using Forest Inventory and Analysis Data. Photogrammetric Engineering and Remote Sensing **74**:1379-1388.

Schaetzl, R. J., S. A. Drzyzga, B. N. Weisenborn, K. A. Kincare, X. C. Lepczyk, K. Shein, C. M. Dowd, and J. Linker. 2002. Measurement, correlation, and mapping of glacial Lake Algonquin shorelines in northern Michigan. Annals of the Association of American Geographers **92**:399-415.

Scheiner, S.M, and J.A. Teeri. 1981. A 53-year record of forest succession following fire in northern Lower Michigan. Michigan Botanist 20: 3-14.

20(1): 3-14. Scheuermann, C. M., L. E. Nave, R. T. Fahey, K. J. Nadelhoffer, and C. M. Gough. 2018. Effects of canopy structure and species diversity on primary production in upper Great Lakes forests. Oecologia **188**:405-415.

Stone, D. M. 2002. Logging options to minimize soil disturbance in the northern Lake States. Northern Journal of Applied Forestry **19**:115-121.

Thom, D., and W. S. Keeton. 2019. Stand structure drives disparities in carbon storage in northern hardwood-conifer forests. Forest Ecology and Management **442**:10-20.

Thom, D., and W. S. Keeton. 2020. Disturbance-based silviculture for habitat diversification: Effects on forest structure, dynamics, and carbon storage. Forest Ecology and

For Review Only

Management **469**.

Thom, D., A. R. Taylor, R. Seidl, W. Thuiller, J. J. Wang, M. Robideau, and W. S. Keeton. 2021. Forest structure, not climate, is the primary driver of functional diversity in northeastern North America. Science of the Total Environment 762.

UMBS. 2024. University of Michigan Biological Station Weather Observations 1980 to Present. https://live-lsa-mfield.pantheonsite.io/dataset/university-michigan-biological-station-weather-observations-1980-present. Link verified 14 June 2024.

Wang, W., J. Xiao, S. V. Ollinger, A. R. Desai, J. Chen, and A. Noormets. 2014. Quantifying the effects of harvesting on carbon fluxes and stocks in northern temperate forests. Biogeosciences 11:6667-6682.

Wardle, D. A., M. Jonsson, S. Bansal, R. D. Bardgett, M. J. Gundale, and D. B. Metcalfe. 2012. Linking vegetation change, carbon sequestration and biodiversity: insights from island ecosystems in a long-term natural experiment. Journal of Ecology **100**:16-30.

White, L. L., D. R. Zak, and B. V. Barnes. 2004. Biomass accumulation and soil nitrogen availability in an 87-year-old Populus grandidentata chronosequence. Forest Ecology and Management **191**:121-127.

Whitney, G. G. 1987. An ecological history of the Great-Lakes forest of Michigan. Journal of Ecology **75**:667-684.

Wiechmann, L. J., M. T. Curzon, and B. J. Palik. 2022. Response of natural tree regeneration to climate adaptation treatments in Pinus resinosa-dominated forests. Forest Ecology and Management 523.

Woodcock, D. W., and A. D. Shier. 2002. Wood specific gravity and its radial variations: the many ways to make a tree. Trees-Structure and Function **16**:437-443.

For Review Only

Yanai, R. D., W. S. Currie, and C. L. Goodale. 2003. Soil carbon dynamics after forest harvest: An ecosystem paradigm reconsidered. Ecosystems **6**:197-212.

For Review Only

Figure Captions

Figure 1. The UMBS landscape. Map shows the locations of plots within the paired chronosequence stands (1x cut+burn and 2x cut+burn) and old reference forests, as well as the US-UMB (reference) and US-UMd (treatment) flux tower plot networks. Shading indicates landscape-level physiography. Inset: UMBS' regional location.

Figure 2. Panel A: Total ecosystem C stocks and their distribution among pools, for plots in both chronosequences and the three old reference forests. Individual plots have been binned into 40-year age classes. Bars are means, errors are standard deviations, and letters denote significant differences between means (Fisher's L.S.D.; overall ANOVA $P<0.001$). See Appendix S1 for statistical test results. **Panel B:** Proportions of total aboveground live tree biomass for three functional tree groups, by 40-year age class (presented for qualitative patterns but not statistically analyzed).

Figure 3. Panel A: NPP_w (mean and standard error) vs. stand age for young (22-48 years), middle-aged (66-84 years), and old (>100 years) stands. **Panel B:** For a multiple regression model for each age category, the proportion of variance in NPP_w explained by individual structural parameters, including leaf area index (LAI; blue), mean maximum canopy height (Max Height; orange), and canopy rugosity as variance of combined vertical and horizontal leaf distributions throughout the canopy (Rugosity; green). The residual (unexplained) variance in each regression model (young, mid, old) is plotted in gray. **Panel C:** Standardized structural parameter values and NPP_w rates for individual plots in young, middle-aged, and old stands. Structural parameters significantly related to NPP_w are indicated with enlarged points and best-fit lines.

For Review Only

Figure 4. Long-term annual leaf litter production in reference and treatment (accelerated succession) tower footprints. Leaf litter production is shown for all vs. only early-successional species (panel A), and for *Q. rubra* vs. *Acer* spp. (panels B, C). Points plotted are means and standard errors for litterfall collections in 10-14 plots per footprint. Best fit lines indicate statistically significant relationships between year and leaf litterfall flux. Note differences in the period of record for reference (1997-2019) vs. treatment (2006-2019) footprints.

Figure 5. Soil CO_2 emissions as a function of stand age. **Panel A:** Annual total soil respiration (RstA) flux and the proportion of the total from heterotrophic sources (Rsh/Rst). **Panel B:** Annual autotrophic (RsaA) and heterotrophic (RshA) soil respiration fluxes. **Panel C:** Growing season total soil respiration (RstGS) flux and the proportion of the total from heterotrophic sources. **Panel D:** Growing season autotrophic (RsaGS) and heterotrophic (RshGS) soil respiration fluxes. Values presented are stand-level means across the 2014-2021 growing seasons. Statistics are for simple linear regression, with best-fit lines added for statistically significant relationships with stand age. In panels A and C, filled circles are Rst fluxes and open circles are Rsh/Rst proportions. In panels B and D, green triangles are Rsa fluxes and purple squares are Rsh fluxes.

Figure 6. Panel A: Growing season fine root production as a function of stand age. **Panel B:** Growing season fine root production vs. annual total soil respiration. Points plotted are stand-level means across all available years of observation; P and r^2 values are for simple linear regression.

Figure 7. Panel A: Relationships between stand age and A horizon properties including total C (%, filled triangles) and microbial biomass C (mg kg^{-1}, open triangles) concentrations, and pH (filled circles). **Panel B:** relationship between A horizon %C and pH. **Panel C:** Relationship

For Review Only

between A horizon pH and α-glucosidase activity. In each panel, r^2 and P values are presented for simple linear regressions relating the individual variables.

Figure 8. Principal coordinates analysis biplot of fungal community dissimilarity across A horizon soil samples from the Burn Plots. Points and ellipses are color-coded according to stand ages (in years, as of 2015 when samples were collected). Ellipses represent 95% confidence intervals for each stand, and vectors represent the top 5 families responsible for community dissimilarity.

Figure 9. Distance based redundancy analysis biplot of fungal community and soil property dissimilarity across A horizon soil samples from the Burn Plots. Points and ellipses are color-coded according to stand ages (in years, as of 2015 when samples were collected). Ellipses represent 95% confidence intervals for each stand, and vectors represent the soil properties that were significantly related to community dissimilarity in a forward stepwise regression model.

Figure 10. ^{15}N signatures of sporocarps collected from ^{15}N-labeled plots in reference and treatment footprints. Plots were labeled with $^{15}NH_4Cl$ in 2010; sporocarps were collected in 2022. Plotted are means and standard errors for 5-15 sporocarps per family, with significant differences ($P<0.05$; Fisher's LSD) between families indicated with letters.

Figure 11. Mineral soil carbon stocks, by genetic horizon, for soil profiles sampled in 1980 and 2009 in an area of unmanipulated 1911-origin reference forest adjacent to the Burn Plots. Plots show means and standard errors; difference of means is significant ($P<0.05$) for A and E horizons.

Figure 12. Panels A-C: Ecosystem C fluxes and water use efficiency, for reference (filled circles) and treatment (open circles) footprints. C fluxes follow eddy-covariance sign

For Review Only

conventions, such that uptake is negative (GPP, NEE) and emissions are positive (R_{eco}). To aid in visualization, timeseries lines connect individual annual values in each plot. Significance of year and treatment are denoted in each panel, with r^2 values provided when only year is significant, and the adjusted R^2 provided when year and treatment are both significant. **Panels D-F:** Mean annual temperature (D), precipitation (E), and bulk inorganic N deposition (F) at UMBS, 1980-2020, with regression P and r^2 values. Climatologic variables are averaged from daily observations from a weather station on the main campus, adjacent to Douglas Lake. Atmospheric deposition data are from the National Atmospheric Deposition Program (UMBS site ID MI09).

Figure 13. Synthesis of ecosystem changes over successional time. The three columns (A, B, C) correspond to the three experimental designs described in section 2.2, which correspond to three semi-discrete developmental phases that collectively span 200 years of succession. Column A shows trends inferred through the paired chronosequences (particularly the Burn Plots) over the first century of stand development. Column B corresponds to FASET, the paired comparison of background reference vs. experimentally accelerated succession footprints, over a 2-decade period from stand age ~90-100. Column C highlights the three old reference forests, with ages ranging from 130 years for the two pine-dominated stands to approximately 200 years in the uneven-aged hemlock-northern hardwoods stand. See section 4.1 for accompanying narrative.

For Review Only

1274 **Figure 1**

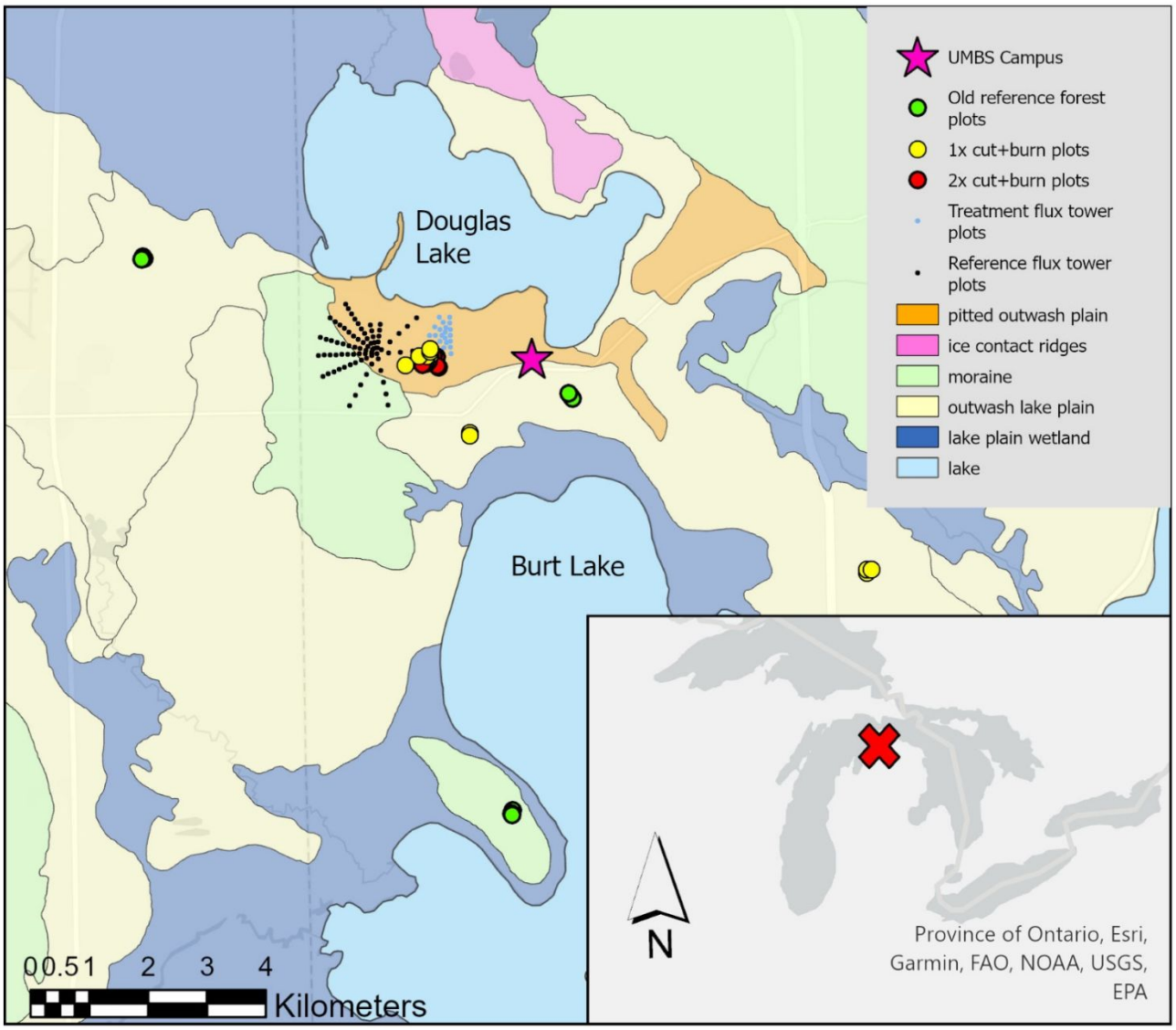

1275

1276

1277

1278

1279

1280

Figure 2

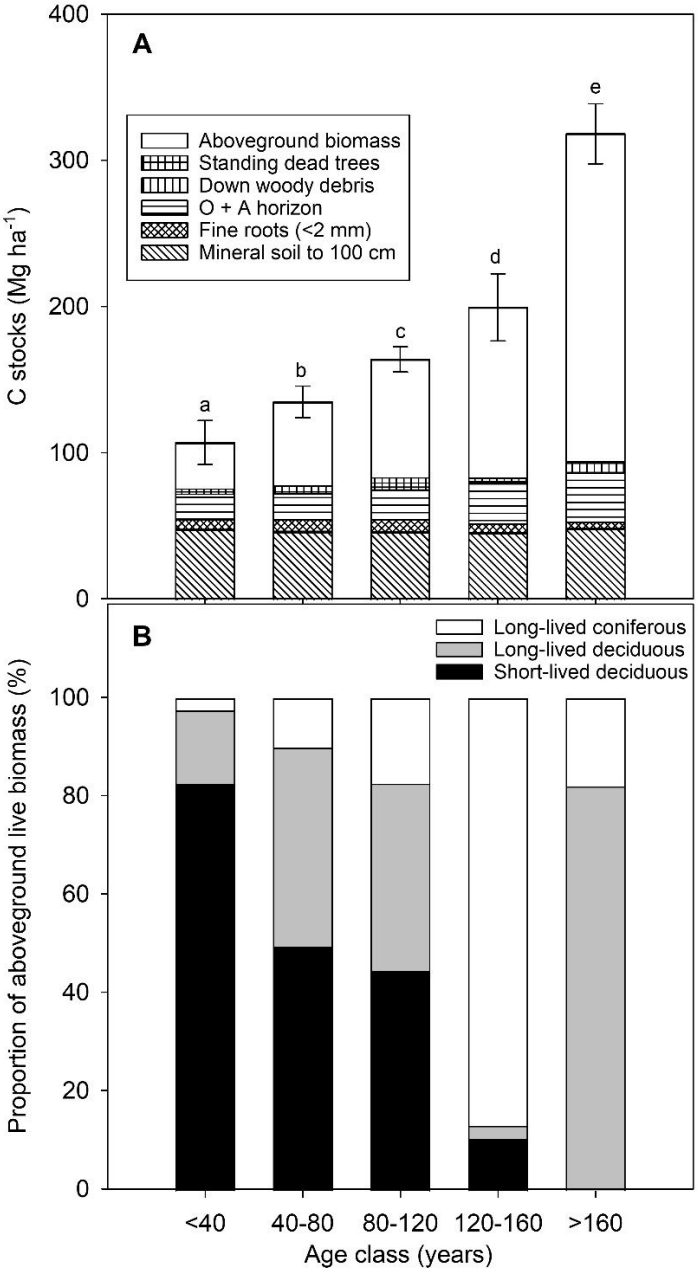

Only

1286 **Figure 3**

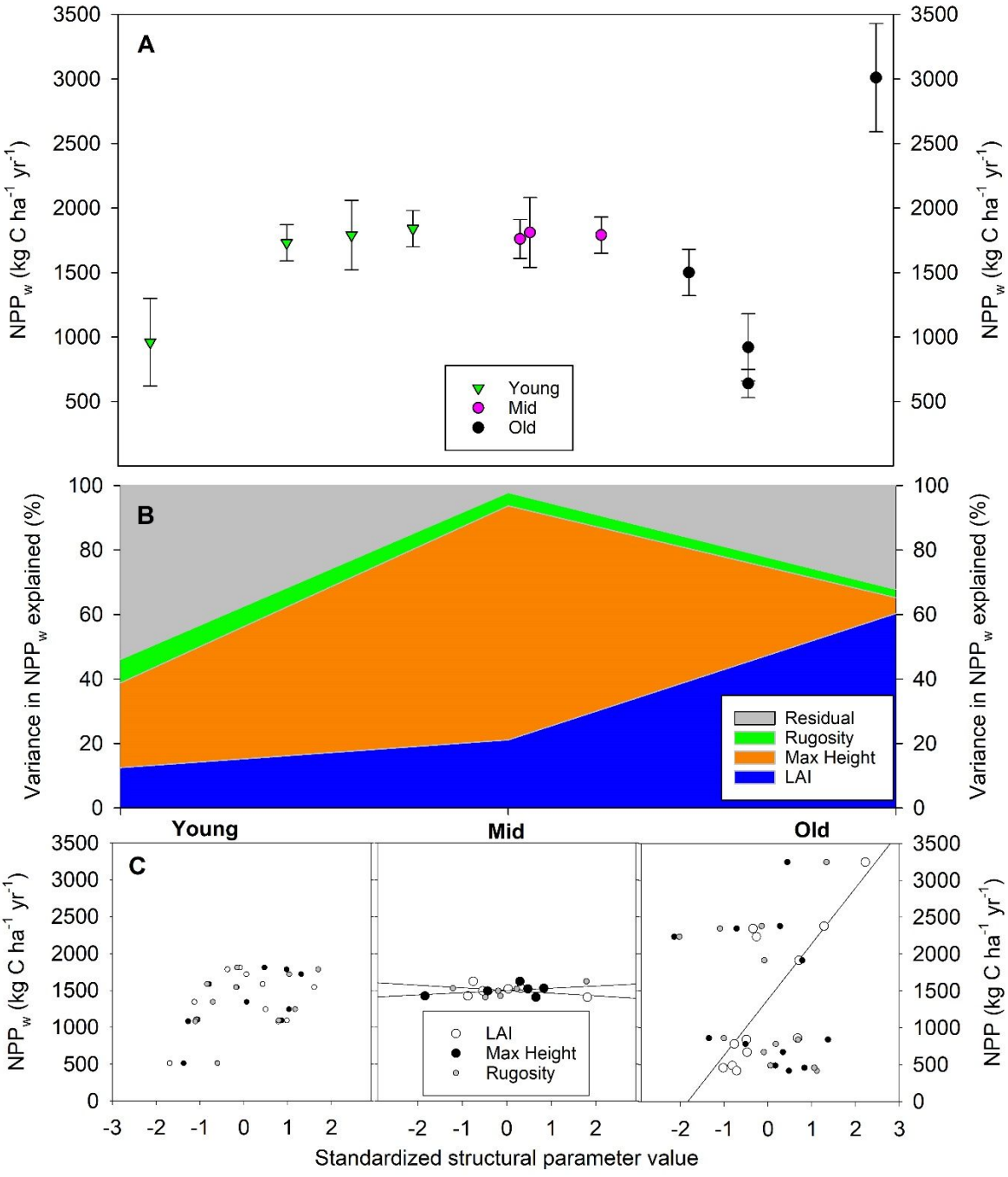

1287

1288

1289

1290 **Figure 4**

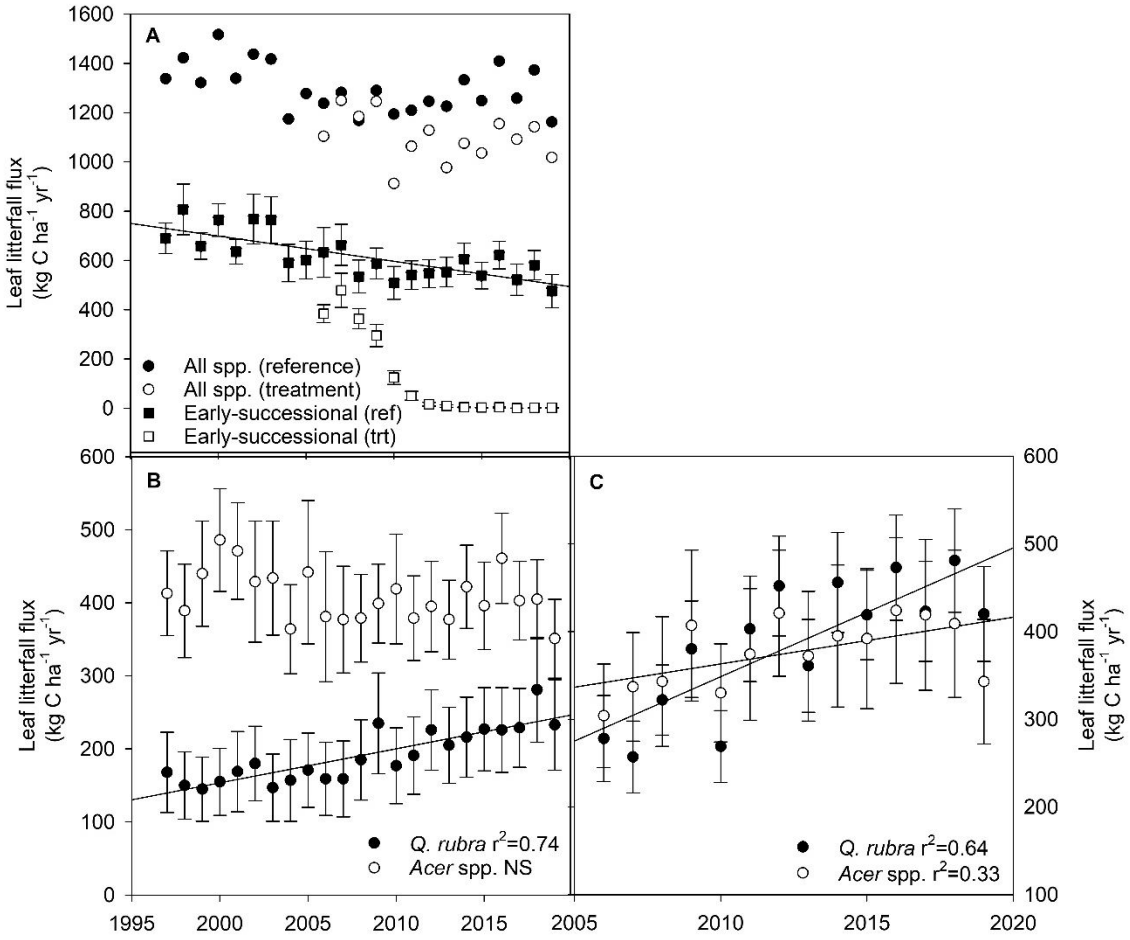

1291

1292

1293

1294

1295

1296

1297

1298

1299 **Figure 5**

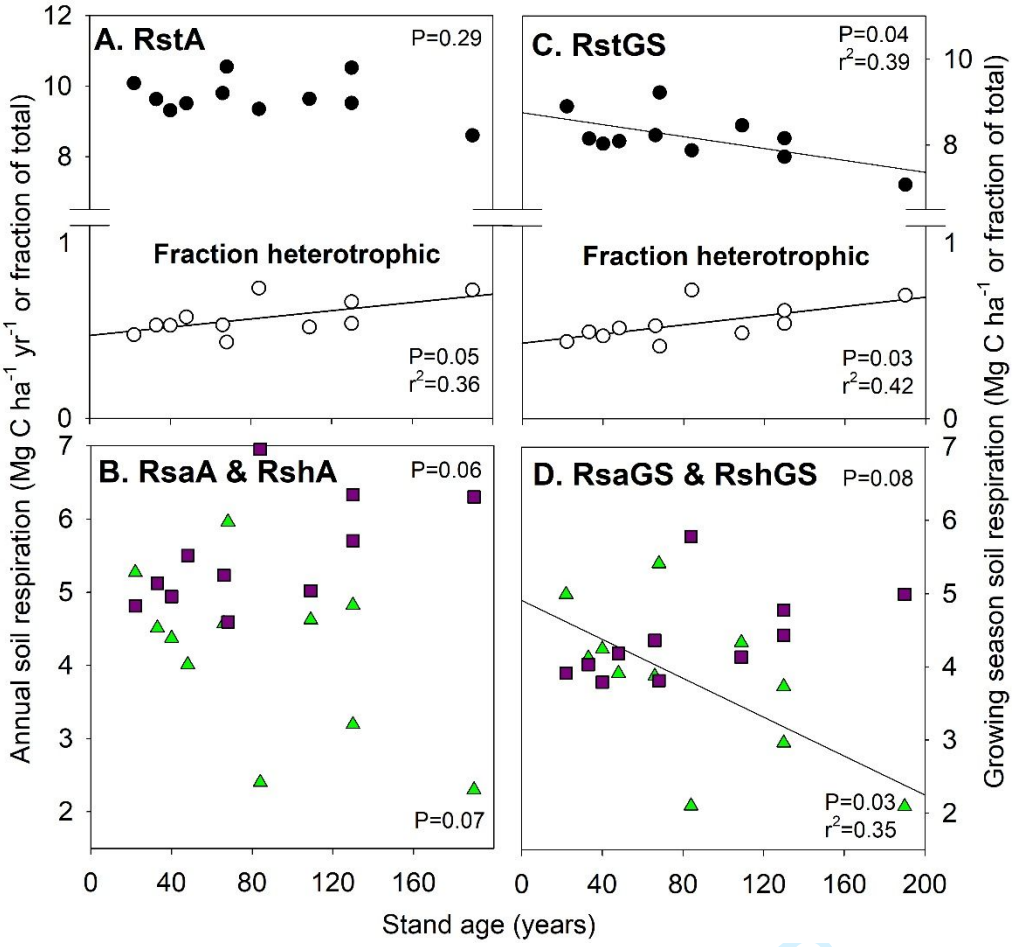

1300

1301

1302

1303

1304

1305

1306

Figure 6

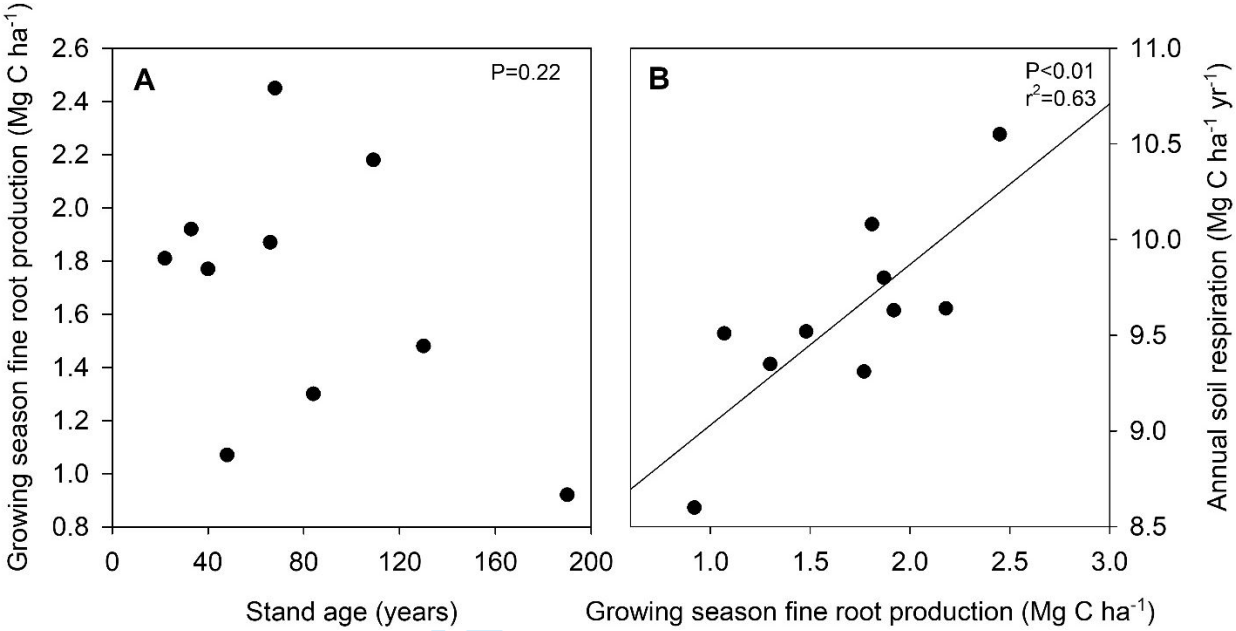

For Review Only

1319 **Figure 7**

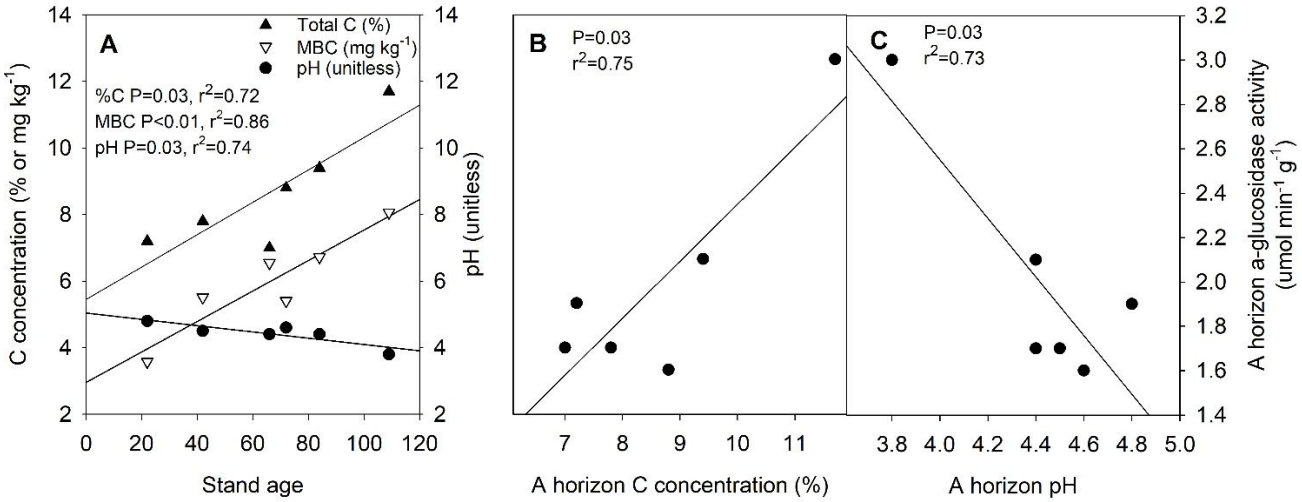

1320

1321

1322

1323

1324

1325

1326

1327

1328

1329

1330

1331

Review Only

1332 **Figure 8**

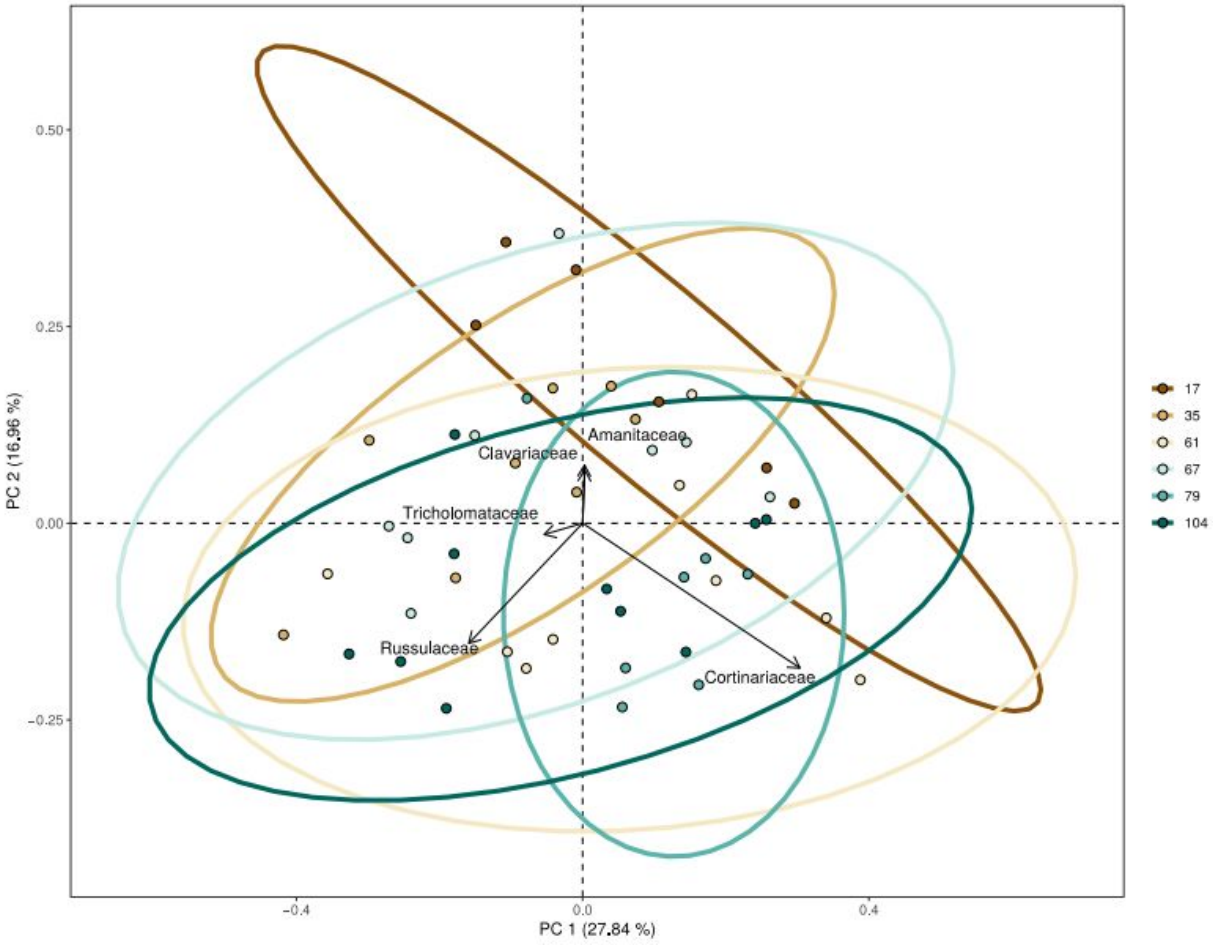

1333

1334

1335

1336

1337

1338

1339

1340 **Figure 9**

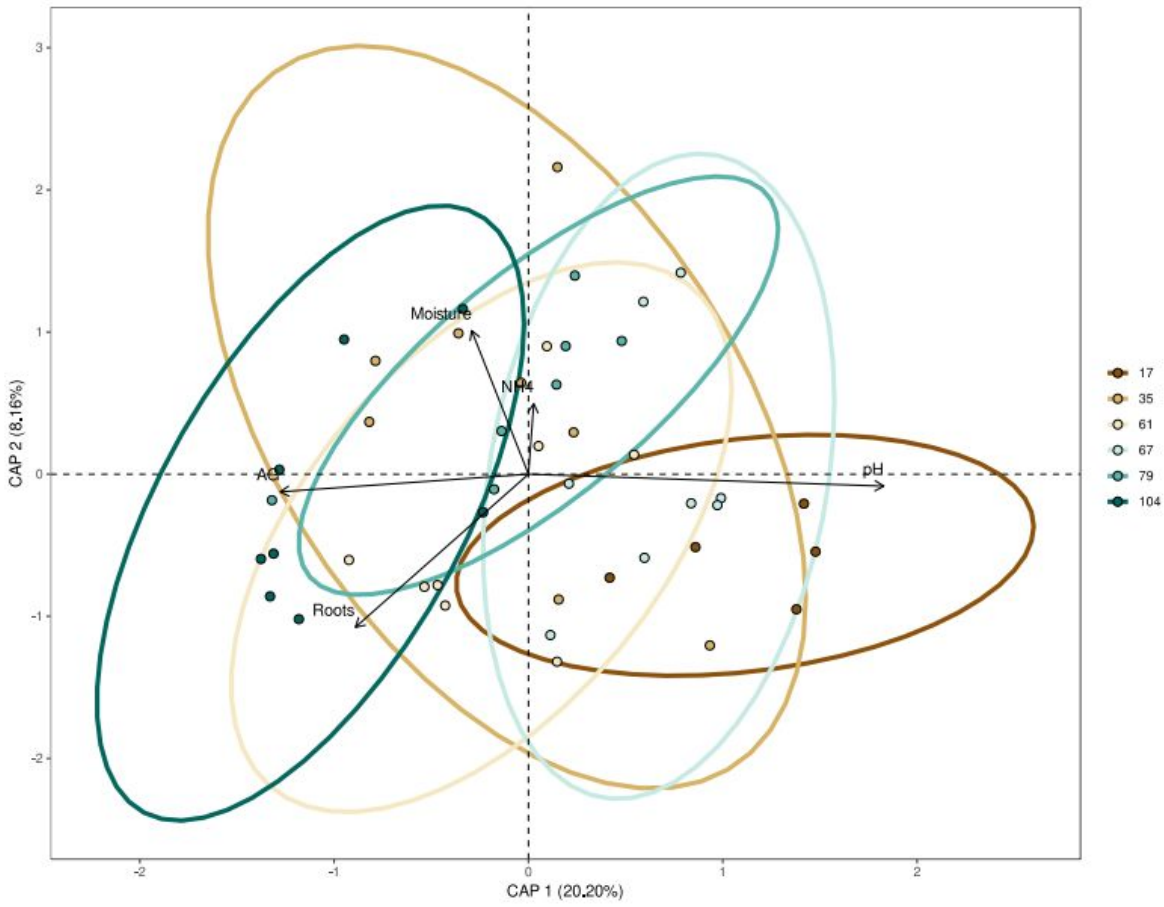

1341

1342

1343

1344

1345

1346

1347

1348

1349 **Figure 10**

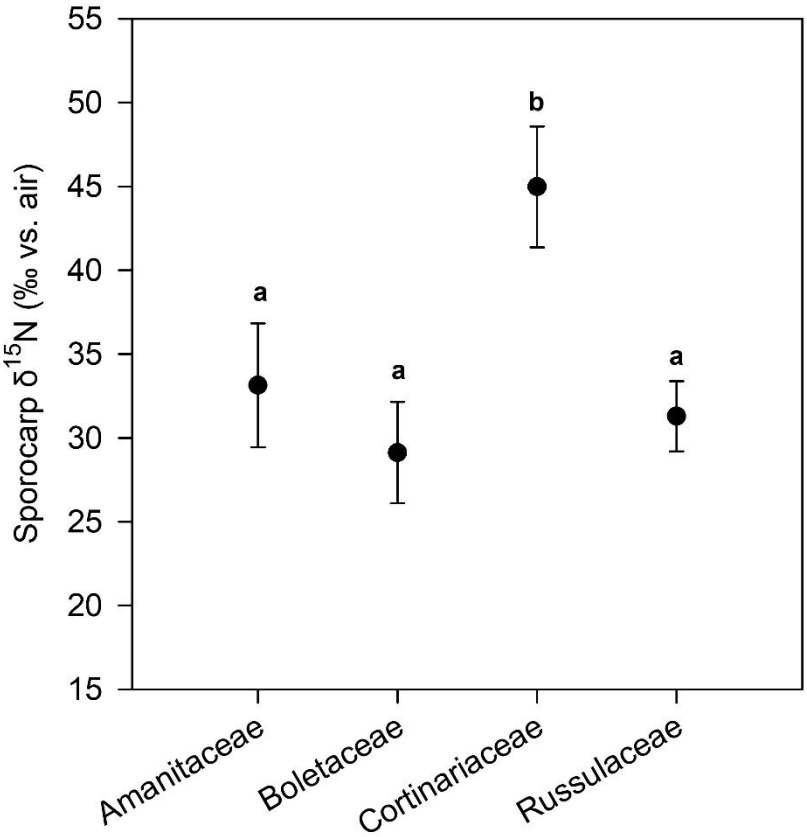

1350

1351

1352

1353

1354

1355

1356

1357

1358 **Figure 11**

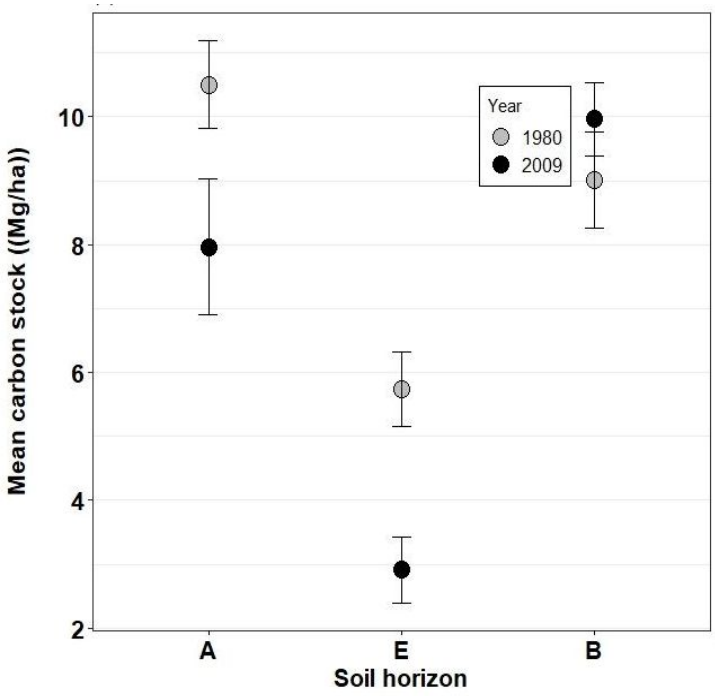

1359

1360

1361

1362

1363

1364

1365

1366

1367

1368

view Only

Figure 12

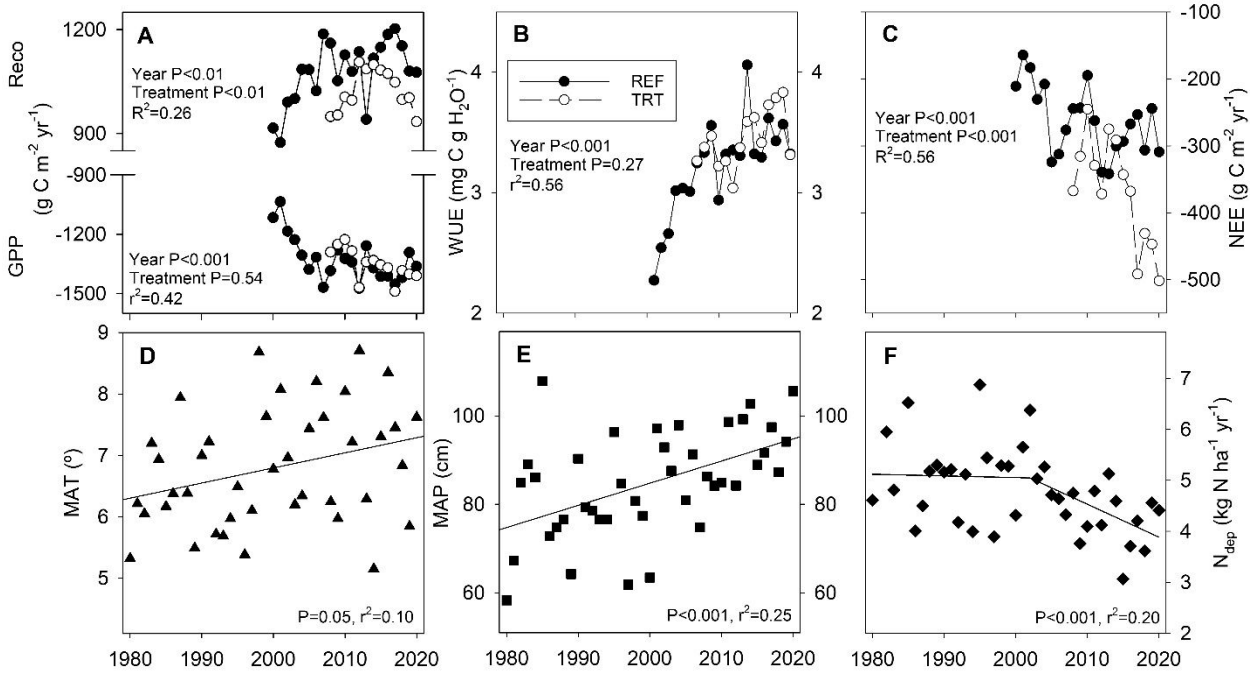

For Review Only

1380 **Figure 13**

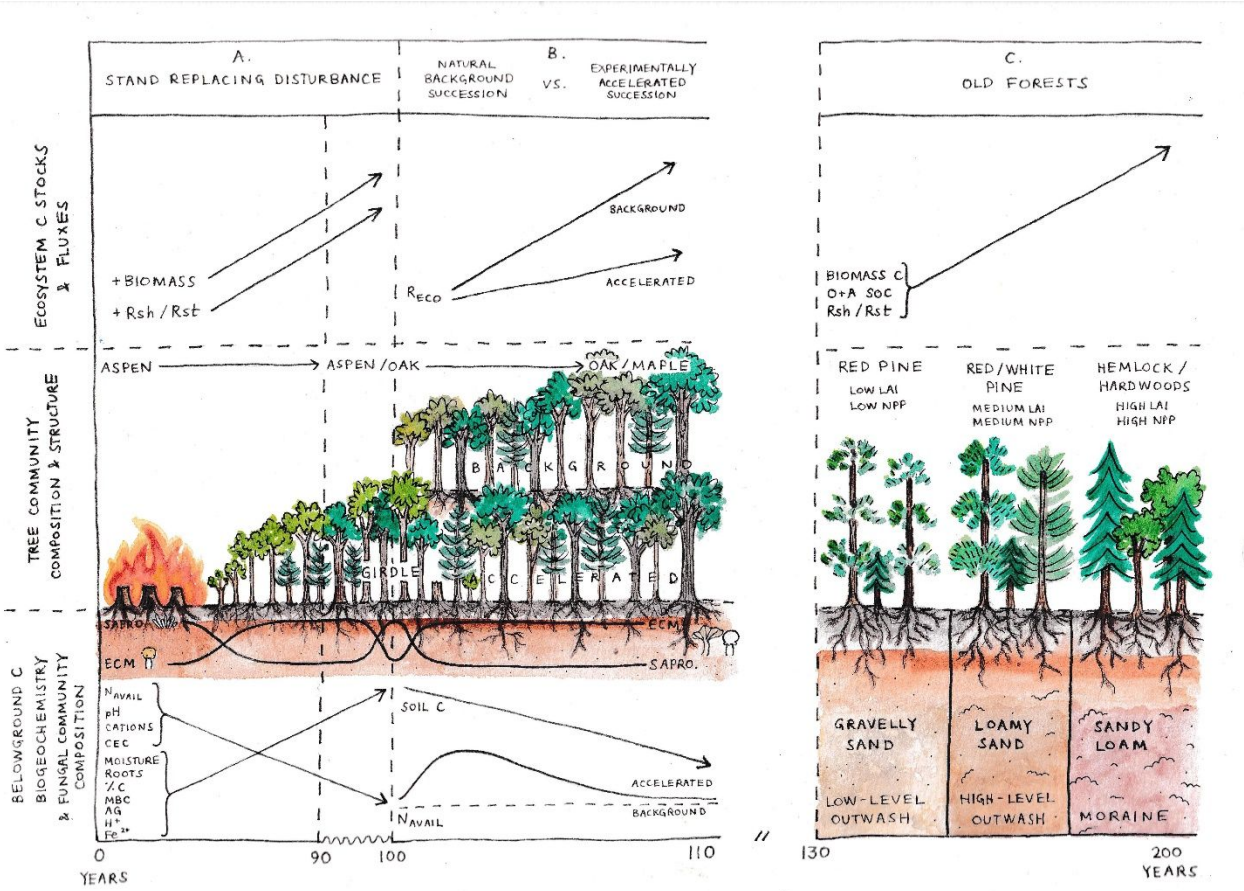

1381

For Peer Review Only

Appendix S1

Lucas Nave, Chris Gough, Cameron Clay, Fernanda Santos, Jeff Atkins, Sonja Benjamins-Carey, Gil Bohrer, Buck Castillo, Robert Fahey, Brady Hardiman, Kathryn Hofmeister, Valeriy Ivanov, Jennifer Kalejs, Ashley Matheny, Angela Menna, Knute Nadelhoffer, Brooke Propson, Adam Schubel, Jason Tallant

Carbon cycling across ecosystem succession in a north temperate forest: controls and management implications. *Ecological Applications.*

1. Detailed Methods

Meta-analysis of organic horizon C stocks across the Burn Plots chronosequence- In order to test for disturbance effects on O horizon C stocks over successional timescales, we synthesized data from 5 known soil sampling campaigns on the Burn Plots, including Schaetzl (1994; sampled 1992), Gough et al. (2007; sampled 2004), and Nave et al. (2019; sampled 2014), and previously unpublished data from collections in 1993 and 2012. The 1993 dataset was collected and documented in a class project (Lehman et al. 1993); the 2012 dataset was collected and documented by a longtime close collaborator to many of the coauthors of this synthesis (Le Moine 2012). Across the five sampling campaigns, frames were used to collect fixed-area O horizon samples, down to the surface of the underlying mineral soil. Fixed-area samples were dried, weighed, ground, and analyzed either for %C (in the case of the three published papers), or, in the case of the unpublished datasets, by loss on ignition, which we multiplied by an assumed C fraction of 0.5 to calculate O horizon C stocks in Mg ha^{-1} as the product of C concentration and dry mass per area. Assuming differences in individual judgment, sampling techniques, and other factors, we chose to use unweighted effect-size meta-analysis to analyze

For Review Only

the data, following the methods of Nave et al. (2021). We computed the response ratio for each experimental treatment stand as its mean O horizon C stock divided by the mean O horizon C stock of the oldest stand in the chronosequence that was sampled at that time. This approach was necessary because individual sampling campaigns sampled different portions of the chronosequence at different times in its history. Collectively, this dataset (Appendix S2) compares chronosequence stands that were 6-56, 18-57, 12-81, 14-76, or 16-78 years old to stands that were 68, 82, 90, 101, or 103 years old when sampled.

Soil respiration scaling- Methods for scaling instantaneous point measurements of Rs to annual and growing season C fluxes in the chronosequence and old reference forest stands are documented in Clay et al. (2022). For scaling point measurements to cumulative fluxes in the tower footprints, where Rs was measured in the 1.1 ha intensive plot surrounding each tower, we first developed temperature-response functions for each footprint (UMB and UMd), utilizing the full span of available Rs measurements (1998-2020 for UMB, 2008-2017 for UMd). These functions were exponential models relating instantaneous Rs to soil temperature, of the form Rs = a * e^(b * Ts), where a and b were footprint-specific parameters and Ts was the simultaneously measured soil temperature at 7.5 cm depth. Next, we used continuous hourly (1998-2006) or half-hourly (2007-present) sensor-based Ts measurements (7.5 cm depth), accessed via AmeriFlux (https://ameriflux.lbl.gov/data/download-data/) to compute cumulative annual Rs efflux, scaled to Mg C ha^{-1} based on collar size and within-plot replication. We only performed these computations for years in which >95% of the Ts data were either measured, or were gap-filled with high confidence (Pastorello et al. 2020). This eliminated 2015-16 from UMB and 2015 from UMd.

For Review Only

Longitudinal sampling of soil C stocks- To assess changes in mineral soil C stocks over recent decades, soil was collected in 1980 and 2009 in an unmanipulated control area adjacent to the Burn Plots. This area consists of 1911-origin forestland that established after the cutting and burning disturbance that was widespread across the UMBS landscape and the wider region. In 1980, a sampling plot with dimensions of 100m x 120m was established, and soils were sampled by genetic horizon (A, E, and Bs1) at sampling points equally spaced along 3 transects. Each soil horizon composite consisted of five individual soil samples collected using a soil corer (0-30cm depth) and at 1-meter radius around each sampling point. In 2009, the same sampling design was implemented approximately 30 m from the perimeter of the 1980 sampling plot. At both campaigns, soils were air-dried and sieved (< 2 mm mesh size), oven dried at 60^{o}C until they reached constant mass, and fine earth bulk densities were measured and used to calculate soil C stocks in Mg C ha^{-1} for each genetic horizon.

Soil biogeochemistry and microbial communities- To characterize long-term successional patterns in soil physicochemical, biogeochemical, microbial properties, we report data from a systematic 2015 sampling campaign on the Burn Plots (Nave et al. 2024). In each Burn Plot (i.e., experimental stand), 5 A horizon samples were collected and composited at each of 3 locations, using a 5.2 cm diameter core, and stored at 4º until processing (within 3 wk). The resulting 3 composite samples per stand were sieved (2mm mesh) to remove rocks and roots from the fine earth fraction. Roots were oven dried at 60º for 24 hours and multiplied by core area to determine root biomass density. Immediately after sieving, the fine earth was subsampled for DNA sequencing, extracellular enzyme activity, microbial biomass C and soil N availability, solid-phase C and N concentrations, pH, and gravimetric water content.

For Review Only

Subsamples for DNA sequencing (2 g) were flash-frozen in liquid nitrogen and stored at -80 C until extraction. Genomic DNA was extracted using a Powersoil DNA Elution Kit (MOBIO, Carlsbad, CA USA), extraction quantity determined using a Qubit Fluorometer (Invitrogen, San Jose, CA, USA) and extracts stored at -80° until amplification. The ITS2 region was amplified using forward primer 5.8S-FUN (5'-AGWGATCCRTTGYYRAAAGTTCCCTGACTGACT) and reverse primer ITS4-FUN (GCAWAWCAAWAAGCGGAGGACCCTGACTGACT). Each subsample had paired forward and reverse barcodes appended to the primer ends for multiplexing. PCR reactions were carried out using Phusion High-Fidelity DNA Polymerase (New England BioLabs, Ipswich, MA) under the following conditions: 5.9ul PCR grade H2O, 4ul 5X Phusion HF Buffer, 0.4ul 10mM dNTP mix, 0.75ul forward primer (10mM), 0.75ul reverse primer (10mM), 8ul DNA template, 0.2ul Phusion Taq. PCR cycle parameters were as follows: 3 min of initial denaturation at 94°, 28 cycles of 30 sec denaturation at 94°, 45 sec annealing at 55°, and 90 sec at 72° with a final extension at 72° for 10 min. PCR products were submitted to the Microbial Systems Molecular Biology Laboratory at the University of Michigan for sequencing and demultiplexing. Sequences were processed using QIIME2 package version qiime2-2019.4. Prior to downstream analysis, forward and reverse reads were analyzed for QC scores in QIIME 2 View. All reverse reads were excluded due to poor quality and only forward reads were used in downstream analyses. Sequences were trimmed for poor quality end reads using denoise-single trimming the first 12 bp and truncating at 245 bp. Sequences were clustered into OTUs at 97% similarity and filtered for chimeras using a vsearch cluster-features-de-novo pipeline. OTUs were then classified using a classifier created from the UNITE database using the classify-sklearn command. A phylogenetic tree was generated with QIIME phylogeny fasttree. The dataset was then filtered for sequences that appeared less than 5 times and fewer than 2

For Review Only

samples with filter-features and rarefied to 6845, representing the minimum sequences total for an individual sample. The most frequent OTUs are presented in Table S1.

For Review Only

Table S1. Fungal OTUs individually accounting for >1% relative abundance of total sequences. Trophic status was assigned to OTUs classified (>97%) at the genus level.

Trophic status	Family	Genus	Species	% relative abundance	Total sequence #
Ectomycorrhizal	Gloniaceae	Cenococcum	*Cenococcum geophilum*	5.7	35496
Ectomycorrhizal	Cortinariaceae	Cortinarius	*Cortinarius alpinus*	5.4	33752
Ericoid mycorrhizal	Helotiaceae	Meliniomyces	*Meliniomyces bicolor*	3.3	20523
Ectomycorrhizal	Russulaceae	Lactifluus	*Lactifluus allardii*	3.1	19456
Ectomycorrhizal	Amanitaceae	Amanita	*Amanita brunnescens*	2.9	18217
Ectomycorrhizal	Cortinariaceae	Cortinarius	*Cortinarius caperatus*	2.8	17664
Unidentified	Russulaceae	unidentified	*unidentified*	2.7	17104
Ectomycorrhizal	Hydnangiaceae	Laccaria	*unidentified*	2.3	14509
Ectomycorrhizal	Atheliaceae	Piloderma	*Piloderma bicolor*	2.0	12364
Ectomycorrhizal	Cortinariaceae	Cortinarius	*unidentified*	1.6	9770
Unidentified	unidentified	unidentified	*unidentified*	1.4	8716
Endophytic	Umbelopsidaceae	Umbelopsis	*Umbelopsis dimorpha*	1.3	8379
unidentified	unidentified	unidentified	*unidentified*	1.3	8055
Ectomycorrhizal	Russulaceae	Russula	*unidentified*	1.3	7883
Ectomycorrhizal	Cortinariaceae	Cortinarius	*Cortinarius cruentiphyllus*	1.2	7590
unidentified	Russulaceae	unidentified	*unidentified*	1.2	7487
Saprobic	Omphalotaceae	Rhodocollybia	*Rhodocollybia butyracea*	1.2	7273
Ectomycorrhizal	Cortinariaceae	Cortinarius	*Cortinarius leiocastaneus*	1.1	6763
Saprobic	Clavariaceae	Clavulinopsis	*Clavulinopsis laeticolor*	1.1	6749
unidentified	Herpotrichiellaceae	unidentified	*unidentified*	1.1	6580
Ectomycorrhizal	Cortinariaceae	Cortinarius	*Cortinarius alboviolaceus*	1.1	6537
Ectomycorrhizal	Cantharellaceae	Craterellus	*Craterellus tubaeformis*	1.0	6378

For Review Only

Soil extracellular enzyme activity, microbial biomass C, and available N determinations followed standard methods. For extracellular enzyme activity (Sinsabaugh and Linkins 1990), three 1 g subsamples from each fine earth sample were extracted in 125 mL of 50mM sodium acetate buffer (pH 5) and α-glucosidase activity was measured after a 4-hour incubation with 4-nitrophenyl a-D-glucopyranoside on a Biotek ELX800 plate reader (Biotek, Winooski, VT, USA). For microbial biomass C (Wu et al. 1990), two 4g subsamples from each fine earth sample were weighed into 15ml polypropylene vials. One subsample was extracted while the other was placed in a sterilized 125 ml Erlenmeyer flask with ~20 boiling chips and 75 ml of ethanol-free chloroform in a desiccator for 48 hours. Both subsamples were extracted for 1 hour with 0.1 M K2SO4 (5:1 solution: soil ratio) on a shaker table (180 strokes per minute). Extracts were filtered, mixed with 15 ml of sodium hexametaphosphate and 2% potassium persulfate, and analyzed for total organic C (TOC) on a Seal AA3 autoanalyzer. Microbial biomass C was calculated as the difference in TOC between non-fumigated and fumigated soils. Soil available N was measured on a 3 g subsample of fine earth as [NH4-N], following extraction with 30 mL of 2 M KCl and quantitation on a Seal AA3 autoanalyzer according to U.S. EPA method 350.1. Concentrations of TOC and NH4-N were scaled to an oven-dry soil basis (mass per mass) using the relevant volumes of extractants and reactants, measured masses of extracted subsamples, and gravimetric moisture content. Alpha glucosidase activity rates were scaled to the quantity of substrate consumed per unit time per mass of soil.

Fine earth subsamples prepared for pH (~5 g, 1:1 soil:water slurry) were measured using a model 8000 pH meter (VWR Scientific, Radnor, PA, USA), and gravimetric moisture content and %C after lyophilization (5 g), with elemental analysis on a Costech ECS 4010 elemental analyzer in the UMBS Analytical Laboratory. The UMBS Analytical Laboratory also housed a Finnigan

For Review Only

Delta V isotope ratio mass spectrometer, which was used to analyze the ^{15}N signatures of ectomycorrhizal (EcM) fungal sporocarps collected in July 2022 from paired plots (n=6 plots) in the reference and treatment flux tower footprints that received ^{15}N tracer additions in 2010 (Nave et al. 2013). We analyzed these fungal samples in order to assess long-term N foraging of several EcM fungal families well represented in Table S1, using ^{15}N-enrichment as an indicator.

Climatology and atmospheric deposition- Daily climatology measurements and weekly atmospheric deposition collections have occurred since the late 1970s on the main "campus" of UMBS, situated on the south shore of 1,700 ha Douglas Lake. The weather station is not inspected by the National Weather Service cooperative network but meets the design standards of its installations, with daily maximum and minimum air temperatures at 2 m height recorded on maximum and minimum Liquid In Glass thermometers, inside a Cotton Region Shelter. Daily water-equivalent precipitation is measured at the UMBS National Atmospheric Deposition Program (NADP) site (site MI09, 45.5608, -84.6783) via a Belfort Universal Precipitation Gage 5-780 (July 1, 1979 to January 7, 2020) or an ETI NOAH IV Total Precipitation Gauge (January 8, 2020 to present). In this paper we present mean annual temperatures as the averages of daily maximum and minimum values, and mean annual precipitation as the sum of daily water-equivalent values. Wet atmospheric deposition is collected weekly in an open field with an Aerochem Metrics Precipitation Collector according to standard NADP protocols (National Trends Network 2019). Weekly samples were mailed to the Central Analytical Laboratory at the University of Illinois (July 1979 to February 2018) or the University of Wisconsin State Lab of Hygiene (March 2018 to present) for analysis. In this paper we accessed NADP National Trends Network data to present annual total inorganic N deposition in kg N ha^{-1} yr^{-1}.

For Review Only

148 *Data analysis*- The results presented in this study are based on community-standard approaches
149 and tests. In most analyses, we used chronosequence stands or flux tower plots as the
150 experimental units, e.g., to test for changes in C pools over time, or to quantify relationships
151 between C fluxes and drivers. For some analyses aimed at uncovering more mechanistic
152 relationships, spatial variation within chronosequence stands facilitated the use of individual
153 plots as experimental units. To analyze tower-based fluxes, we treated the two footprints as
154 experimental units. Table S2 provides, for each relationship tested using inferential statistics,
155 information about which units of observation were treated as the experimental units, the response
156 and predictor variables used in the statistical test, and information about the statistical test. This
157 tabular detail is offered as supplementary to the data analysis section (2.4) and results narrative
158 (section 3) of the main paper. After table S2, further detail is provided in section 2 of this
159 Appendix in the form of statistical test outputs.
160
161
162
163
164
165
166
167
168

For Review Only

Table S2. Summary of relationships tested using inferential statistics.

Relationship	Experimental Units	Response Variable	Predictor Variable(s)	Test	Additional Notes
Ecosystem C vs. stand age	Individual plots in each chronosequence & old reference stand, binned into 40-yr age classes	Individual pool & total ecosystem C stocks	Age class	ANOVA	ANOVA of C stock in each pool, by plot (n=30 total)
Canopy structure vs. C uptake	Individual plots in each chronosequence & old reference stand	Wood NPP	LAI, canopy height, rugosity	multiple linear regression	One regression each for young (22 - 48 yr), middle (66-84), & old (>100) stands. Predictor variables standardized (subtract from mean, divide by stdev) prior to analysis. Predictive capacity of individual variables assessed by partial r^2 values.
Leaf production over time, by taxon	Individual plots in reference and treatment tower footprints	Annual leaf litterfall flux	Year, footprint, taxon	simple linear regression	Separate regressions for each species, genus, or functional group and footprint
Soil respiration vs. stand age	Individual chronosequence & old reference stands	Rst, Rsa, Rsh, Rsh/Rst	Stand age	simple linear regression	Separate regressions for annual and growing season means for each response variable
Fine root production, stand age, and soil respiration	Individual chronosequence & old reference stands	Growing season root production; annual Rst	Stand age; growing season root production	simple linear regression	Two separate regressions, all values averaged across all available years of observation

For Review Only

Table S2 continued.

Relationship	Experimental Units	Response Variable	Predictor Variable(s)	Test	Additional Notes
O horizon C stocks vs. stand age	Individual chronosequence stands	O horion C stock	Treatment, Stand age	unweighted meta-analysis	Categorical meta-analysis to test for disturbance effect; tested for significant temporal pattern with continuous meta-analysis
Soil properties vs. stand age	Individual chronosequence stands	%C, microbial biomass C, and pH	Stand age	simple linear regression	A horizons, data from 2x cut+burn stands only, sampled in 2015
Soil enzymes vs. properties	Individual chronosequence stands	α-glucosidase activity rate	%C, pH	simple linear regression	A horizons, data from 2x cut+burn stands only, sampled in 2015
Fungal community composition vs. stand age	Soil samples from individual chronosequence stands	Bray-Curtis community dissimilarity	principal coordinate axes	Principal coordinates analysis	Mantel test of significant differences in community dissimilarity across stand ages
Fungal community composition vs. stand age and soil properties	Soil samples from individual chronosequence stands	Distance-based dissimilarity values	pH, %C, %N α-glucosidase, NH4, soil moisture, fine root biomass	dbRDA, forward stepwise regression	Forward stepwise regression to identify significant predictors of variation in community dissimilarity

For Review Only

Table S2 continued.

Relationship	Experimental Units	Response Variable	Predictor Variable(s)	Test	Additional Notes
Fungal N foraging and competition	Individual plots in reference and treatment tower footprints	Sporocarp 15N enrichment	EcM family	ANOVA	ANOVA of 15N values of bulk sporocarps in each family from each plot
Soil C stock change in recent decades	Individual soil profiles from common control area	A, E, B horizon C stocks	Year, Horizon	2-way ANOVA	Samples collected in 1980 vs. 2009, within 30 m distance of each other, processed and analyzed using common methodology.
C uptake and losses	Reference and treatment tower footprints	Annual GPP, Reco, NEE	Year, treatment	multiple linear regression	One regression for each response variable, with year (continuous) and treatment (dummy) as predictors
Canopy water use efficiency	Reference and treatment tower footprints	Growing season WUE	Year, treatment	multiple linear regression	Year (continuous) and treatment (dummy) as predictors
Climate change	Weather station	MAT, MAP	Year	simple linear regression	Simple linear regressions to test for significant slope (change) in climate variables over time
N deposition over time	NADP station	Total inorganic N	Year	piecewise regression	Regression to test for significant change in N deposition over time

For Review Only

2. Statistical output

This section provides the output of the statistical tests underpinning each of the figures in the main manuscript, except for Figures 8 and 9. Data and code (QIIME) for the statistical analyses underlying those figures are in Nave et al (2024).

Figure 2a: Ecosystem C stocks vs. stand age

One Way Analysis of Variance Wednesday, February 06, 2019, 11:52:08 AM

Data source: Data 3 in C pools stats

Dependent Variable: Total ecosystem (Mg C ha-1)

Normality Test (Shapiro-Wilk) Passed (P = 0.751)

Equal Variance Test: Passed (P = 0.400)

Group Name	N	Missing	Mean	Std Dev	SEM
<40	8	0	106.927	19.231	6.799
40-80	9	0	134.753	10.911	3.637
80-120	3	0	163.911	7.137	4.121
120-160	6	0	199.419	24.362	9.946
>160	3	0	318.182	14.476	8.358

Source of Variation	DF	SS	MS	F	P
Between Groups	4	112530.034	28132.509	96.045	<0.001
Residual	24	7029.862	292.911		
Total	28	119559.896			

The differences in the mean values among the treatment groups are greater than would be expected by chance; there is a statistically significant difference (P = <0.001).

Power of performed test with alpha = 0.050: 1.000

All Pairwise Multiple Comparison Procedures (Fisher LSD Method):

Comparisons for factor: **Age class**

Comparison	Diff of Means	LSD(alpha=0.050)	P	Diff >= LSD
>160 vs. <40	211.254	23.914	<0.001	Yes
>160 vs. 40-80	183.428	23.549	<0.001	Yes
>160 vs. 80-120	154.271	28.841	<0.001	Yes
>160 vs. 120-160	118.762	24.977	<0.001	Yes
120-160 vs. <40	92.492	19.077	<0.001	Yes
120-160 vs. 40-80	64.666	18.617	<0.001	Yes
120-160 vs. 80-120	35.509	24.977	0.007	Yes
80-120 vs. <40	56.983	23.914	<0.001	Yes
80-120 vs. 40-80	29.158	23.549	0.017	Yes
40-80 vs. <40	27.826	17.164	0.003	Yes

For Review Only

One Way Analysis of Variance Wednesday, February 06, 2019, 11:46:14 AM

Data source: Data 2 in C pools stats

Dependent Variable: Live biomass total (Mg C ha-1)

Normality Test (Shapiro-Wilk) Passed (P = 0.426)

Equal Variance Test: Passed (P = 0.322)

Group Name	N	Missing	Mean	Std Dev	SEM
<40	8	0	31.979	8.593	3.038
40-80	9	0	57.849	8.559	2.853
80-120	3	0	81.212	3.850	2.223
120-160	6	0	117.000	14.595	5.958
>160	3	0	224.343	18.597	10.737

Source of Variation	DF	SS	MS	F	P
Between Groups	4	93392.159	23348.040	193.936	<0.001
Residual	24	2889.372	120.390		
Total	28	96281.531			

The differences in the mean values among the treatment groups are greater than would be expected by chance; there is a statistically significant difference (P = <0.001).

Power of performed test with alpha = 0.050: 1.000

All Pairwise Multiple Comparison Procedures (Fisher LSD Method):

Comparisons for factor: **Age class**

Comparison	Diff of Means	LSD(alpha=0.050)	P	Diff >= LSD
>160 vs. <40	192.363	15.331	<0.001	Yes
>160 vs. 40-80	166.494	15.097	<0.001	Yes
>160 vs. 80-120	143.131	18.490	<0.001	Yes
>160 vs. 120-160	107.343	16.013	<0.001	Yes
120-160 vs. <40	85.020	12.230	<0.001	Yes
120-160 vs. 40-80	59.151	11.935	<0.001	Yes
120-160 vs. 80-120	35.788	16.013	<0.001	Yes
80-120 vs. <40	49.232	15.331	<0.001	Yes
80-120 vs. 40-80	23.363	15.097	0.004	Yes
40-80 vs. <40	25.869	11.004	<0.001	Yes

For Review only

One Way Analysis of Variance Wednesday, February 06, 2019, 11:47:26 AM

Data source: Data 2 in C pools stats

Dependent Variable: sqrt_STD _DEAD

Normality Test (Shapiro-Wilk) Passed (P = 0.634)

Equal Variance Test: Passed (P = 0.224)

Group Name	N	Missing	Mean	Std Dev	SEM
<40	8	0	1.293	0.308	0.109
40-80	9	0	1.882	0.361	0.120
80-120	3	0	2.474	0.583	0.337
120-160	6	0	1.358	0.506	0.207
>160	3	0	1.090	0.0684	0.0395

Source of Variation	DF	SS	MS	F	P
Between Groups	4	4.890	1.222	7.987	<0.001
Residual	24	3.673	0.153		
Total	28	8.563			

The differences in the mean values among the treatment groups are greater than would be expected by chance; there is a statistically significant difference (P = <0.001).

Power of performed test with alpha = 0.050: 0.986

All Pairwise Multiple Comparison Procedures (Fisher LSD Method):

Comparisons for factor: **Age class**

Comparison	Diff of Means	LSD(alpha=0.050)	P	Diff >= LSD
80-120 vs. >160	1.384	0.659	<0.001	Yes
80-120 vs. <40	1.181	0.547	<0.001	Yes
80-120 vs. 120-160	1.116	0.571	<0.001	Yes
80-120 vs. 40-80	0.592	0.538	0.033	Yes
40-80 vs. >160	0.792	0.538	0.006	Yes
40-80 vs. <40	0.589	0.392	0.005	Yes
40-80 vs. 120-160	0.524	0.426	0.018	Yes
120-160 vs. >160	0.268	0.571	0.342	No
120-160 vs. <40	0.0647	0.436	0.762	Do Not Test
<40 vs. >160	0.204	0.547	0.450	Do Not Test

For Review Only

One Way Analysis of Variance Wednesday, February 06, 2019, 11:53:36 AM

Data source: Data 2 in C pools stats

Dependent Variable: DWD Mg C ha-1

Normality Test (Shapiro-Wilk) Passed (P = 0.059)

Equal Variance Test: Passed (P = 0.059)

Group Name	N	Missing	Mean	Std Dev	SEM
<40	8	0	1.700	1.335	0.472
40-80	9	0	1.369	0.765	0.255
80-120	3	0	1.839	0.530	0.306
120-160	6	0	0.872	0.928	0.379
>160	3	0	6.332	3.838	2.216

Source of Variation	DF	SS	MS	F	P
Between Groups	4	68.123	17.031	7.940	<0.001
Residual	24	51.480	2.145		
Total	28	119.603			

The differences in the mean values among the treatment groups are greater than would be expected by chance; there is a statistically significant difference (P = <0.001).

Power of performed test with alpha = 0.050: 0.985

All Pairwise Multiple Comparison Procedures (Fisher LSD Method):

Comparisons for factor: **Age class**

Comparison	Diff of Means	LSD(alpha=0.050)	P	Diff >= LSD
>160 vs. 120-160	5.460	2.137	<0.001	Yes
>160 vs. 40-80	4.963	2.015	<0.001	Yes
>160 vs. <40	4.631	2.046	<0.001	Yes
>160 vs. 80-120	4.493	2.468	<0.001	Yes
80-120 vs. 120-160	0.967	2.137	0.360	No
80-120 vs. 40-80	0.470	2.015	0.635	Do Not Test
80-120 vs. <40	0.138	2.046	0.890	Do Not Test
<40 vs. 120-160	0.828	1.632	0.305	Do Not Test
<40 vs. 40-80	0.332	1.469	0.645	Do Not Test
40-80 vs. 120-160	0.497	1.593	0.526	Do Not Test

For Review only

One Way Analysis of Variance Wednesday, February 06, 2019, 10:34:48 AM

Data source: Data 2 in C pools stats

Dependent Variable: O+A horiz Mg C ha-1

Normality Test (Shapiro-Wilk) Passed (P = 0.058)

Equal Variance Test: Passed (P = 0.550)

Group Name	N	Missing	Mean	Std Dev	SEM
<40	8	0	17.407	5.929	2.096
40-80	9	0	18.066	5.410	1.803
80-120	3	0	20.781	3.220	1.859
120-160	6	0	28.416	13.118	5.355
>160	3	0	34.103	6.082	3.512

Source of Variation	DF	SS	MS	F	P
Between Groups	4	998.886	249.722	4.175	0.010
Residual	24	1435.368	59.807		
Total	28	2434.254			

The differences in the mean values among the treatment groups are greater than would be expected by chance; there is a statistically significant difference (P = 0.010).

Power of performed test with alpha = 0.050: 0.739

All Pairwise Multiple Comparison Procedures (Fisher LSD Method):

Comparisons for factor: **Age class**

Comparison	Diff of Means	LSD(alpha=0.050)	P	Diff >= LSD
>160 vs. <40	16.696	10.806	0.004	Yes
>160 vs. 40-80	16.037	10.641	0.005	Yes
>160 vs. 80-120	13.322	13.032	0.045	Yes
>160 vs. 120-160	5.687	11.286	0.309	No
120-160 vs. <40	11.009	8.620	0.014	Yes
120-160 vs. 40-80	10.350	8.412	0.018	Yes
120-160 vs. 80-120	7.636	11.286	0.175	No
80-120 vs. <40	3.373	10.806	0.526	No
80-120 vs. 40-80	2.714	10.641	0.603	Do Not Test
40-80 vs. <40	0.659	7.756	0.862	Do Not Test

For Review Only

One Way Analysis of Variance Wednesday, February 06, 2019, 10:37:23 AM

Data source: Data 2 in C pools stats

Dependent Variable: Fine root Mg C ha-1

Normality Test (Shapiro-Wilk) Passed (P = 0.648)

Equal Variance Test: Passed (P = 0.772)

Group Name	N	Missing	Mean	Std Dev	SEM
<40	8	0	6.539	1.956	0.692
40-80	9	0	7.778	1.533	0.511
80-120	3	0	7.944	0.579	0.334
120-160	6	0	5.917	2.480	1.012
>160	3	0	4.154	1.377	0.795

Source of Variation	DF	SS	MS	F	P
Between Groups	4	38.437	9.609	2.854	0.046
Residual	24	80.799	3.367		
Total	28	119.236			

The differences in the mean values among the treatment groups are greater than would be expected by chance; there is a statistically significant difference (P = 0.046).

Power of performed test with alpha = 0.050: 0.473

All Pairwise Multiple Comparison Procedures (Fisher LSD Method):

Comparisons for factor: **Age class**

Comparison	Diff of Means	LSD(alpha=0.050)	P	Diff >= LSD
80-120 vs. >160	3.791	3.092	0.018	Yes
80-120 vs. 120-160	2.027	2.678	0.131	No
80-120 vs. <40	1.405	2.564	0.269	Do Not Test
80-120 vs. 40-80	0.166	2.525	0.893	Do Not Test
40-80 vs. >160	3.624	2.525	0.007	Yes
40-80 vs. 120-160	1.861	1.996	0.066	Do Not Test
40-80 vs. <40	1.238	1.840	0.178	Do Not Test
<40 vs. >160	2.386	2.564	0.067	No
<40 vs. 120-160	0.623	2.045	0.536	Do Not Test
120-160 vs. >160	1.763	2.678	0.187	Do Not Test

For Review Only

One Way Analysis of Variance Wednesday, February 06, 2019, 10:36:57 AM

Data source: Data 2 in C pools stats

Dependent Variable: Minsoil 0-100 Mg C ha-1

Normality Test (Shapiro-Wilk) Passed (P = 0.952)

Equal Variance Test: Passed (P = 0.362)

Group Name	N	Missing	Mean	Std Dev	SEM
<40	8	0	47.545	10.585	3.742
40-80	9	0	46.034	3.170	1.057
80-120	3	0	45.788	6.348	3.665
120-160	6	0	45.157	11.554	4.717
>160	3	0	48.059	4.609	2.661

Source of Variation	DF	SS	MS	F	P
Between Groups	4	30.262	7.566	0.110	0.978
Residual	24	1655.114	68.963		
Total	28	1685.376			

For Review Only

Figure 3: Canopy complexity and NPP_w

Multiple Linear Regression Tuesday, November 21, 2023 11:39:46 AM

Data source: Data 1 in Notebook3

Young NPPkgC/ha = -386.904 + (212.141 * LAI 4 Ring) + (165.573 * mean.max.ht) - (122.763 * rugosity)

N = 11

R = 0.680 Rsqr = 0.462 Adj Rsqr = 0.232

Standard Error of Estimate = 344.238

	Coefficient	Std. Error	t	P	VIF
Constant	-386.904	786.526	-0.492	0.638	
LAI 4 Ring	212.141	325.718	0.651	0.536	1.089
mean.max.ht	165.573	95.641	1.731	0.127	4.918
rugosity	-122.763	125.903	-0.975	0.362	4.771

Warning: Multicollinearity is present among the independent variables. The variables with the largest values of VIF are causing the problem. Consider getting more data or eliminating one or more variables from the equation. The likely candidates for elimination are: mean.max.ht , rugosity

Analysis of Variance:

	DF	SS	MS	F	P
Regression	3	712988.378	237662.793	2.006	0.202
Residual	7	829499.816	118499.974		
Total	10	1542488.194	154248.819		

Multiple Linear Regression Tuesday, November 21, 2023 11:49:45 AM

Data source: Data 1 in complexity.JNB

Mid NPP = 929.574 - (347.274 * LAI) + (80.977 * Max) + (9.149 * Rug)

N = 6

R = 0.989 Rsqr = 0.978 Adj Rsqr = 0.945

Standard Error of Estimate = 18.296

	Coefficient	Std. Error	t	P	VIF
Constant	929.574	141.049	6.590	0.022	
LAI	-347.274	57.516	-6.038	0.026	2.302
Max	80.977	11.407	7.099	0.019	1.797
Rug	9.149	4.701	1.946	0.191	1.435

Analysis of Variance:

	DF	SS	MS	F	P
Regression	3	30031.531	10010.510	29.904	0.033
Residual	2	669.513	334.757		
Total	5	30701.045	6140.209		

For Review Only

Multiple Linear Regression Tuesday, November 21, 2023 11:50:11 AM

Data source: Data 1 in complexity.JNB

Old NPP = -299.893 + (1108.522 * LAI) + (9.847 * Max) - (38.737 * Rug)

N = 12

R = 0.823 Rsqr = 0.678 Adj Rsqr = 0.557

Standard Error of Estimate = 647.868

	Coefficient	Std. Error	t	P	VIF
Constant	-299.893	1933.172	-0.155	0.881	
LAI	1108.522	281.843	3.933	0.004	1.009
Max	9.847	128.494	0.0766	0.941	3.345
Rug	-38.737	47.973	-0.807	0.443	3.354

Analysis of Variance:

	DF	SS	MS	F	P
Regression	3	7072270.398	2357423.466	5.616	0.023
Residual	8	3357863.244	419732.905		
Total	11	10430133.641	948193.967		

For Review Only

Figure 4: Leaf litterfall compositional change

Linear Regression Wednesday, May 3, 2023 2:59:38 PM

Data source: summaries in Myco_succession_litterfall.JNB

REF POP+BEPA = 21211.587 - (10.256 * Year)

N = 23

R = 0.760 Rsqr = 0.578 Adj Rsqr = 0.558

Standard Error of Estimate = 60.794

	Coefficient	Std. Error	t	P
Constant	21211.587	3837.366	5.528	<0.001
Year	-10.256	1.911	-5.367	<0.001

Analysis of Variance:

	DF	SS	MS	F	P
Regression	1	106452.737	106452.737	28.803	<0.001
Residual	21	77612.942	3695.854		
Total	22	184065.680	8366.622		

Normality Test (Shapiro-Wilk) Passed (P = 0.051)

Constant Variance Test (Spearman Rank Correlation): Passed (P = 0.061)

Linear Regression Wednesday, May 3, 2023 1:50:13 PM

Data source: summaries in Myco_succession_litterfall.JNB

REF QURU = -9152.636 + (4.653 * Year)

N = 23

R = 0.857 Rsqr = 0.735 Adj Rsqr = 0.722

Standard Error of Estimate = 19.393

	Coefficient	Std. Error	t	P
Constant	-9152.636	1224.129	-7.477	<0.001
Year	4.653	0.610	7.633	<0.001

Analysis of Variance:

	DF	SS	MS	F	P
Regression	1	21911.740	21911.740	58.261	<0.001
Residual	21	7898.086	376.099		
Total	22	29809.826	1354.992		

Normality Test (Shapiro-Wilk) Passed (P = 0.127)

Constant Variance Test (Spearman Rank Correlation): Passed (P = 0.630)

For Review Only

Linear Regression Wednesday, May 3, 2023 2:04:42 PM

Data source: summaries in Myco_succession_litterfall.JNB

TRT QURU = -29196.253 + (14.699 * Year)

N = 14

R = 0.802 Rsqr = 0.643 Adj Rsqr = 0.613

Standard Error of Estimate = 47.735

	Coefficient	Std. Error	t	P
Constant	-29196.253	6369.192	-4.584	<0.001
Year	14.699	3.165	4.644	<0.001

Analysis of Variance:

	DF	SS	MS	F	P
Regression	1	49153.125	49153.125	21.571	<0.001
Residual	12	27343.732	2278.644		
Total	13	76496.857	5884.374		

Normality Test (Shapiro-Wilk) Passed (P = 0.894)

Constant Variance Test (Spearman Rank Correlation): Passed (P = 0.904)

Linear Regression Wednesday, May 3, 2023 2:04:55 PM

Data source: summaries in Myco_succession_litterfall.JNB

TRT Acer = -10353.956 + (5.332 * Year)

N = 14

R = 0.571 Rsqr = 0.326 Adj Rsqr = 0.269

Standard Error of Estimate = 33.409

	Coefficient	Std. Error	t	P
Constant	-10353.956	4457.676	-2.323	0.039
Year	5.332	2.215	2.407	0.033

Analysis of Variance:

	DF	SS	MS	F	P
Regression	1	6467.556	6467.556	5.794	0.033
Residual	12	13393.873	1116.156		
Total	13	19861.429	1527.802		

Normality Test (Shapiro-Wilk) Passed (P = 0.793)

Constant Variance Test (Spearman Rank Correlation): Passed (P = 0.715)

For Review Only

Figure 5: Soil respiration vs stand age

Linear Regression Wednesday, May 22, 2024 11:27:25 AM

Data source: Data 1 in synthesis figs.JNB

RshA/RstA = 0.473 + (0.00118 * Stand Age)

N = 11

R = 0.605 Rsqr = 0.366 Adj Rsqr = 0.295

Standard Error of Estimate = 0.084

	Coefficient	Std. Error	t	P
Constant	0.473	0.0501	9.451	<0.001
Stand Age	0.00118	0.000517	2.279	0.049

Analysis of Variance:

	DF	SS	MS	F	P
Regression	1	0.0365	0.0365	5.193	0.049
Residual	9	0.0633	0.00704		
Total	10	0.0999	0.00999		

Normality Test (Shapiro-Wilk) Passed (P = 0.520)

Constant Variance Test (Spearman Rank Correlation): Passed (P = 0.116)

Linear Regression Wednesday, May 22, 2024 11:28:13 AM

Data source: Data 1 in synthesis figs.JNB

RsaA = 5.220 - (0.0124 * Stand Age)

N = 11

R = 0.559 Rsqr = 0.312 Adj Rsqr = 0.236

Standard Error of Estimate = 0.996

	Coefficient	Std. Error	t	P
Constant	5.220	0.594	8.782	<0.001
Stand Age	-0.0124	0.00613	-2.020	0.074

Analysis of Variance:

	DF	SS	MS	F	P
Regression	1	4.046	4.046	4.082	0.074
Residual	9	8.922	0.991		
Total	10	12.968	1.297		

Normality Test (Shapiro-Wilk) Passed (P = 0.784)

Constant Variance Test (Spearman Rank Correlation): Passed (P = 0.102)

For Review Only

Linear Regression Thursday, May 9, 2024 11:36:43 AM

Data source: Data 1 in synthesis figs.JNB

RshA = 4.780 + (0.00859 * Stand Age)

N = 11

R = 0.593 Rsqr = 0.351 Adj Rsqr = 0.279

Standard Error of Estimate = 0.632

	Coefficient	Std. Error	t	P
Constant	4.780	0.377	12.676	<0.001
Stand Age	0.00859	0.00389	2.208	0.055

Analysis of Variance:

	DF	SS	MS	F	P
Regression	1	1.945	1.945	4.875	0.055
Residual	9	3.592	0.399		
Total	10	5.537	0.554		

Normality Test (Shapiro-Wilk) Passed (P = 0.085)

Constant Variance Test (Spearman Rank Correlation): Passed (P = 0.369)

Linear Regression Tuesday, April 25, 2023 11:31:04 AM

Data source: Data 1 in synthesis figs.JNB

RstGS = 8.753 - (0.00691 * Stand Age)

N = 11 Missing Observations = 1

R = 0.625 Rsqr = 0.391 Adj Rsqr = 0.324

Standard Error of Estimate = 0.466

	Coefficient	Std. Error	t	P
Constant	8.753	0.278	31.442	<0.001
Stand Age	-0.00691	0.00287	-2.405	0.040

Analysis of Variance:

	DF	SS	MS	F	P
Regression	1	1.258	1.258	5.784	0.040
Residual	9	1.957	0.217		
Total	10	3.215	0.322		

Normality Test (Shapiro-Wilk) Passed (P = 0.088)

Constant Variance Test (Spearman Rank Correlation): Passed (P = 0.776)

For Review Only

Linear Regression Wednesday, May 22, 2024 11:29:01 AM

Data source: Data 1 in synthesis figs.JNB

RshGS/RstGS = 0.432 + (0.00131 * Stand Age)

N = 11

R = 0.650 Rsqr = 0.422 Adj Rsqr = 0.358

Standard Error of Estimate = 0.083

	Coefficient	Std. Error	t	P
Constant	0.432	0.0494	8.734	<0.001
Stand Age	0.00131	0.000510	2.564	0.030

Analysis of Variance:

	DF	SS	MS	F	P
Regression	1	0.0451	0.0451	6.576	0.030
Residual	9	0.0617	0.00686		
Total	10	0.107	0.0107		

Normality Test (Shapiro-Wilk) Passed (P = 0.058)

Constant Variance Test (Spearman Rank Correlation): Passed (P = 0.221)

Linear Regression Wednesday, May 22, 2024 11:29:58 AM

Data source: Data 1 in synthesis figs.JNB

RsaGS = 4.907 - (0.0133 * Stand Age)

N = 11

R = 0.647 Rsqr = 0.419 Adj Rsqr = 0.354

Standard Error of Estimate = 0.848

	Coefficient	Std. Error	t	P
Constant	4.907	0.506	9.696	<0.001
Stand Age	-0.0133	0.00522	-2.546	0.031

Analysis of Variance:

	DF	SS	MS	F	P
Regression	1	4.658	4.658	6.481	0.031
Residual	9	6.469	0.719		
Total	10	11.126	1.113		

Normality Test (Shapiro-Wilk) Passed (P = 0.371)

Constant Variance Test (Spearman Rank Correlation): Passed (P = 0.673)

For Review Only

Linear Regression Wednesday, May 22, 2024 11:30:33 AM

Data source: Data 1 in synthesis figs.JNB

RhGS = 3.846 + (0.00639 * Stand Age)

N = 11

R = 0.546 Rsqr = 0.298 Adj Rsqr = 0.220

Standard Error of Estimate = 0.530

	Coefficient	Std. Error	t	P
Constant	3.846	0.317	12.147	<0.001
Stand Age	0.00639	0.00327	1.955	0.082

Analysis of Variance:

	DF	SS	MS	F	P
Regression	1	1.075	1.075	3.821	0.082
Residual	9	2.531	0.281		
Total	10	3.606	0.361		

Normality Test (Shapiro-Wilk) Failed (P = <0.001)

Constant Variance Test (Spearman Rank Correlation): Passed (P = 0.353)

For Review Only

Figure 6: Fine roots, stand age, soil respiration

Linear Regression Wednesday, May 22, 2024 11:32:51 AM

Data source: Data 1 in synthesis figs.JNB

Root_prod = 1.991 - (0.00398 * Stand Age)

N = 10 Missing Observations = 1

R = 0.426 Rsqr = 0.181 Adj Rsqr = 0.0789

Standard Error of Estimate = 0.463

	Coefficient	Std. Error	t	P
Constant	1.991	0.278	7.165	<0.001
Stand Age	-0.00398	0.00299	-1.331	0.220

Analysis of Variance:

	DF	SS	MS	F	P
Regression	1	0.380	0.380	1.771	0.220
Residual	8	1.716	0.214		
Total	9	2.096	0.233		

Normality Test (Shapiro-Wilk) Passed (P = 0.711)

Constant Variance Test (Spearman Rank Correlation): Passed (P = 0.583)

Linear Regression Wednesday, May 22, 2024 11:33:54 AM

Data source: Data 1 in synthesis figs.JNB

RstA = 8.191 + (0.839 * Root_prod)

N = 10 Missing Observations = 1

R = 0.795 Rsqr = 0.632 Adj Rsqr = 0.586

Standard Error of Estimate = 0.328

	Coefficient	Std. Error	t	P
Constant	8.191	0.394	20.802	<0.001
NPPfr	0.839	0.227	3.705	0.006

Analysis of Variance:

	DF	SS	MS	F	P
Regression	1	1.476	1.476	13.728	0.006
Residual	8	0.860	0.108		
Total	9	2.336	0.260		

Normality Test (Shapiro-Wilk) Passed (P = 0.197)

Constant Variance Test (Spearman Rank Correlation): Passed (P = 0.838)

For Review Only

Burn Plots O horizon C stocks: meta-analysis

Structure: Grouped

→ Citation: Hedges and Olkin (1985)

→ Effect Sizes: lnR
→ Effect Size Variances: var_un
→ Groups: Author
→ Fixed Effects Model

→ Standard confidence intervals around means based on Student's t distribution
→ Use bootstrap for confidence intervals around means: 999 iterations
→ Citations: Adams *et al.* (1997), Dixon (1993)

23 studies will be included in this analysis

Group Results

Heterogeneity

Source	Q	df	P(χ^2)
Gough (within)	0.49	3	0.92
Le Moine (within)	0.06	4	1.00
Lehman (within)	0.21	3	0.98
Nave (within)	0.02	3	1.00
Schaetzl (within)	1.17	5	0.95

Source	I^2	95% CI
Gough (within)	0.00	0.00 to 6.30
Le Moine (within)	0.00	0.00 to 0.00
Lehman (within)	0.00	0.00 to 0.00
Nave (within)	0.00	0.00 to 0.00
Schaetzl (within)	0.00	0.00 to 0.00

→ Citations: Higgins and Thompson (2002), Huedo-Medina *et al.* (2006)

Source	Q	df	P(χ^2)
Model (Between)	3.73	4	0.44
Error (Within)	1.94	18	1.00
Total	5.67	22	1.00

Mean Effect Sizes

	n	Mean	Median	95% CI	Bootstrap CI	Bias-corrected CI
Gough	lnR	4	0.00	0.02	-1.59 to 1.59	-0.33 to 0.32	-0.40 to 0.24
Le Moine	lnR	5	-0.04	-0.07	-1.28 to 1.20	-0.13 to 0.06	-0.13 to 0.06
Lehman	lnR	4	-0.29	-0.33	-1.88 to 1.30	-0.51 to -0.08	-0.52 to -0.10
Nave	lnR	4	-0.13	-0.12	-1.72 to 1.46	-0.20 to -0.07	-0.20 to -0.07
Schaetzl	lnR	6	-1.00	-1.12	-2.05 to 0.05	-1.31 to -0.63	-1.29 to -0.61
Gough	exp(lnR)	4	1.00	1.02	0.20 to 4.91	0.72 to 1.37	0.67 to 1.27

For Review Only

```
Le Moine exp(lnR) 5 0.96 0.93 0.28 to 3.32 0.88 to 1.06 0.88 to 1.06
Lehman exp(lnR) 4 0.75 0.72 0.15 to 3.67 0.60 to 0.93 0.60 to 0.90
Nave exp(lnR) 4 0.88 0.89 0.18 to 4.32 0.82 to 0.93 0.82 to 0.93
Schaetzl exp(lnR) 6 0.37 0.33 0.13 to 1.05 0.27 to 0.53 0.27 to 0.54
```

Global Results

Heterogeneity

```
Source Q df P(χ²)
-------------------------
Total 5.67 22 1.00
```

→ Citation: Hedges and Olkin (1985)

```
Source I² 95% CI
---------------------------
Total 0.00 0.00 to 0.00
```

→ Citations: Higgins and Thompson (2002), Huedo-Medina *et al.* (2006)

Mean Effect Size

```
n Mean Median 95% CI Bootstrap CI Bias-corrected CI
-------------------------------------------------------------------------------------
----
Global lnR 23 -0.34 -0.16 -0.78 to 0.09 -0.54 to -0.15 -0.55 to -0.16
-------------------------------------------------------------------------------------
----
Global exp(lnR) 23 0.71 0.85 0.46 to 1.09 0.58 to 0.86 0.58 to 0.85
```

Structure: Linear Regression

→ Citations: Hedges and Olkin (1985), Greenland (1987)

→ Effect Sizes: lnR
→ Effect Size Variances: var_un
→ Independent Variable: Time
→ Fixed Effects Model

→ Standard confidence intervals around means based on Student's t distribution
→ Use bootstrap for confidence intervals around means: 999 iterations
→ Citations: Adams *et al.* (1997), Dixon (1993)

23 studies will be included in this analysis

Regression Results

Predictors

```
Predictor Value SE 95% CI P(Normal)
-------------------------------------------------
Intercept -0.48 0.47 -1.41 to 0.44 0.31
Slope 0.00 0.01 -0.02 to 0.02 0.74
```

Heterogeneity

```
Source Q df P(χ²)
-------------------------
Model 0.11 1 0.74
Error 5.56 21 1.00
-------------------------
Total 5.67 22 1.00
```

For Review Only

Figure 7: Stand age, soil properties, biogeochemical functions

Linear Regression Monday, May 1, 2023 2:41:37 PM

Data source: Data 2 in synthesis figs.JNB

%C = 5.446 + (0.0487 * Stand age)

N = 6

R = 0.851 Rsqr = 0.724 Adj Rsqr = 0.656

Standard Error of Estimate = 1.031

	Coefficient	Std. Error	t	P
Constant	5.446	1.074	5.071	0.007
Stand age	0.0487	0.0150	3.243	0.032

Analysis of Variance:

	DF	SS	MS	F	P
Regression	1	11.181	11.181	10.514	0.032
Residual	4	4.254	1.063		
Total	5	15.435	3.087		

Normality Test (Shapiro-Wilk) Passed (P = 0.337)

Constant Variance Test (Spearman Rank Correlation): Passed (P = 0.060)

Linear Regression Monday, May 1, 2023 2:42:08 PM

Data source: Data 2 in synthesis figs.JNB

MBC = 295.573 + (4.579 * Stand age)

N = 6

R = 0.927 Rsqr = 0.859 Adj Rsqr = 0.824

Standard Error of Estimate = 63.617

	Coefficient	Std. Error	t	P
Constant	295.573	66.258	4.461	0.011
Stand age	4.579	0.926	4.945	0.008

Analysis of Variance:

	DF	SS	MS	F	P
Regression	1	98967.320	98967.320	24.453	0.008
Residual	4	16188.680	4047.170		
Total	5	115156.000	23031.200		

Normality Test (Shapiro-Wilk) Passed (P = 0.730)

Constant Variance Test (Spearman Rank Correlation): Passed (P = 0.060)

For Review Only

Linear Regression Monday, May 1, 2023 2:53:15 PM

Data source: Data 2 in synthesis figs.JNB

pH = 5.038 - (0.00944 * Stand age)

N = 6

R = 0.861 Rsqr = 0.741 Adj Rsqr = 0.676

Standard Error of Estimate = 0.192

	Coefficient	Std. Error	t	P
Constant	5.038	0.200	25.210	<0.001
Stand age	-0.00944	0.00279	-3.381	0.028

Analysis of Variance:

	DF	SS	MS	F	P
Regression	1	0.421	0.421	11.434	0.028
Residual	4	0.147	0.0368		
Total	5	0.568	0.114		

Normality Test (Shapiro-Wilk) Passed (P = 0.752)

Constant Variance Test (Spearman Rank Correlation): Passed (P = 0.060)

Linear Regression Monday, May 1, 2023 3:12:45 PM

Data source: Data 2 in synthesis figs.JNB

AlphaG = 7.828 - (1.320 * pH)

N = 6

R = 0.853 Rsqr = 0.728 Adj Rsqr = 0.660

Standard Error of Estimate = 0.304

	Coefficient	Std. Error	t	P
Constant	7.828	1.787	4.381	0.012
pH	-1.320	0.404	-3.270	0.031

Analysis of Variance:

	DF	SS	MS	F	P
Regression	1	0.990	0.990	10.692	0.031
Residual	4	0.370	0.0926		
Total	5	1.360	0.272		

Normality Test (Shapiro-Wilk) Passed (P = 0.775)

Constant Variance Test (Spearman Rank Correlation): Passed (P = 0.060)

For Review Only

Linear Regression Monday, May 1, 2023 3:05:30 PM

Data source: Data 2 in synthesis figs.JNB

AlphaG = -0.219 + (0.257 * %C)

N = 6

R = 0.864 Rsqr = 0.747 Adj Rsqr = 0.684

Standard Error of Estimate = 0.293

	Coefficient	Std. Error	t	P
Constant	-0.219	0.657	-0.334	0.755
%C	0.257	0.0746	3.437	0.026

Analysis of Variance:

	DF	SS	MS	F	P
Regression	1	1.016	1.016	11.813	0.026
Residual	4	0.344	0.0860		
Total	5	1.360	0.272		

Normality Test (Shapiro-Wilk) Passed (P = 0.490)

Constant Variance Test (Spearman Rank Correlation): Passed (P = 0.060)

For Review Only

Figure 10: Fungal 15N tracer recovery

One Way Analysis of Variance Monday, December 11, 2023 12:41:29 PM

Data source: Data 1 in Notebook1

Dependent Variable: d15N

Normality Test (Shapiro-Wilk): Passed (P = 0.135)

Equal Variance Test (Brown-Forsythe): Passed (P = 0.821)

Group Name	N	Missing	Mean	Std Dev	SEM
Cortinariaceae	4	0	44.977	7.208	3.604
Russulaceae	7	0	31.294	5.531	2.090
Amanitaceae	3	0	33.147	6.395	3.692
Boletaceae	4	0	29.125	6.060	3.030

Source of Variation	DF	SS	MS	F	P
Between Groups	3	630.045	210.015	5.533	0.010
Residual	14	531.363	37.955		
Total	17	1161.408			

The differences in the mean values among the treatment groups are greater than would be expected by chance; there is a statistically significant difference (P = 0.010).

Power of performed test with alpha = 0.050: 0.773

All Pairwise Multiple Comparison Procedures (Fisher LSD Method):

Comparisons for factor: **Family**

Comparison	Diff of Means	LSD(alpha=0.050)	P	Diff >= LSD
Cortinariaceae vs. Boletaceae	15.852	9.343	0.003	Yes
Cortinariaceae vs. Russulaceae	13.683	8.282	0.003	Yes
Cortinariaceae vs. Amanitaceae	11.831	10.092	0.025	Yes
Amanitaceae vs. Boletaceae	4.022	10.092	0.407	No
Amanitaceae vs. Russulaceae	1.852	9.118	0.670	Do Not Test
Russulaceae vs. Boletaceae	2.169	8.282	0.583	Do Not Test

For Review Only

Figure 11 (Decadal change in SOC stocks)

Two Way Analysis of Variance Wednesday, October 27, 2021 1:51:20 PM

Data source: Data 1 in Notebook1

General Linear Model

Dependent Variable: stock_c

Normality Test (Shapiro-Wilk): Passed (P = 0.858)

Equal Variance Test (Brown-Forsythe): Passed (P = 0.105)

Source of Variation	DF	SS	MS	F	P
year	1	38.275	38.275	6.299	0.015
horizon	2	403.051	201.526	33.163	<0.001
year x horizon	2	51.667	25.834	4.251	0.018
Residual	65	394.992	6.077		
Total	70	891.787	12.740		

Main effects cannot be properly interpreted if significant interaction is determined. This is because the size of a factor's effect depends upon the level of the other factor.

The effect of different levels of year depends on what level of horizon is present. There is a statistically significant interaction between year and horizon. (P = 0.018)

Power of performed test with alpha = 0.0500: for year : 0.621

Power of performed test with alpha = 0.0500: for horizon : 1.000

Power of performed test with alpha = 0.0500: for year x horizon : 0.600

Least square means for year :

Group	Mean	SEM
1980.000	8.415	0.417
2009.000	6.946	0.411

Least square means for horizon :

Group	Mean	SEM
A	9.233	0.503
E	4.324	0.503
B	9.486	0.514

Least square means for year x horizon :

Group	Mean	SEM
1980.000 x A	10.500	0.712
1980.000 x E	5.739	0.712
1980.000 x B	9.007	0.743
2009.000 x A	7.966	0.712
2009.000 x E	2.908	0.712
2009.000 x B	9.964	0.712

All Pairwise Multiple Comparison Procedures (Tukey Test):

For Review Only

Comparisons for factor: **horizon within 1980**

Comparison	Diff of Means	p	q	P	P<0.050
A vs. E	4.761	3	6.691	<0.001	Yes
A vs. B	1.493	3	2.052	0.321	No
B vs. E	3.268	3	4.492	0.006	Yes

Comparisons for factor: **horizon within 2009**

Comparison	Diff of Means	p	q	P	P<0.050
B vs. E	7.055	3	9.915	<0.001	Yes
B vs. A	1.998	3	2.807	0.124	No
A vs. E	5.058	3	7.107	<0.001	Yes

Comparisons for factor: **year within A**

Comparison	Diff of Means	p	q	P	P<0.050
1980.000 vs. 2009.000	2.534	2	3.561	0.014	Yes

Comparisons for factor: **year within E**

Comparison	Diff of Means	p	q	P	P<0.050
1980.000 vs. 2009.000	2.830	2	3.977	0.007	Yes

Comparisons for factor: **year within B**

Comparison	Diff of Means	p	q	P	P<0.050
2009.000 vs. 1980.000	0.957	2	1.315	0.356	No

For Review Only

Figure 12: C and water fluxes and climatology

Multiple Linear Regression Wednesday, May 22, 2024 12:36:27 PM

Data source: Data 1 in fluxes_thru_2020.JNB

GPP = -22700.350 + (11.953 * Year) - (18.329 * +RC-TRT)

N = 34 Missing Observations = 1

R = 0.650 Rsqr = 0.422 Adj Rsqr = 0.385

Standard Error of Estimate = 79.439

	Coefficient	Std. Error	t	P	VIF
Constant	-22700.350	5175.015	-4.387	<0.001	
Year	11.953	2.575	4.643	<0.001	1.135
+RC-TRT	-18.329	29.866	-0.614	0.544	1.135

Analysis of Variance:

	DF	SS	MS	F	P
Regression	2	142991.433	71495.716	11.330	<0.001
Residual	31	195625.223	6310.491		
Total	33	338616.656	10261.111		

Column	SSIncr	SSMarg
Year	140614.569	136012.398
+RC-TRT	2376.864	2376.864

The dependent variable GPP can be predicted from a linear combination of the independent variables:

	P
Year	<0.001
+RC-TRT	0.544

Not all of the independent variables appear necessary (or the multiple linear model may be underspecified).
The following appear to account for the ability to predict GPP (P < 0.05): Year

Normality Test (Shapiro-Wilk) Passed (P = 0.440)

Constant Variance Test (Spearman Rank Correlation): Passed (P = 0.131)

For Review Only

Multiple Linear Regression Wednesday, May 22, 2024 12:37:21 PM

Data source: Data 1 in fluxes_thru_2020.JNB

ER = -13566.763 + (7.285 * Year) - (80.589 * +RC-TRT)

N = 34 Missing Observations = 1

R = 0.555 Rsqr = 0.308 Adj Rsqr = 0.263

Standard Error of Estimate = 72.109

	Coefficient	Std. Error	t	P	VIF
Constant	-13566.763	4697.522	-2.888	0.007	
Year	7.285	2.337	3.117	0.004	1.135
+RC-TRT	-80.589	27.110	-2.973	0.006	1.135

Analysis of Variance:

	DF	SS	MS	F	P
Regression	2	71782.416	35891.208	6.903	0.003
Residual	31	161190.446	5199.692		
Total	33	232972.861	7059.784		

Column	SSIncr	SSMarg
Year	25835.295	50530.152
+RC-TRT	45947.120	45947.120

The dependent variable ER can be predicted from a linear combination of the independent variables:

	P
Year	0.004
+RC-TRT	0.006

All independent variables appear to contribute to predicting ER ($P < 0.05$).

Normality Test (Shapiro-Wilk) Passed (P = 0.571)

Constant Variance Test (Spearman Rank Correlation): Passed (P = 0.575)

For Review Only

Multiple Linear Regression Wednesday, May 22, 2024 12:34:30 PM

Data source: Data 1 in fluxes_thru_2020.JNB

NEE = 12729.804 - (6.464 * Year) - (79.240 * +RC-TRT)

N = 34 Missing Observations = 1

R = 0.764 Rsqr = 0.584 Adj Rsqr = 0.557

Standard Error of Estimate = 54.343

	Coefficient	Std. Error	t	P	VIF
Constant	12729.804	3540.151	3.596	0.001	
Year	-6.464	1.761	-3.670	<0.001	1.135
+RC-TRT	-79.240	20.431	-3.878	<0.001	1.135

Analysis of Variance:

	DF	SS	MS	F	P
Regression	2	128459.783	64229.891	21.750	<0.001
Residual	31	91547.223	2953.136		
Total	33	220007.005	6666.879		

Column	SSIncr	SSMarg
Year	84038.265	39775.358
+RC-TRT	44421.518	44421.518

The dependent variable NEE can be predicted from a linear combination of the independent variables:

	P
Year	<0.001
+RC-TRT	<0.001

All independent variables appear to contribute to predicting NEE (P < 0.05).

Normality Test (Shapiro-Wilk) Passed (P = 0.552)

Constant Variance Test (Spearman Rank Correlation): Passed (P = 0.087)

For Review Only

Multiple Linear Regression Wednesday, May 22, 2024 12:39:59 PM

Data source: Data 1 in fluxes_thru_2020.JNB

WUE = -89.783 + (0.0463 * Year) + (0.101 * +RC-TRT)

N = 34 Missing Observations = 1

R = 0.747 Rsqr = 0.558 Adj Rsqr = 0.529

Standard Error of Estimate = 0.247

	Coefficient	Std. Error	t	P	VIF
Constant	-89.783	16.616	-5.404	<0.001	
Year	0.0463	0.00826	5.597	<0.001	1.083
+RC-TRT	0.101	0.0895	1.127	0.268	1.083

Analysis of Variance:

	DF	SS	MS	F	P
Regression	2	2.383	1.191	19.543	<0.001
Residual	31	1.890	0.0610		
Total	33	4.272	0.129		

Column	SSIncr	SSMarg
Year	2.305	1.909
+RC-TRT	0.0775	0.0775

The dependent variable WUE can be predicted from a linear combination of the independent variables:

	P
Year	<0.001
+RC-TRT	0.268

Not all of the independent variables appear necessary (or the multiple linear model may be underspecified).
The following appear to account for the ability to predict WUE (P < 0.05): Year

Normality Test (Shapiro-Wilk) Passed (P = 0.302)

Constant Variance Test (Spearman Rank Correlation): Passed (P = 0.661)

For Review Only

Linear Regression Tuesday, May 14, 2024 9:48:58 AM

Data source: Data 1 in fluxes_thru_2020.JNB

MAT = -42.520 + (0.0247 * Year)

N = 41

R = 0.309 Rsqr = 0.0957 Adj Rsqr = 0.0725

Standard Error of Estimate = 0.919

	Coefficient	Std. Error	t	P
Constant	-42.520	24.273	-1.752	0.088
Year	0.0247	0.0121	2.032	0.049

Analysis of Variance:

	DF	SS	MS	F	P
Regression	1	3.490	3.490	4.128	0.049
Residual	39	32.971	0.845		
Total	40	36.461	0.912		

Normality Test (Shapiro-Wilk) Passed (P = 0.948)

Constant Variance Test (Spearman Rank Correlation): Passed (P = 0.280)

Linear Regression Wednesday, May 22, 2024 1:16:54 PM

Data source: Data 1 in fluxes_thru_2020.JNB

MAP = -917.074 + (0.501 * Year)

N = 41

R = 0.501 Rsqr = 0.251 Adj Rsqr = 0.231

Standard Error of Estimate = 10.508

	Coefficient	Std. Error	t	P
Constant	-917.074	277.388	-3.306	0.002
Year	0.501	0.139	3.612	<0.001

Analysis of Variance:

	DF	SS	MS	F	P
Regression	1	1440.310	1440.310	13.045	<0.001
Residual	39	4306.019	110.411		
Total	40	5746.329	143.658		

Normality Test (Shapiro-Wilk) Passed (P = 0.164)

Constant Variance Test (Spearman Rank Correlation): Passed (P = 0.107)

For Review Only

Nonlinear Regression- N deposition **Wednesday, May 22, 2024 1:20:43 PM**

Data Source: Data 1 in fluxes_thru_2020.JNB
Equation: Piecewise, 2 segment linear

t1 = min(t)
t2 = max(t)
region1(t) = (y1*(T1-t) + y2*(t-t1))/(T1-t1)
region2(t) = (y2*(t2-t) + y3*(t-T1))/(t2-T1)
f = if(t <= T1, region1(t), region2(t))

R	Rsqr	Adj Rsqr	Standard Error of Estimate
0.5096	0.2597	0.1962	0.7304

	Coefficient	Std. Error	t	P
y1	5.1214	0.3373	15.1853	<0.0001
y2	5.0494	0.3221	15.6755	<0.0001
y3	3.8862	0.3304	11.7622	<0.0001
T1	2002.0000	7.7335	258.8753	<0.0001

Analysis of Variance:

	DF	SS	MS
Regression	4	898.0858	224.5215
Residual	35	18.6721	0.5335
Total	39	916.7579	23.5066

Corrected for the mean of the observations:

	DF	SS	MS
Regression	3	6.5489	2.1830
Residual	35	18.6721	0.5335
Total	38	25.2210	0.6637

Statistical Tests:

Normality Test (Shapiro-Wilk) Passed (P = 0.3501)
W Statistic= 0.9690 Significance Level = 0.0500

Constant Variance Test (Spearman Rank Correlation) Passed (P = 0.7571)

For Review Only

Soil respiration: US-UMB vs. US-UMd

Factor	df	t	P
Footprint	10	14.781	0.00000004

Group Means

UMd	6.54
UMB	7.37

Difference of Means

0.83

For Review Only

Appendix S1 References

Clay, C., L. Nave, K. Nadelhoffer, C. Vogel, B. Propson, J. Den Uyl, L. J. Hickey, A. Barry, and C. M. Gough. 2022. Fire after clear-cut harvesting minimally affects the recovery of ecosystem carbon pools and fluxes in a Great Lakes forest. Forest Ecology and Management **519**.

Gough, C. M., C. S. Vogel, K. H. Harrold, K. George, and P. S. Curtis. 2007. The legacy of harvest and fire on ecosystem carbon storage in a north temperate forest. Global Change Biology 13:1935-1949.

Lehman E., N. Mahowald, M. Olender, B. Plater, and P. Speck. 1993. Forest fires, organic soil carbon and global warming. University of Michigan Biological Station Working Paper. 47pp., including appendices. Available from University of Michigan Deep Blue Documents. https://hdl.handle.net/2027.42/54462.

National Trends Network. 2019. NTN Site Operations Manual. NADP Program Office. < https://nadp.slh.wisc.edu/wp-content/uploads/2021/04/NTN-2000_Operations_Manual_v_3-0.pdf>

Nave, L. E., K. DeLyser, G. M. Domke, M. K. Janowiak, T. A. Ontl, E. Sprague, B. F. Walters, and C. W. Swanston. 2021. Land use and management effects on soil carbon in US Lake States, with emphasis on forestry, fire, and reforestation. Ecological Applications **31**.

Nave L., C. Gough, and K. Nadelhoffer. 2024. Forest tree, woody debris, root ingrowth, soil respiration and characterization data from long-term research plots for LTREB at the University of Michigan Biological Station. Version 9. Environmental Data Initiative. https://doi.org/10.6073/pasta/b47e7e6f05d6fcd7136c1e28f23e5217 Link last verified 15 February 2024.

For Review Only

Nave, L. E., J. M. Le Moine, C. M. Gough, and K. J. Nadelhoffer. 2019. Multidecadal trajectories of soil chemistry and nutrient availability following cutting vs. burning disturbances in Upper Great Lakes forests. Canadian Journal of Forest Research 49:731-742.

Nave, L. E., K. J. Nadelhoffer, J. M. Le Moine, L. T. A. van Diepen, J. K. Cooch, and N. J. Van Dyke. 2013. Nitrogen Uptake by Trees and Mycorrhizal Fungi in a Successional Northern Temperate Forest: Insights from Multiple Isotopic Methods. Ecosystems **16**:590-603.

Pastorello, G., C. Trotta, E. Canfora, H. S. Chu, D. Christianson, Y. W. Cheah, C. Poindexter, J. Q. Chen, A. Elbashandy, M. Humphrey, P. Isaac, D. Polidori, A. Ribeca, C. van Ingen, L. M. Zhang, B. Amiro, C. Ammann, M. A. Arain, J. Ardö, T. Arkebauer, S. K. Arndt, N. Arriga, M. Aubinet, M. Aurela, D. Baldocchi,, et al.. 2020. The FLUXNET2015 dataset and the ONEFlux processing pipeline for eddy covariance data. Scientific Data **7**.

Schaetzl, R. J. 1994. Changes in O-horizon mass, thickness and carbon content following fire in northern hardwood forests. Vegetatio **115**:41-50.

Sinsabaugh, R.L., and A.E. Linkins. 1990. Enzymic and chemical analysis of particulate organic matter from a boreal river. Freshw. Biol. **23**: 301–309.

Wu, J., R.G. Jorgensen, B. Pommerening, R. Chaussod, and P.C. Brookes. 1990. Measurement of soil microbial biomass C by fumigation-extraction—an automated procedure. Soil Biology and Biochemistry **22**:1167-1169.

For Review Only

Author	Control_age	Stand_age	CTRL C stock	TRT C stock	lnR	var_un
Schaetzl 1994	90	12	2	0.5	-1.492	1
Schaetzl 1994	90	38	2	0.5	-1.328	1
Schaetzl 1994	90	44	2	0.7	-1.064	1
Schaetzl 1994	90	56	2	0.9	-0.832	1
Schaetzl 1994	90	69	2	1.8	-0.128	1
Schaetzl 1994	90	81	2	0.6	-1.171	1
Nave 2019	103	16	4.4	3.8	-0.157	1
Nave 2019	103	34	4.4	4.1	-0.064	1
Nave 2019	103	60	4.4	4.1	-0.077	1
Nave 2019	103	78	4.4	3.6	-0.216	1
Gough 2007	68	6	6.2	3.8	-0.495	1
Gough 2007	68	24	6.2	7.2	0.149	1
Gough 2007	68	50	6.2	9.8	0.459	1
Gough 2007	68	56	6.2	5.6	-0.11	1
Lehman 1993	82	57	16.6	17	0.024	1
Lehman 1993	82	45	20.1	16.9	-0.175	1
Lehman 1993	82	39	18.4	11.3	-0.486	1
Lehman 1993	82	18	22.1	13.1	-0.526	1
Le Moine 2012	101	76	8	7.7	-0.029	1
Le Moine 2012	101	64	8	7.4	-0.07	1
Le Moine 2012	101	58	8	7.4	-0.07	1
Le Moine 2012	101	32	8	9.2	0.147	1
Le Moine 2012	101	14	8	6.6	-0.183	1

Author identifies the source dataset
Control_age indicates which stand age was used as the control for each source dataset
Stand_age indicates the stand age, in years, since the experimental cut+burn manipulation
CTRL C stock is the O horizon C stock in Mg ha-1 for the control condition
TRT C stock is the O horizon C stock in Mg ha-1 for the treatment plot
lnR is the ln-transformed response ratio
var_un is set at 1 in order to conduct an unweighted meta-analysis (all weights the same)

For Review Only